

## **General Disclaimer**

### **One or more of the Following Statements may affect this Document**

- This document has been reproduced from the best copy furnished by the organizational source. It is being released in the interest of making available as much information as possible.
- This document may contain data, which exceeds the sheet parameters. It was furnished in this condition by the organizational source and is the best copy available.
- This document may contain tone-on-tone or color graphs, charts and/or pictures, which have been reproduced in black and white.
- This document is paginated as submitted by the original source.
- Portions of this document are not fully legible due to the historical nature of some of the material. However, it is the best reproduction available from the original submission.

(NASA-CR-175735) LAND VEHICLE ANTENNAS FOR  
SATELLITE MOBILE COMMUNICATIONS Final  
Report (Ball Aerospace Systems Div.,  
Boulder) 121 p HC A06/MF A01 CSCI 17B

N85-25682  
Unclas  
21104  
G3/32

**LAND VEHICLE ANTENNAS**  
**FOR**  
**SATELLITE MOBILE COMMUNICATIONS**

**FINAL REPORT**  
**F85-02**

**FEBRUARY 1985**  
956686



**SUBMITTED TO:**

**JET PROPULSION LABORATORY**  
**CALIFORNIA INSTITUTE OF TECHNOLOGY**  
**PASADENA, CALIFORNIA**



**BOULDER, COLORADO 80306**



Final Report

F85-02

LAND VEHICLE ANTENNAS  
FOR SATELLITE MOBILE  
COMMUNICATIONS

H.A. Haddad, B.V. Pieper and D.B. McKenna

February 1985

Submitted to:

Jet Propulsion Laboratory (JPL)  
California Institute of Technology  
Pasadena, CA



## FOREWORD

Ball Aerospace Systems Division (BASD), Boulder, CO submits this final report to JPL Pasadena, California in fulfillment of JPL Contract Number 956686, Mod. No. 2.

This report is a summary of the work that was performed by the following individuals:

- H.A. Haddad - System Engineer and Program Manager
- R.E. Brown - Large Volume cost Estimator
- B.V. Pieper - Antenna Pointing System
- A.M. Muckle - Mechanical Steering and Control System
- T.A. Pett - RF Antenna Performance
- D.B. McKenna - RF Antenna Performance

We would like to acknowledge the helpful comments made by the JPL staff during the course of this study, specifically Dr. John Huang, Mr. Dave Bell, Dr. Ken Woo, Dr. Y. Rahmat-Samii, Dr. Firuz Naderi and Dr. Farmaz Davarian.



## SUMMARY

This report summarizes the work performed during the second phase of a study program on concepts development of Land Mobile Vehicle (LMV) Antennas for Satellite Mobile Communications. Three types of antennas have been investigated as to their RF performance, size, pointing system and cost. The three concepts are:

- (1) The mechanically steered 1 x 4 tilted microstrip array
- (2) The mechanically steered fixed-beam conformal array
- (3) The electronically steered conformal phased array

A summary of their expected cost and system performance is summarized in Table S-1.

Depending on the type of design, the antenna height can be 2" to 7.5", the gain may vary from 9 to 11 dB and the elevation pattern rolloffs from 70° to horizon can be 5 to 6 dB. The two satellite isolations are estimated for satellites located at 80°W and 113°W and with the assumption of having amplitude taper in the LMV antenna.

The breadboard (B.B.) and prototype costs include the costs for designing, fabricating, essential testing and detail drawings of the functioning antenna system. The per unit costs for quantities of 100, 10,000 and 100,000 units are based on concept's parts and material breakdown with a complexity factor assigned to each design. It is very difficult at this phase of the program to determine the cost with high degree of accuracy. A more accurate prices can be established once the breadboard and prototype units are made. Then a rigorous learning curve method would be used to determine the prices in large quantities.



Table S-1  
ANTENNA CANDIDATE CONCEPTS

No.	Size (Inches)		Technical Features				Cost (Thousands of Dollars)			Development Time (Months)		Comments		
	Height	Base	Gain	Two Satellite Isolation* (dB)	Polarization (db)	Drop Off Rate 70° to horizon (db)	B. B.	Development	Manufacturer	B. B.	Proto-type		Date Available	
1	7.5	36	11	20	5	5	220	125	2-3 Lots of 100	.7-.8 Lots of 10,000	.5-.6 Lots of 100,000	9-12	6-9	<ul style="list-style-type: none"> <li>• CONUS operation</li> <li>• Can be adjusted for Alaska operation with essentially the same gain</li> <li>• Single channel monopulse tracking or magnetometry</li> </ul>
2	3.5	36	9	20	0	6	230	125	3-4 Lots of 10,000	1.0-1.4 Lots of 10,000	.7-.9 Lots of 100,000	9-12	6-9	<ul style="list-style-type: none"> <li>• CONUS only</li> <li>• Reduced gain for Alaska operation</li> <li>• Single channel monopulse tracking or magnetometry</li> </ul>
3	2.0	36	10	20	0	6	250	150	6-8 Lots of 10,000	2.5-3.5 Lots of 10,000	1-2 Lots of 100,000	12-15	9	<ul style="list-style-type: none"> <li>• CONUS only</li> <li>• Reduced gain for Alaska operation</li> <li>• Sequential lobing with/without magnetometry</li> </ul>

\* Satellites' positions are at 80°W and 113°W; LMV antenna has a taper.



## TABLE OF CONTENTS

<u>Section</u>	<u>Title</u>	<u>Page</u>
	Foreword	ii
	Summary	iii
1.0	Introduction.....	1-1
2.0	Land Mobile Vehicle Antennas.....	2-1
2.1	Mechanically Steered Antenna Arrays.....	2-1
2.1.1	1 x 4 Tilted Microstrip Array.....	2-11
2.1.2	Reduction of Low-Angle Radiation.....	2-23
2.1.2	Conformal Fixed-beam Array.....	2-35
2.2	Electronically Steered Conformal Array.....	2-39
3.0	Vehicle Antenna Pointing Systems.....	3-1
3.1	Monopulse Tracking Systems - Phase Detection.....	3-1
3.1.1	System Concept Description.....	3-1
3.1.2	Performance.....	3-18
3.1.3	Reliability.....	3-19
3.1.4	Heritage.....	3-20
3.1.5	Cost.....	3-20
3.2	Monopulse Tracking - Amplitude Detection.....	3-21
3.2.1	System Concept Description.....	3-21
3.2.2	Performance.....	3-26
3.2.3	Reliability.....	3-28
3.2.4	Heritage.....	3-28
3.2.5	Costs.....	3-29
3.3	Sequential Lobe Tracking.....	3-29
3.3.1	System Concept Description.....	3-29
3.3.2	Performance.....	3-39
3.3.3	Reliability.....	3-40
3.3.4	Heritage.....	3-40
3.3.5	Costs.....	3-40
3.4	Magnetometer Pointing System.....	3-40
3.4.1	System Concept Description.....	3-40
3.4.2	Performance.....	3-45



TABLE OF CONTENTS (Continued)

<u>Section</u>	<u>Title</u>	<u>Page</u>
	3.4.3 Reliability.....	3-46
	3.4.4 Heritage.....	3-46
	3.4.5 Cost.....	3-46
3.5	Performance Summary.....	3-47
4.0	Antenna System Cost.....	4-1

FIGURES

<u>Figure</u>		<u>Page</u>
1-1	The Three LMV Antenna Concepts Shown Configured atop a Car Roof.....	1-2
2-1	Cut-Away View of Antenna Drive Assembly.....	2-4
2-2	Concept 1 - Antenna with Drive Assembly.....	2-5
2-3	Concept 2 - Antenna and Drive Assembly.....	2-6
2-4	1 x 4 Antenna Array Showing the Front Radiating Patches and the Rear Quadrature Hybrids.....	2-13
2-5	Narrow Beam Pattern of the 1 x 4 Array, Flat on Finite Ground Plane, F = .845 GHz.....	2-15
2-6	Wide Beam Pattern of the 1 x 4 Array, Flat on Finite Ground Plane, F = .845 GHz.....	2-16
2-7	Elevation Pattern Cut of the 1 x 4 Array Tilted 35° Over Finite Ground Plane, F = .845 GHz.....	2-18
2-8	Impedance Plot of Uniformly Illuminated 1 x 4 Array: Power Divider, Hybrids and Patches, F = .82 - .87 GHz.....	2-19
2-9	Narrow Beam Pattern of Tapered 1 x 4 Array with Cross Polarization, F = .84 GHz.....	2-21
2-10	Impedance Plot of Tapered 1 x 4 Array, Power Divider, Hybrids and Patches, F = .82 - .87 GHz.....	2-22
2-11	Corrugated Surface Model.....	2-25
2-12	C-band Corrugation Model with Finite Ground Plane.....	2-26
2-13	UHF Corrugation Model with Finite Ground Plane.....	2-28
2-14	Calculated Pattern of the Uniformly Fed Tilted 1 x 4 Array.....	2-30



TABLE OF CONTENTS (Continued)

<u>Figure</u>		<u>Page</u>
2-15	Measured Pattern of the Uniformly Fed Tilted 1 x 4 Array.....	2-31
2-16	Calculated Pattern of the Tapered Tilted 1 x 4 Array.....	2-32
2-17	Measured Pattern of the Tapered Tilted 1 x 4 Array.....	2-33
2-18	Calculated Difference Patterns of the Uniformly Fed Tilted 1 x 4 Array.....	2-36
2-19	Calculated Difference Pattern of the Tapered Tilted 1 x 4 Array.....	2-37
2-20	Mechanically Steered Fixed-Beam Conformal Array.....	2-38
2-21	Electronically Steered Conformal Phased Array.....	2-40
3-1	Single-Channel Monopulse Tracking - Phase Detection.....	3-2
3-2	Phasor Diagram Showing Phase Modulation.....	3-6
3-3	Mobile Terminal Block Diagram.....	3-7
3-4	Basic Phaselock Loop Can Detect Pointing Errors.....	3-8
3-5	Pointing Error Determination.....	3-10
3-6	Phase Modulation.....	3-11
3-7	Monopulse Tracking System Operations Flow Diagram.....	3-13
3-8	Worst Case Reacquisition Sequence.....	3-17
3-9	Single-Channel Monopulse Tracking - Amplitude Detection.....	3-22
3-10	Phasor Diagram Showing Amplitude Modulation.....	3-24
3-11	Pointing Error Determined by Synchronously Demodulating Transients in AGC and Phase Shifts of $\Delta$ Signal.....	3-25
3-12	Amplitude Modulation of the Received Signal.....	3-27
3-13	Sequential Lobing Tracking System.....	3-31
3-14	Pointing Error Determination.....	3-33
3-15	Amplitude Modulation Determination.....	3-34
3-16	Effects of Steering Beam $\pm 10^\circ$ .....	3-35
3-17	Sequential Lobe Tracking System.....	3-37
3-18	Magnetometer Fluxgate.....	3-42
3-19	Magnetometer Block Diagram.....	3-43



TABLE OF CONTENTS (Continued)

TABLES

<u>Table</u>		<u>Page</u>
S-1	Antenna Candidate Concepts.....	iv
1-1	Summary of Antenna Concept Performance.....	1-3
2-1	Gain of a Uniformly Fed 1 x 4 Array.....	2-20
2-2	Beamwidths and Pattern Rolloff for a Uniformly Fed 1 x 4 Array	2-20
2-3	Gain of a Tapered 1 x 4 Array.....	2-24
2-4	Beamwidths and Pattern Rolloff for a Tapered 1 x 4 Array.....	2-24
2-5	Calculated/Measured Pattern Isolation (dB Down from Main Lobe) Two Satellite System Located at 80° and 113° W Longitude.....	2-34
2-6	Calculated/Measured Pattern Isolation (dB Down from Main Lobe) Two Satellite System Located at 105° and 135° W Longitude....	2-34
3-1	Pointing System Performance Comparison.....	3-1
4-1	Antenna Major Cost Driver.....	4-3
4-2	Cost Estimates.....	4-3
4-3	Per Unit Cost Breakdown in Quantities of 10,000 for Three Types of Antennas.....	4-4

APPENDICES

<u>Appendix</u>		<u>Page</u>
A	Single Channel Monopulse Tracking System Using Phase Modulation.....	A-1
B	Pointing Accuracy of a Monopulse Tracking System Using Phase Detection.....	B-1



## SECTION 1.0

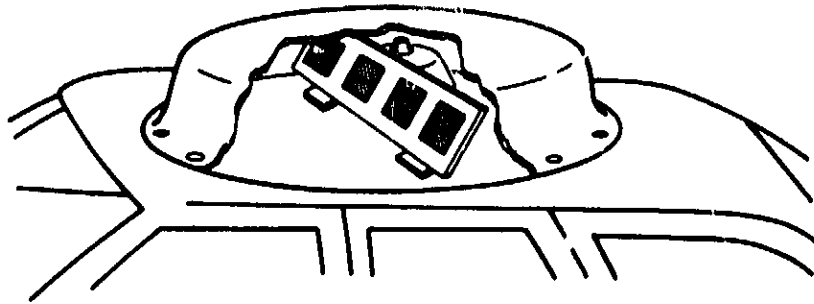
### INTRODUCTION

We have investigated three types of antenna systems with two types of steering mechanisms. The 1 x 4 tilted microstrip array and the conformal fixed-beam array are two of the antennas that are mechanically steered. The 19-element conformal array with solid state phase shifter is steered electronically. Figure 1-1 shows their configurations on the roof of a car. Some preliminary RF and system study was previously made and documented in a separate report.<sup>1</sup> Table 1-1 summarizes the basic performances for each of the three antenna concepts.

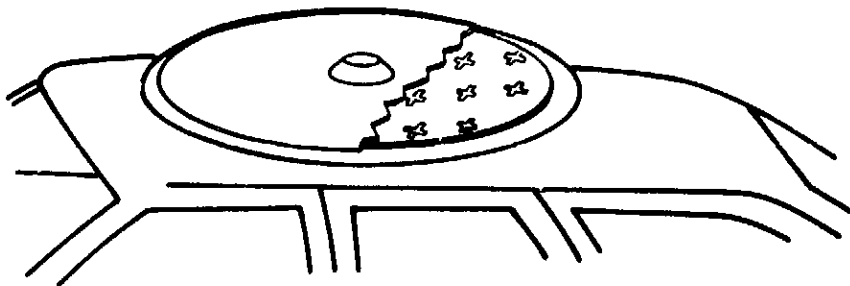
In this report, the emphasis of the study is on the RF performance of the tilted 1 x 4 antenna array and on the methods for pointing the various antennas to a geosynchronous satellite. The results of this study are detailed in Sections 2 and 3. We also present in Section 2 an updated version of satellite isolations in two-satellite system.

Finally, cost estimates for the various antenna concepts in quantities of 10,000 and 100,000 units are summarized in Section 4.

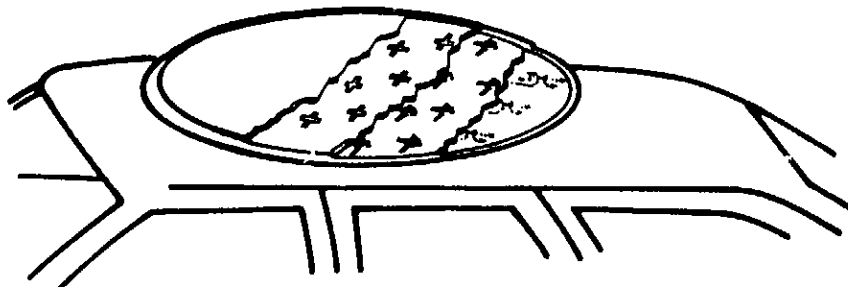
<sup>1</sup>"CONCEPT AND COST TRADE-OFFS FOR LAND VEHICLE ANTENNAS IN SATELLITE MOBILE COMMUNICATIONS." Final Report F84-10, Ball Aerospace Systems Division, July 1984.



Mechanically Steered 1 x 4 Tilted Microstrip Array



Mechanically Steered Fixed-Beam Conformal Array



Electronically Steered Conformal Array

Figure 1-1. The three LMV Concepts Shown Configured atop a Car Roof



Table 1-1  
SUMMARY OF ANTENNA CONCEPT PERFORMANCE

	1 x 4 Tilted	Conformal Mech.	Phased Array
Transmit Frequency 821-825 MHz	YES	YES	YES
Receive Frequency 866-870 MHz	YES	YES	YES
CONUS Gain (dB) (Minimum)	11	9	10
# Elev. Positions - CONUS	1	1	2
VSWR ( $\leq 2:1$ )	YES	YES	YES
HPBW - Azimuth (Degrees)	18	26	26
HPBW - Elevation (Degrees)	65	50	26
Axial Ratio - CONUS (dB)	4	9	9
Pattern Roll Off - from 70° to Horizon	5	6	6
Size - Base Diameter (Inches)	36	36	36
Size - Height (Inches)	7.5	3.5	2
Peak Power (100W)	YES	YES	YES
Average Power (5W)	YES	YES	YES



## SECTION 2.0

### LAND MOBILE VEHICLE ANTENNAS

#### 2.1 MECHANICALLY STEERED ANTENNA ARRAYS

Since submitting our first report, we have made a significant improvement to the mechanically steered antenna systems which has substantially relieved the requirements on the pointing system. Simply stated, we've rediscovered the basic law of physics that a body at rest tends to stay at rest. If the antenna steering mechanism is designed such that it acts like a "pivot-point," then, as the host vehicle turns corners and in general changes its orientation, the inertia in the antenna will tend to keep it pointed in the same direction. The only pointing errors are those caused by friction which tend to make the antenna follow the motion of the host vehicle.

This is the same basic concept used to point antennas on dual spin communication spacecraft and its benefits are obvious. First of all, the reaction time of the pointing system can be substantially reduced. The pointing system no longer has to try to maintain lock during  $45^\circ/\text{second}$  turns. Instead, the pointing system only needs to compensate for the slow varying drifts caused by friction (roughly  $5^\circ/\text{second}$ ). This means the problems of high speeds, high torques and over-shooting the target when making a correction are all but eliminated. Finally, this approach adds a measure of open-loop tracking allowing rapid reacquisition after short drop-outs in the signal. In the following, we will describe the details of how this new steering mechanism works.

#### Steering Mechanism Concept Description

The steering mechanism has essentially two modes of operation, i.e., an acquisition mode and a tracking mode. In the acquisition mode, the antenna is rotated at a constant rate until a signal, indicating a near target condition, is received from the AGC. At this time the velocity is rapidly reduced, and the system switches to the tracking mode. The reader is referred to Section 3 for a complete description of the acquisition and tracking methods.

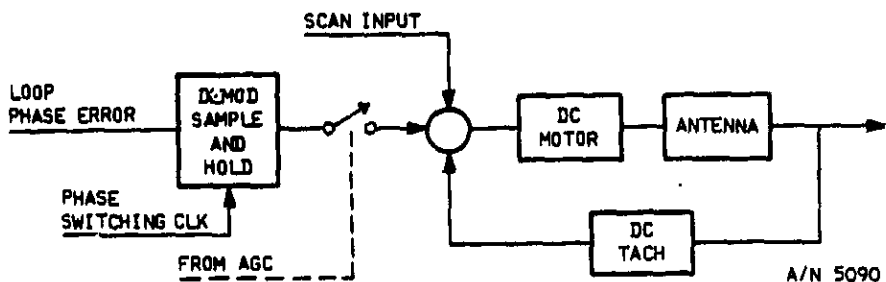


We will restate the requirements so they will be handy for the reader. When the system is tracking, the tracking error will be held to  $1^\circ$  or less. This will keep the antenna gain high and the phase shift in the received signal low. When the vehicle, on which the antenna is mounted, is turning rapidly at  $45^\circ/\text{second}$ , the pointing error will increase. But we still expect to point to within about  $5^\circ$  or boresite. The increase in error during turn is a direct result of the requirement that the tracking error can only be updated at a 10 Hz rate.

The acquisition mode has two aspects: initial acquisition and reacquisition. Initial acquisition starts by rotating the antenna at a constant rate in one direction. When a signal is obtained from the receiver, indicating a near target condition, the system goes into the tracking mode. Should the signal strength drop below the threshold for more than 4 seconds when the system is in the tracking mode, reacquisition will be initiated. Here a small raster scan will be used so that reacquisition time will be short.

There is one major constraint related to the steering system, which is due to the 10 Hz limit on signal modulation. This means the tracking error signal can only be updated at a 10 Hz rate. Thus we have a sampled-data servo system, which is sampled at the above rate. We prefer not to develop a full blown sampled-data servo with its attendant complexity and cost. We can avoid this by limiting the bandwidth of the tracking loop to less than one hertz, which is what we propose to do.

The functional block diagram, shown below, gives the configuration.

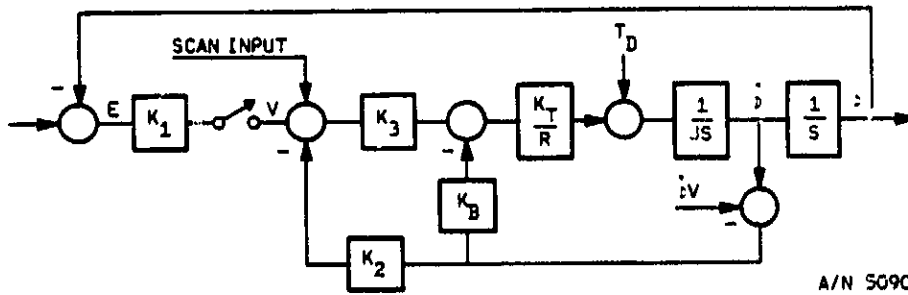


The system is comprised of a velocity control servo with either a tracking error or a search input. The electro-mechanical part of the system is quite simple; it consists of:



- the antenna
- a DC motor
- a DC tachometer
- a two channel coaxial rotary joint
- and a pair of bearings

All these components rotate around a common axis, without gears, belts or cables. The motor and tachometer have center holes which will accommodate the rotary joint. Figure 2-1 shows a cut-away view of the drive assembly and Figures 2-2 and 2-3 show conceptual concepts of how the antenna could be attached. The system can be described by the servo block diagram given below.



where:

- $K_1, K_2, K_3$  = Gains to Be Chosen
- $K_B$  = Motor Back EMF Constant
- $K_T$  = Motor Torque Constant
- $R$  = Motor Resistance
- $J$  = Assembly Moment of Inertia
- $\phi$  = Antenna Position
- $\phi_v$  = Vehicle Position
- $T_D$  = Friction
- $E$  = Tracking Error

### Parameters Definition

To get started we need to choose a reasonable motor and tachometer. Inland Motors shows the following information.

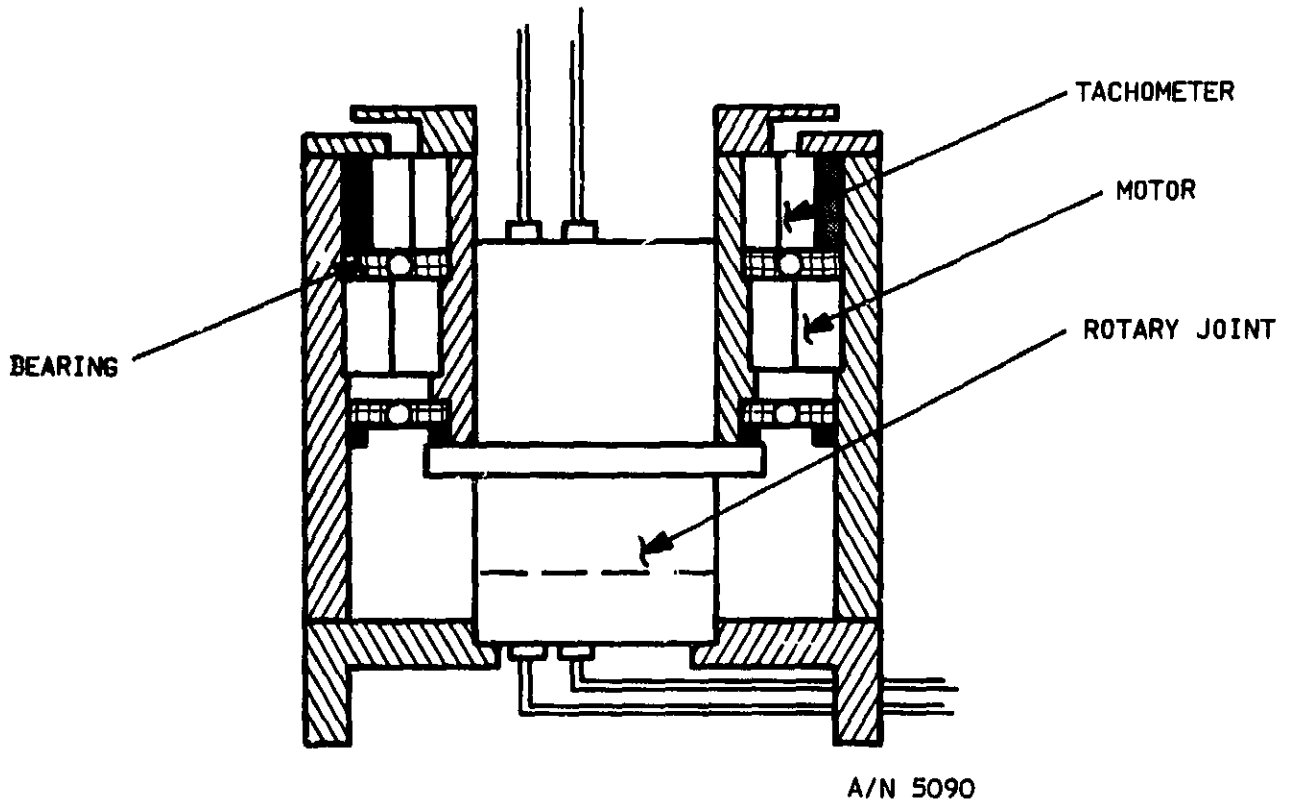
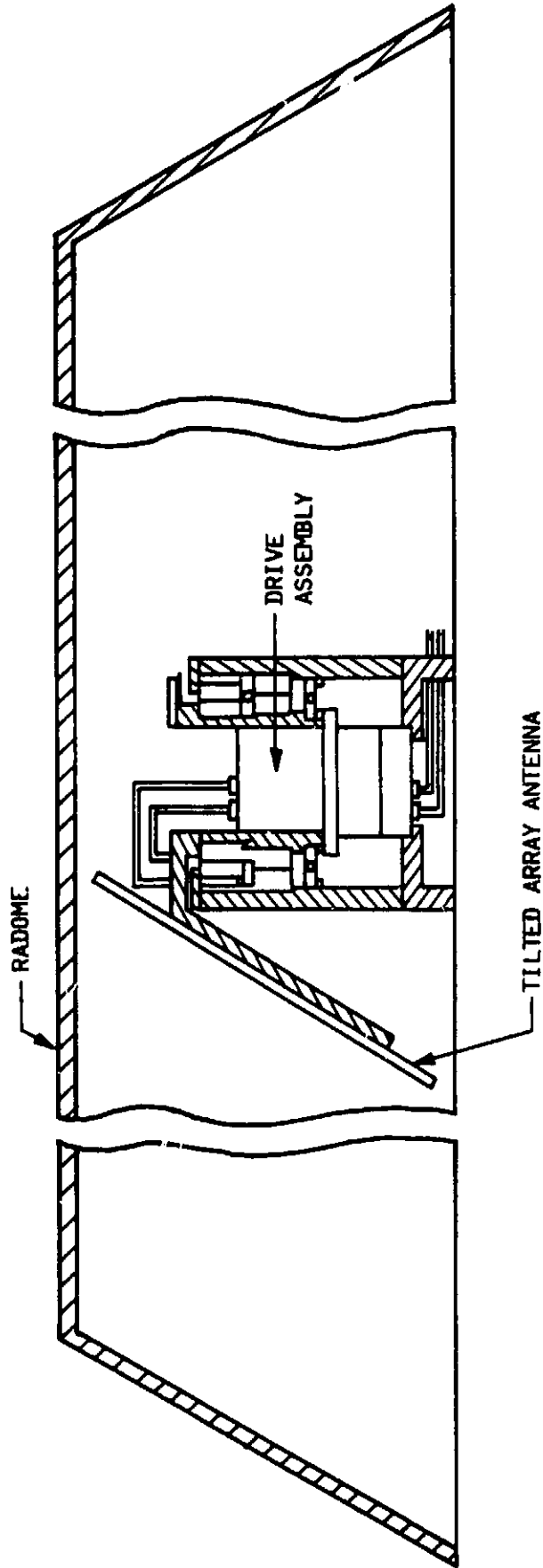
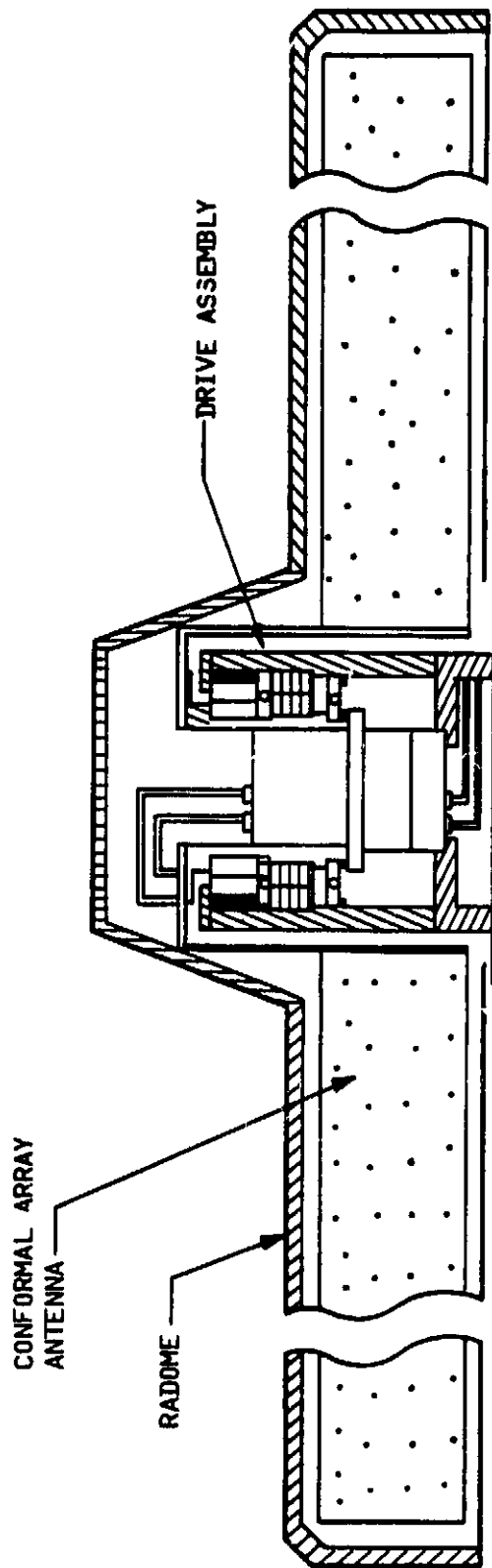


Figure 2-1 Cut-Away View of Antenna Drive Assembly



A/N 5090

Figure 2-2 Concept 1 - Antenna with Drive Assembly



A/N 5090

Figure 2-3 Concept 2 - Antenna and Drive Assembly



Motor T-3912            R = 3.2 Ohms  
                               $K_T = 0.46 \text{ lb-ft/amp}$   
                               $K_B = 0.36 \text{ V/rad/sec}$   
                              Friction = .05 lb-ft  
                              ID = 2.937 in.  
                              OD = 4.562 in.  
                              Weight = 1.5 lbs.

Tachometer TG-4413     $K_G = 8.58 \text{ Volts/rad/sec}$   
                              Friction = 0.04 lb-ft.  
                              ID = 3.5 in.  
                              OD = 5.12 in.  
                              Weight = 2.2 lbs.

To complete the drive mechanism we need parameters for the rotary joint and bearings.

Rotary Joint            Friction = 0.02 lb-ft.  
                              Weight = 2.2 lbs.

Bearings                Friction = 0.03 lb-ft.

The total friction  $T_D = 0.14 \text{ lb-ft.}$

The weight of the antenna should be around 12 pounds so the total should be around

Weight = 20 lbs.

excluding the radome.

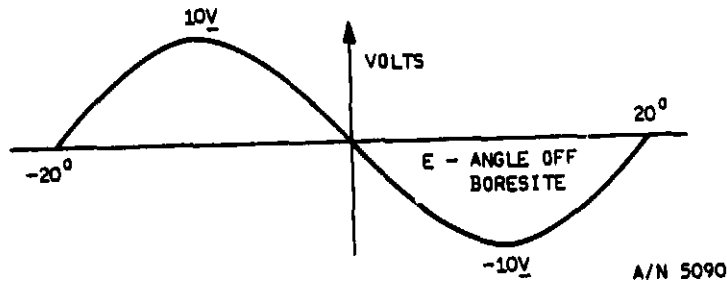
The moment of inertia of the rotating assembly is estimated to be

$J = 0.6 \text{ slug-ft}^2$



Now we have all the essential parameters except for the gain on the tracking error channel.

The tracking error is a sinusoidal function.



In the linear region the gain is

$$K = 96 \text{ volts/rad}$$

### Analysis

Now we need to choose reasonable values for the parameters  $K_1$ ,  $K_2$ , and  $K_3$ . Because we wish to keep the error due to friction disturbance torques to 1.0 degree or less we have the following relationship.

$$K_1 K_3 > \frac{R}{K_T} \frac{T_D}{E}$$

Thus 
$$K_1 K_3 > \frac{3.2}{.46} \frac{0.14}{.01745}$$

$$K_1 K_3 > 55.8$$

To get reasonable damping the bandwidth of velocity servo needs to be around 4.0 rad/sec. This means that



$$K_2K_3 = 4 \frac{RJ}{K_T} - KB$$

$$K_2K_3 = 16.3$$

When the vehicle is turning at 25°/sec we want to keep the error to 3°.

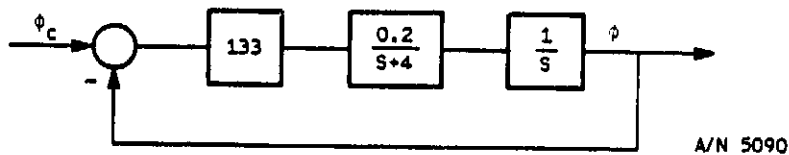
$$\dot{\phi}_v \left[ K_2K_3 + \frac{K_B}{K_3} \right] = EK_1$$

so 
$$K_1 = 136 - \frac{3}{K_3}$$

Let 
$$K_1K_3 = 111.6$$

Thus 
$$\begin{aligned} K_3 &= 0.84 \\ K_2 &= 19.4 \\ K_1 &= 133 \end{aligned}$$

Using these numbers we get the diagram below.



The closed loop transfer function is

$$\frac{\phi}{\phi_c} = \frac{26.6}{s^2 + 4s + 26.6}$$



The bandwidth is

$$W = 4.75 \text{ rad/sec}$$

and the damping factor is  $\zeta = 0.4$

This damping is reasonable and the frequency ( $f = .76 \text{ Hz}$ ) is less than  $1.0 \text{ Hz}$  as desired.

Note that

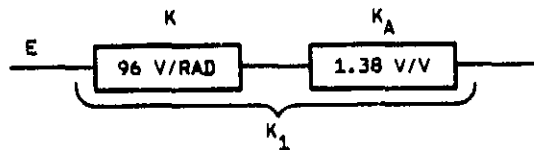
$$K_1 = KK_A$$

where

$K = \text{Tracking Signal Gain}$

$K_A = \text{Amplifier}$

So



Also

$$K_2 = K_{\delta}^* K_a$$

where

$K_{\delta}^* = \text{Tach Gain}$

$K_a = \text{Amplifier}$



50



## Conclusions

The steering servo system is simple and straightforward. It will point to within about  $0.5^\circ$  most of the time while tracking. In the worst case, while the vehicle is cornering rapidly, the error will be around  $3^\circ$  for a few seconds. The servo can tolerate the low sampling rate of 10 Hz in the error channel. Target acquisition will not be a problem.

### 2.1.1 1 x 4 Tilted Microstrip Array

The mechanically steered 1 x 4 tilted array is an excellent choice for meeting the required specifications. The elevation coverage is nearly optimal for CONUS operation. The gain is achieved by effective use of the aperture in the azimuth direction which also achieves an excellent axial ratio. The design features a simple antenna and a low loss feed network.

The tilted panel contains the following components: antenna elements, polarization hybrid, and power divider. The microstrip patch antenna is constructed on a honeycomb substrate for low cost and weight while maintaining near optimal elevation pattern coverage. In addition, this substrate yields low dielectric losses and wider antenna bandwidth.

A major benefit of this type of antenna is the excellent beam shape for achieving isolation between desired and undesired satellites. Plus, the cost of the mechanically steered tilted array is the lowest of all concepts studied. The only real disadvantage is the 7.5" vertical dimension resulting in a non-conformal configuration. An antenna width of 10.5 inches, when tilted at 35 degrees, will have a vertical height of 6 inches. Clearances above and below the mechanically rotated antenna, together with radome thickness, will increase the overall height to 7.5 inches.



## 2.1.1.1 Experimental and Analytical Evaluation of Antenna Performance

### Single microstrip patch development

Initially, only single patches were designed and tested. The substrate thickness was varied from 3/8" to 3/4" to determine effects on patch bandwidth. It was confirmed experimentally that a 3/8" substrate yields a bandwidth of 9 percent. The antenna feed evolved from a single pin feed, which required a matching network to cancel pin inductance, to a 3/8" piece of semi-rigid coaxial cable inserted into the honeycomb substrate.

A single square patch constructed on a honeycomb substrate can achieve a gain of approximately 9 dB. This gain corresponds to an aperture area of 11 by 11 inches. Due to the overlap between the effective apertures in an array environment, the directivity for the 1 x 4 array is expected to be lower than 4 separate patches with each having 9 dB of gain. As we will see later, the directivity of the 1 x 4 array is lower than 14.0 dB.

A 3 dB polarization hybrid was developed on 1/8" honeycomb and at 845.5 MHz performed as follows: .1 dB power split imbalance, 2.1 degree phase error, and a measured efficiency of 98.5%.

Similarly, a four-way microstrip power divider was constructed on an 1/8" honeycomb. The measured efficiency at 845.5 MHz is 95.7%.

### Microstrip Array Development

Figure 2-4 shows the complete front and rear views of the full scale 1 x 4 antenna array. A spherical radiation pattern was performed on this antenna using a computer-controlled anechoic chamber. This system measures and records radiated amplitudes at user selected locations. For the LMV 1 x 4 array Radiation Distribution Plots (RDP's), data points were taken at every 2 x 3 degree matrix position: 91 scans (1 to 91) in theta by 181 data points (1 to 181) in phi. This corresponds to 16,200 data points which are recorded on magnetic tape and transferred to the VAX computer for analysis: contour

ORIGINAL PAGE IS  
OF POOR QUALITY

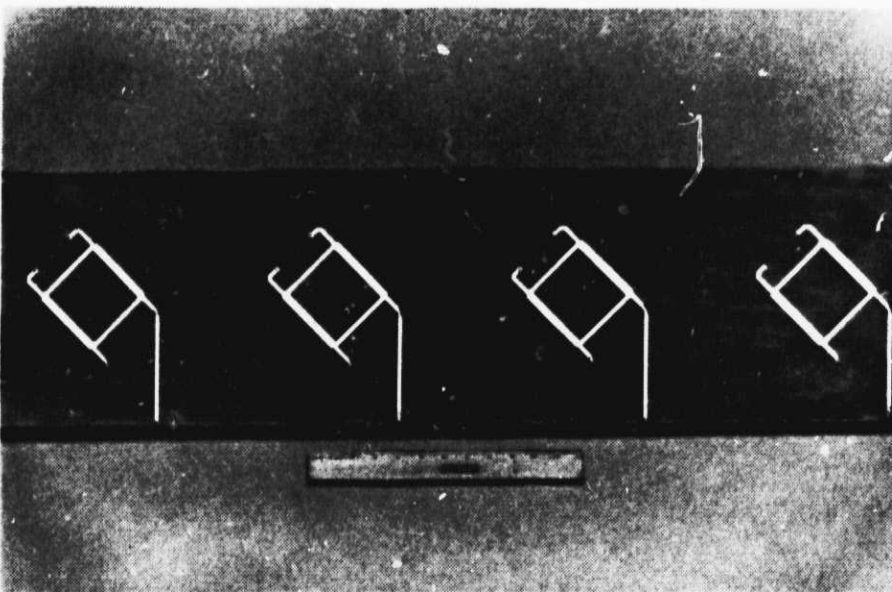
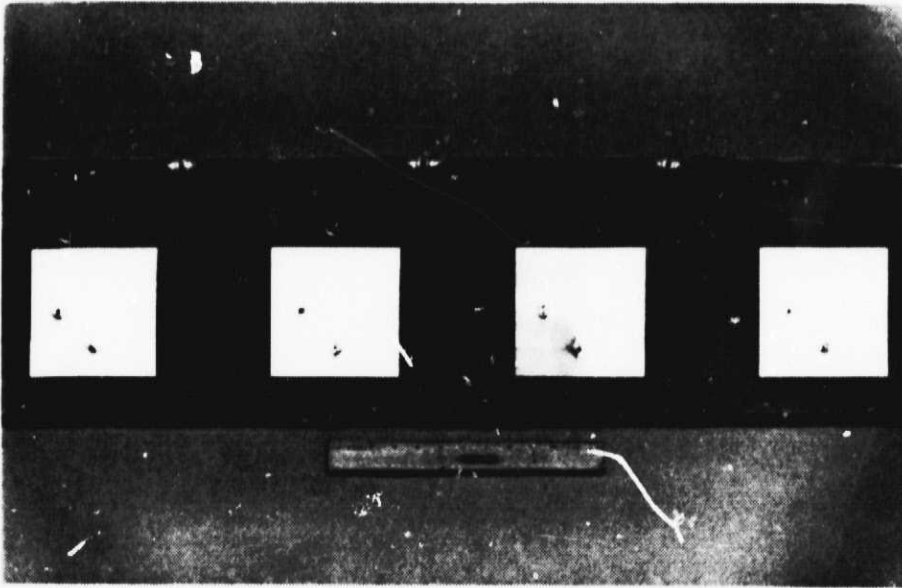


Figure 2-4. 1x4 Antenna Array Showing the Front Radiating Patches and the Rear Quadrature Hybrids



selection, pattern rotation, directivity calculation and output plotting routines.

Two RDP's (Radiation Distribution Plots) were performed: the first with a uniformly illuminated aperture tilted 35 degrees over a finite ground plane (simulating actual installation), the second with a tapered array having .707 amplitude (i.e., .5 power split) on the outer two elements. Both RDP's were measured with a circularly polarized source horn. Antenna performance is therefore referenced to this right-hand circularly polarized source (RHCP).

#### Uniformly Illuminated Array

The uniformly illuminated array utilized a microstrip power divider feeding four (4) quadrature hybrids in phase. These hybrids, in turn, individually feed one patch at two orthogonal points, 0 and 90 degrees, in order to develop RHCP.

Test data from the uniformly illuminated array indicates a close correspondence to the computer-predicted performance. Azimuth and elevation patterns were taken with the array flat as well as tilted at 35 degrees. When tilted, the antenna performance did exhibit some changes. These are an increase in the axial ratio of the main lobe from 1 to 3 dB and minor increase in sidelobe levels and axial ratio. However, note that overall performance, as evidenced by gain and adjacent satellite isolation data, generally remains unaffected.

Single azimuth cuts were performed with a rotating linearly polarized source to generate spinning linear patterns. Polarization loss is observed by a level drop in the sidelobes relative to the optimum computer model. This condition, although valuable for isolation with similarly polarized satellites, will reduce the isolation of an opposite polarization sense satellite located at or near a sidelobe.

Azimuth and elevation cuts for the flat array can be seen in Figures 2-5 and 2-6, respectively. Their corresponding spinning linear plots can be seen as



QUALITY OF POOR QUALITY

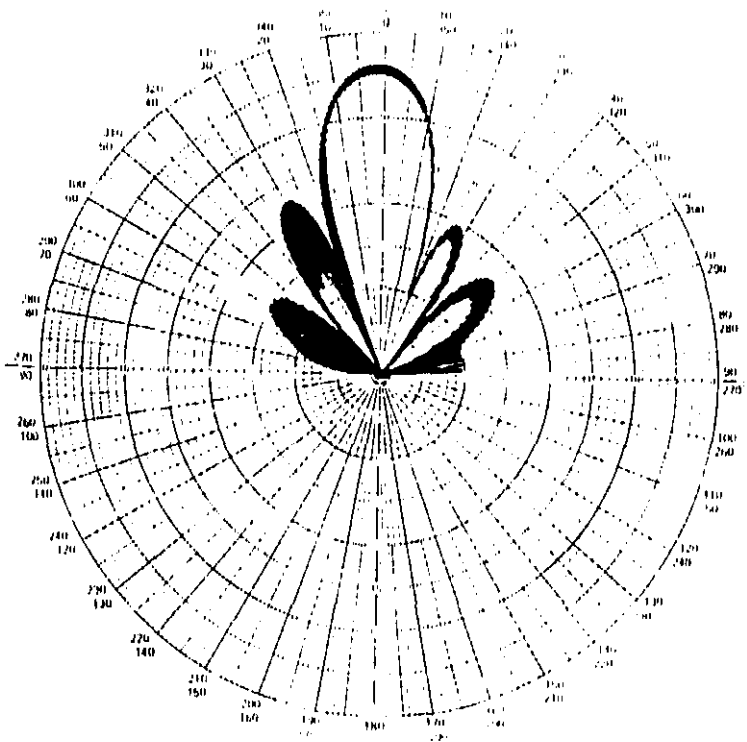
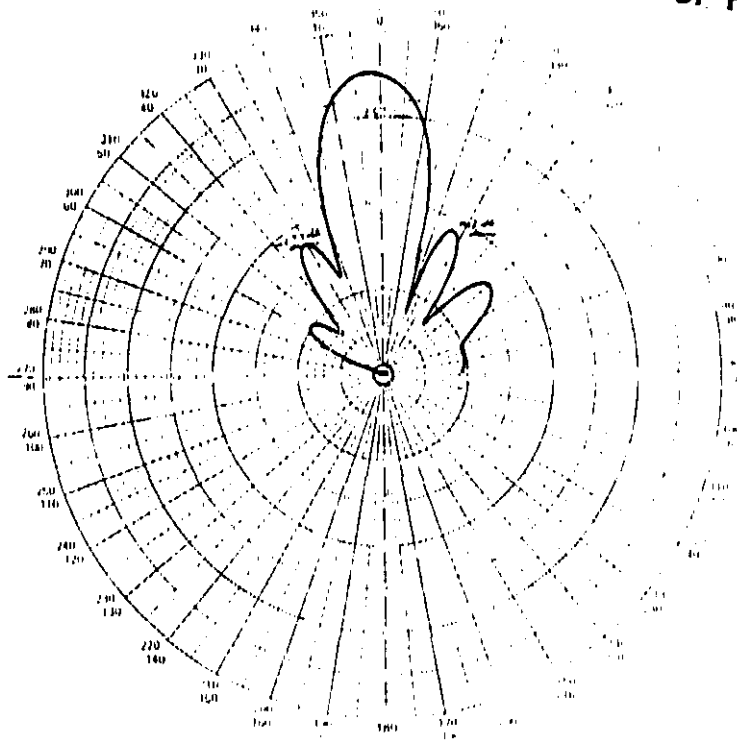


Figure 2-5. Narrow Beam Pattern of the 1x4 Array, Fiat on Finite Ground Plane,  $f=.845$  GHz

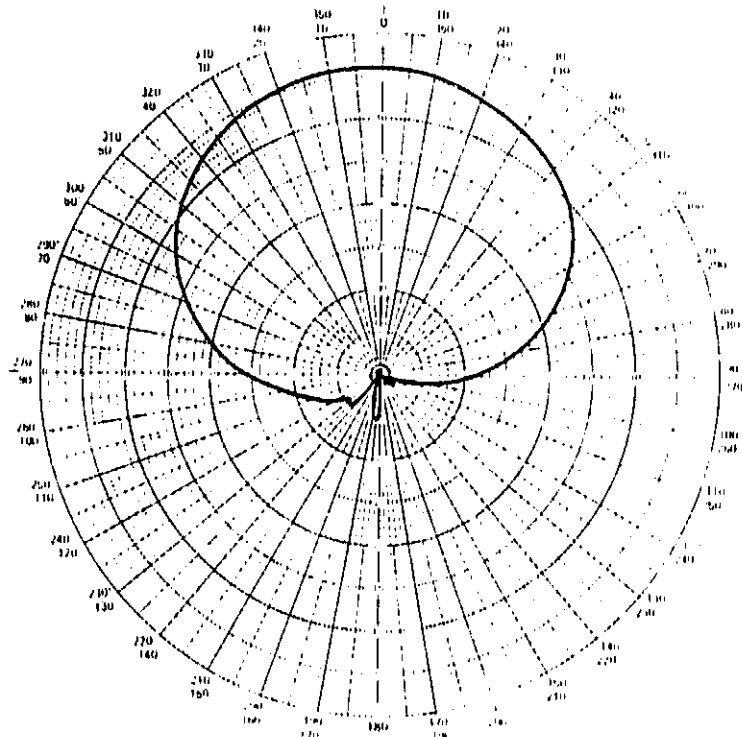


Figure 2-6

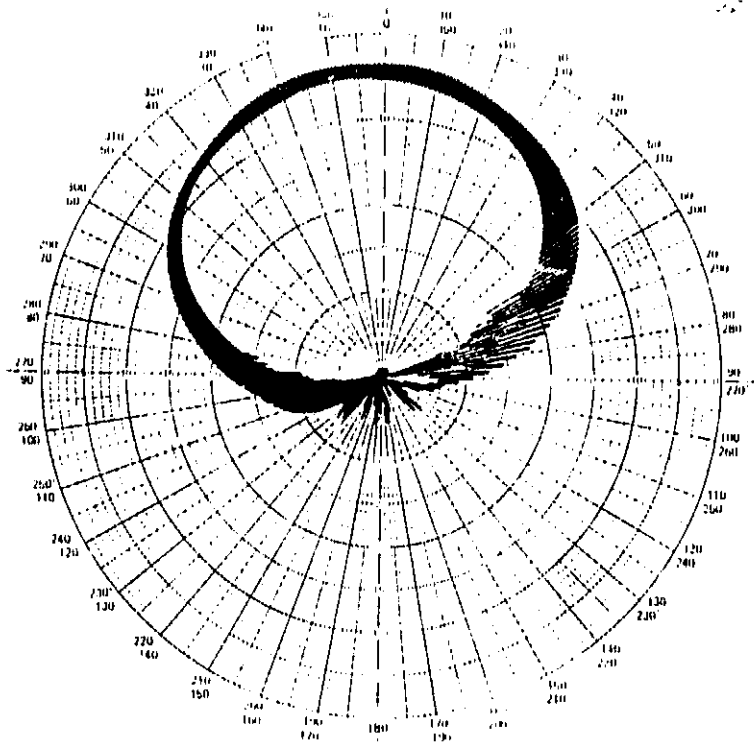


Figure 2-6. Wide Beam Pattern of the 1x4 Array, Flat on Finite Ground Plane,  $f=0.845$  GHz



well. Note that the spinning linears more accurately reflect antenna performance since the source horn is rotating. Elevation cuts for the tilted array on a finite ground plane can be seen in Figure 2-7.

The antenna input impedance Smith chart can be seen in Figure 2-8. The antenna is matched better than 1.5:1 VSWR.

Table 2-1 shows the directivity, system losses, and antenna gain. These results agree very well with measured data. The measured beamwidths in azimuth and elevation and the elevation pattern rolloff (from 70° to horizon) are shown in Table 2-2.

### Tapered Amplitude Array

Tradeoffs exist in choosing the taper level to be used. The use of amplitude tapering causes a decrease in gain; therefore, only the minimum taper level should be used to reduce the sidelobes. In addition, beam broadening occurs which can cause undesirable satellite positions to end up on the skirts of the main beam. For undesired satellite locations in the sidelobe region, amplitude tapering can be employed, but the level of tapering should be only that required to achieve the proper isolation.

The second breadboard is a 1 x 4 array with the following amplitude taper: .707, 1.0, 1.0, .707. The primary purpose of this array was to further investigate improving multiple-satellite isolation without significantly affecting the beamwidth or reducing overall gain. As in the first antenna, the tapered array used coaxial feeds from hybrid-to-patch, but differed by using an external power splitter to develop the taper. The matched coaxial power divider was quickly assembled and tested. The input arm is split three ways, two of which are fed to the center two patches, and the third arm is split equally to feed the outer two elements. Therefore, what is needed is a 3-way power divider at the input port and a 2-way power divider for the outer elements.

Test data for the tapered array depicts a slight overall reduction in directivity (.4 dB) and beamwidth changes of a degree or less. Figure 2-9 shows a typical pattern at  $f = 840$  MHz. Figure 2-10 shows the input impedance on a Smith chart.

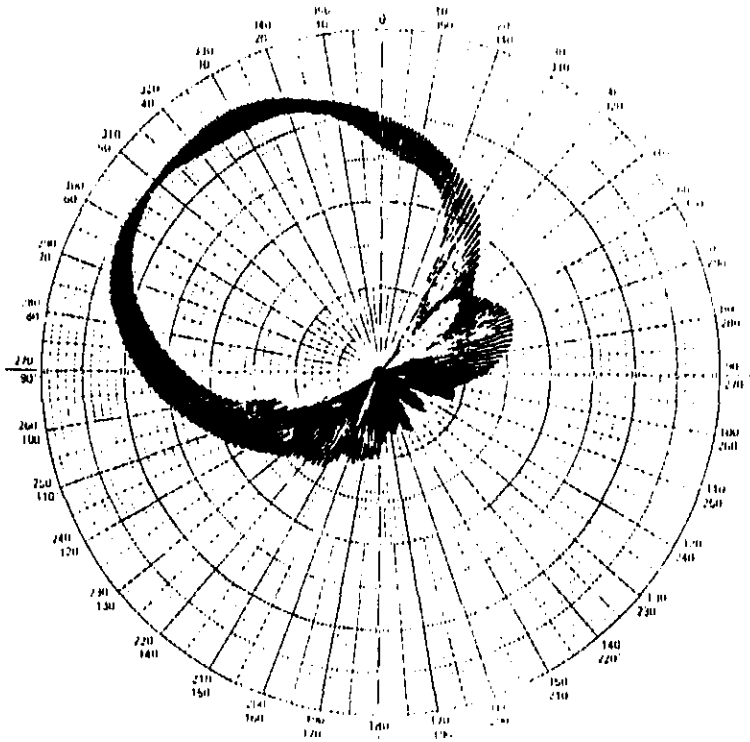
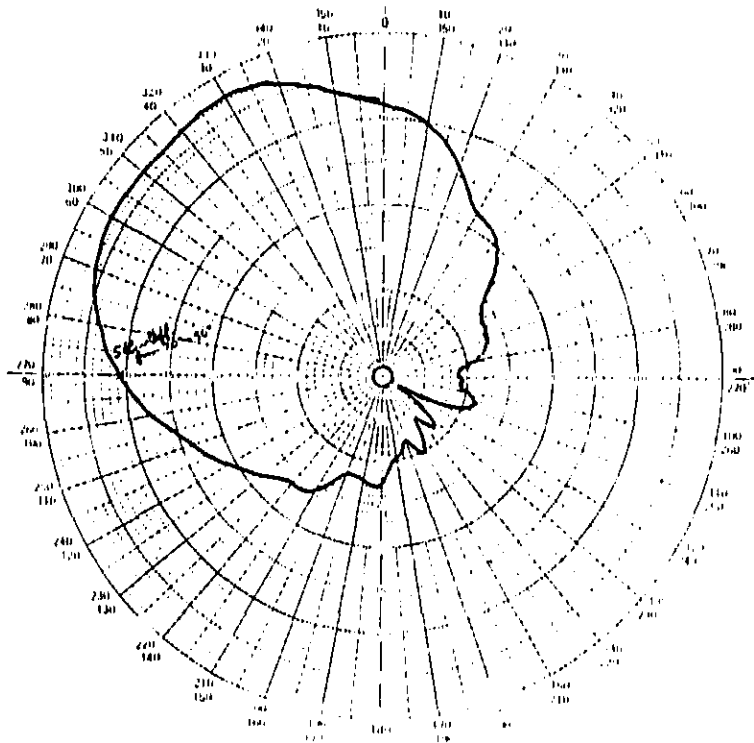


Figure 2-7. Elevation Pattern Cut of the 1x4 Array Tilted 35 Degrees Over Finite Ground Plane,  $f=.845$  GHz

ORIGINAL PAGE IS  
OF POOR QUALITY

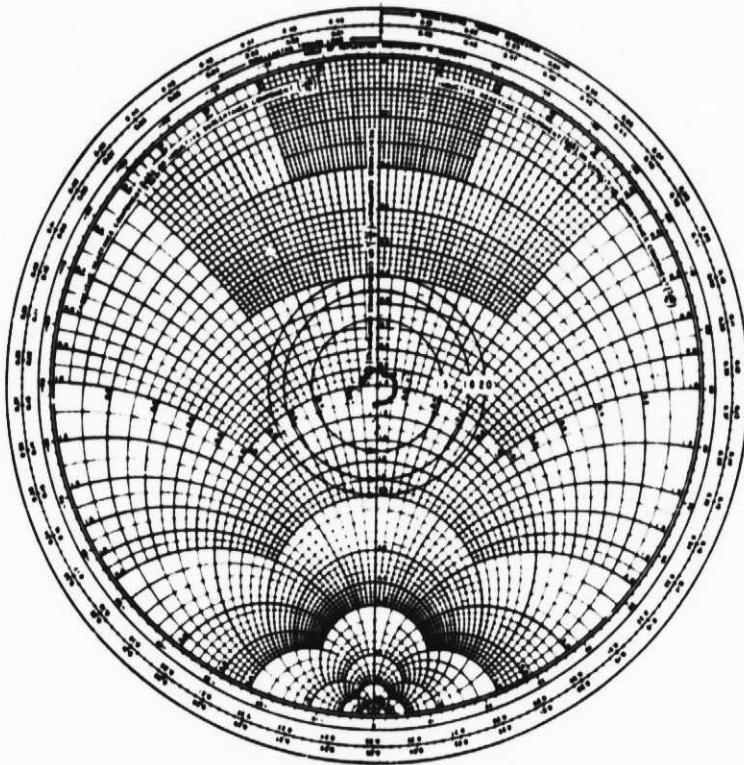


Figure 2-8. Impedance Plot of Uniformly Illuminated 1x4 Array:  
Power Divider, Hybrids, and Patches.  $f=.820-.870$  GHz



Table 2-1

GAIN OF A UNIFORMLY FED 1 x 4 ARRAY

	<u>dB</u>
Measured Directivity (Computer Predicted = 13.8 dB)	13.8
Microstrip Radiating Element	-.1
Hybrid	-.1
Power Divider	-.2
Axial Ratio	-.25
2:1 Mismatch at Input	<u>-.5</u>
Peak Gain	12.7
Worse Pattern Rolloff (30° to 70° from Broadside)	-1.0
Gain over Full Coverage Region	<u>11.7</u>

Table 2-2

BEAMWIDTHS AND PATTERN ROLLOFF  
FOR A UNIFORMLY FED 1 x 4 ARRAY

Azimuth Beamwidth	18 degrees
Elevation Beamwidth	66 degrees
Elevation Rolloff	5 dB (from 70 degrees to horizon)

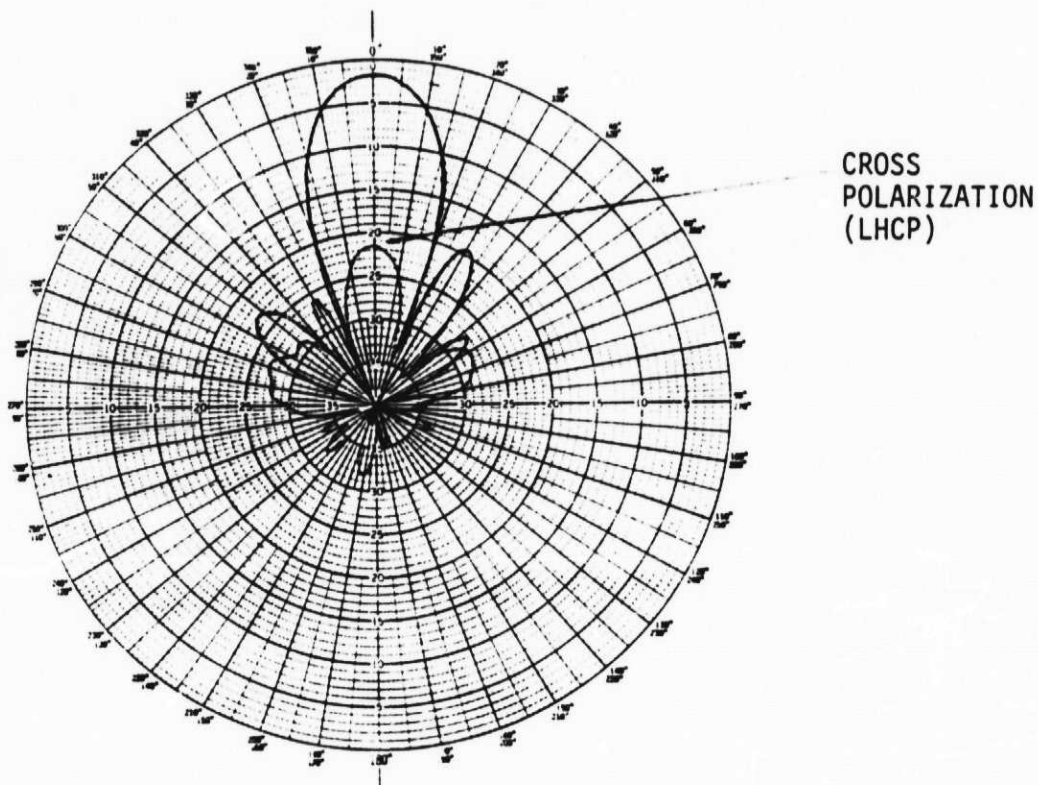


Figure 2-9. Narrow-Beam Pattern of Tapered 1x4 Array with Cross-Polarization Pattern,  $f = .840$  GHz

ORIGINAL PAGE IS  
OF POOR QUALITY

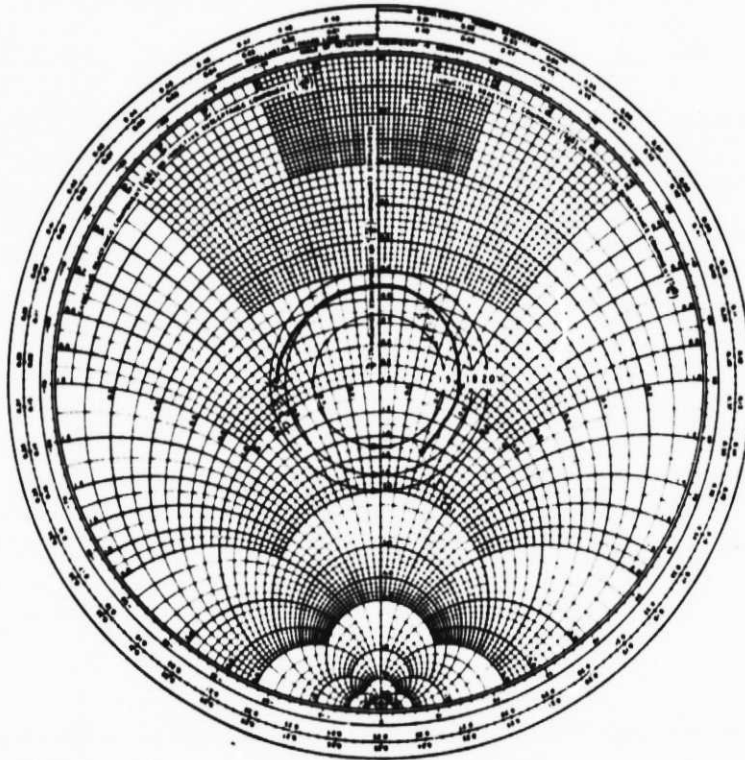


Figure 2-10. Impedance Plot of Tapered 1x4 Array: Power Divider, Hybrids, and Patches.  $F = .820 - .870$  GHz



In Table 2-3 we show the directivity, system losses, and antenna gain. Note that these results exemplify a worst-case condition in terms of rolloff and VSWR. Table 2-4 shows the measured beamwidths and pattern rolloffs (from  $70^\circ$  to horizon).

### 2.1.2 Reduction of Low-Angle Radiation

Corrugated surfaces will support a longitudinal electric field. When the direction of free-space propagation is normal to the corrugation alignment, energy is coupled and a TM propagating mode exists. For the TM mode to be supported, the height "d" of the corrugations must be  $0 < d < \lambda/4$  or  $\lambda/2 < d < 3/4\lambda$ . These fin height regions correspond to an inductive surface impedance and, in general, the following criteria must be satisfied:  $W \geq t$  and  $W + t < \lambda/5$ , where W is the fin-fin spacing and t is the fin thickness.

Corrugation models were designed and constructed for scaled C-band tests which were followed by full scale UHF corrugation tests. In each case, aluminum fins were attached to a planar piece of aluminum. Parameters such as fin height, fin separation, and number of fins were varied in order to determine the optimum configuration for maximum horizon rolloff. The best case physical criteria from the C-band studies were exactly emulated for the UHF tests (dimensions relative to wavelength).

#### C-Band Corrugation Studies

Frequency scaling was used to conduct initial corrugation tests at C-band. Model dimensions may be observed in Figures 2-11 and 2-12. As shown, only one patch was used in the center of a square corrugation region. Note that this single patch is "seeing" a large corrugation surface area. The following is a summary of the C-band corrugation results:

- Two of the corrugation depths tested,  $D = .20\lambda$  and  $.25\lambda$ , showed increases in the horizon rolloff rate ( $\Theta = 80^\circ$  to horizon) relative to a ground plane alone.



Table 2-3

GAIN OF A TAPERED 1 x 4 ARRAY

	<u>dB</u>
Measured Directivity (Computer Predicted = 13.7 dB)	13.4
Microstrip Radiating Element	-.1
Hybrid	-.1
Power Divider	-.2
Axial Ratio	-.25
2:1 Mismatch at Input	<u>-.5</u>
Peak Gain	12.3
Worse Pattern Rolloff (30° to 70° from Broadside)	-1.0
Gain over Full Coverage	<u>11.3</u>

Table 2-4

BEAMWIDTHS AND PATTERN ROLLOFF  
FOR A TAPERED 1 x 4 ARRAY

Azimuth Beamwidth	20 degrees
Elevation Beamwidth	67 degrees
Elevation Rolloff	5 dB

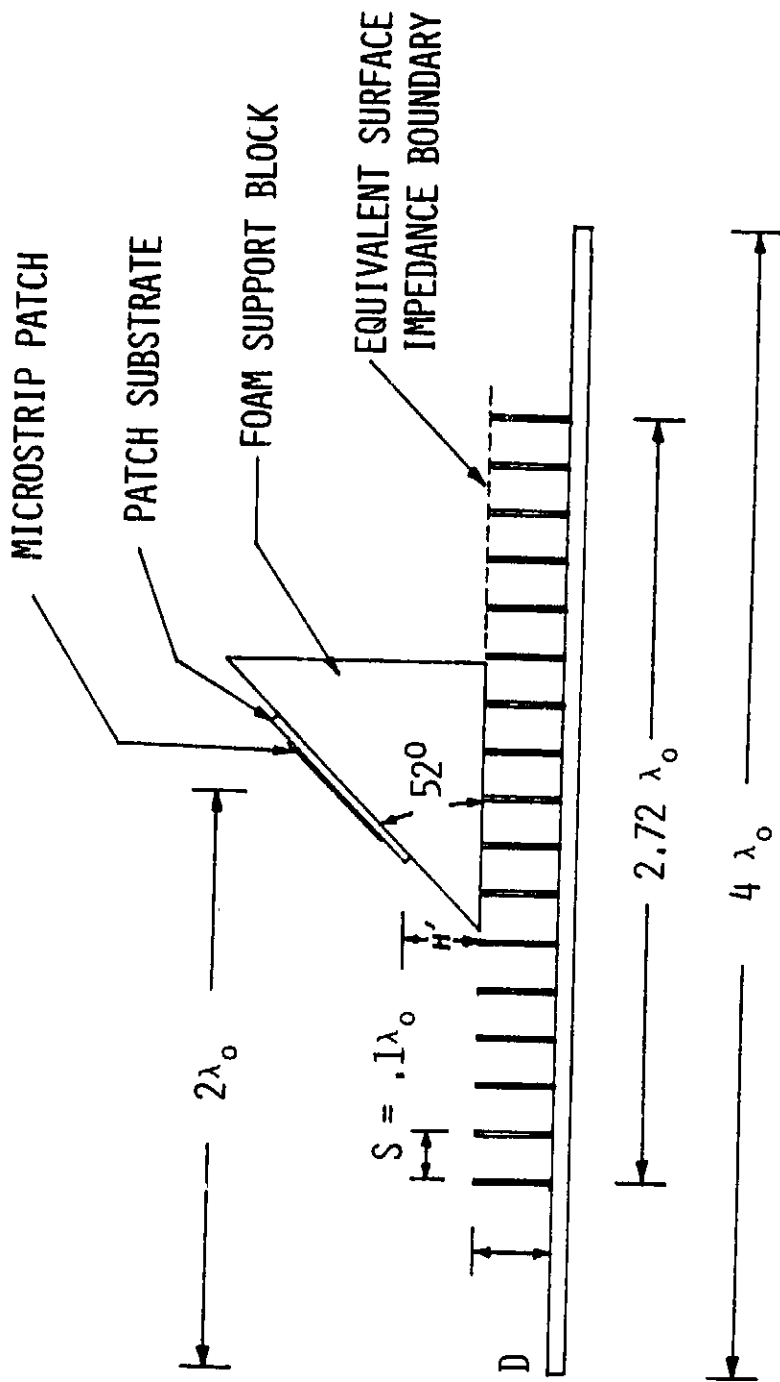
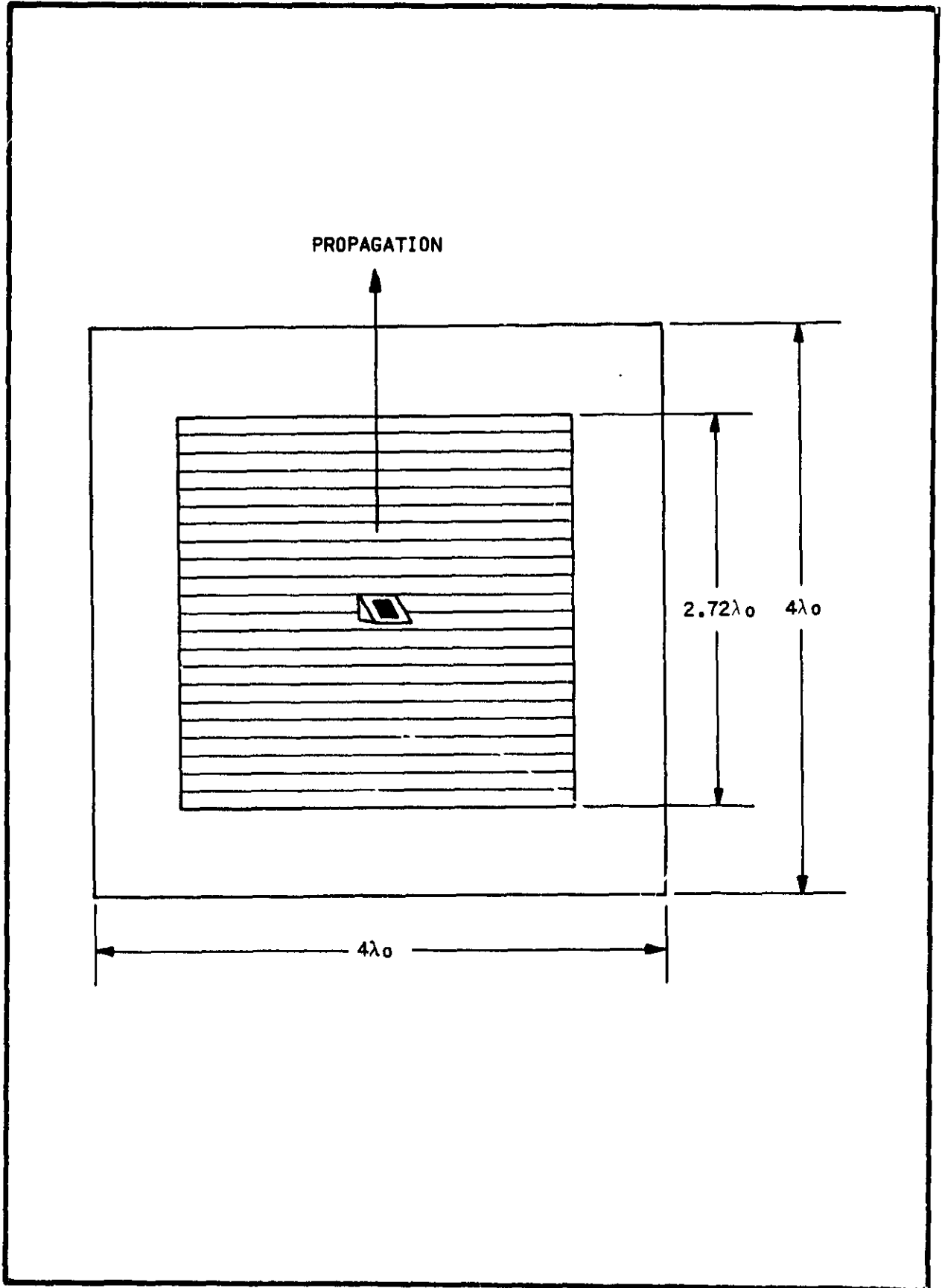


Figure 2-11. Corrugated Surface Model





C-Band Corrugation Model with Finite Ground Plane  
Figure 2-12



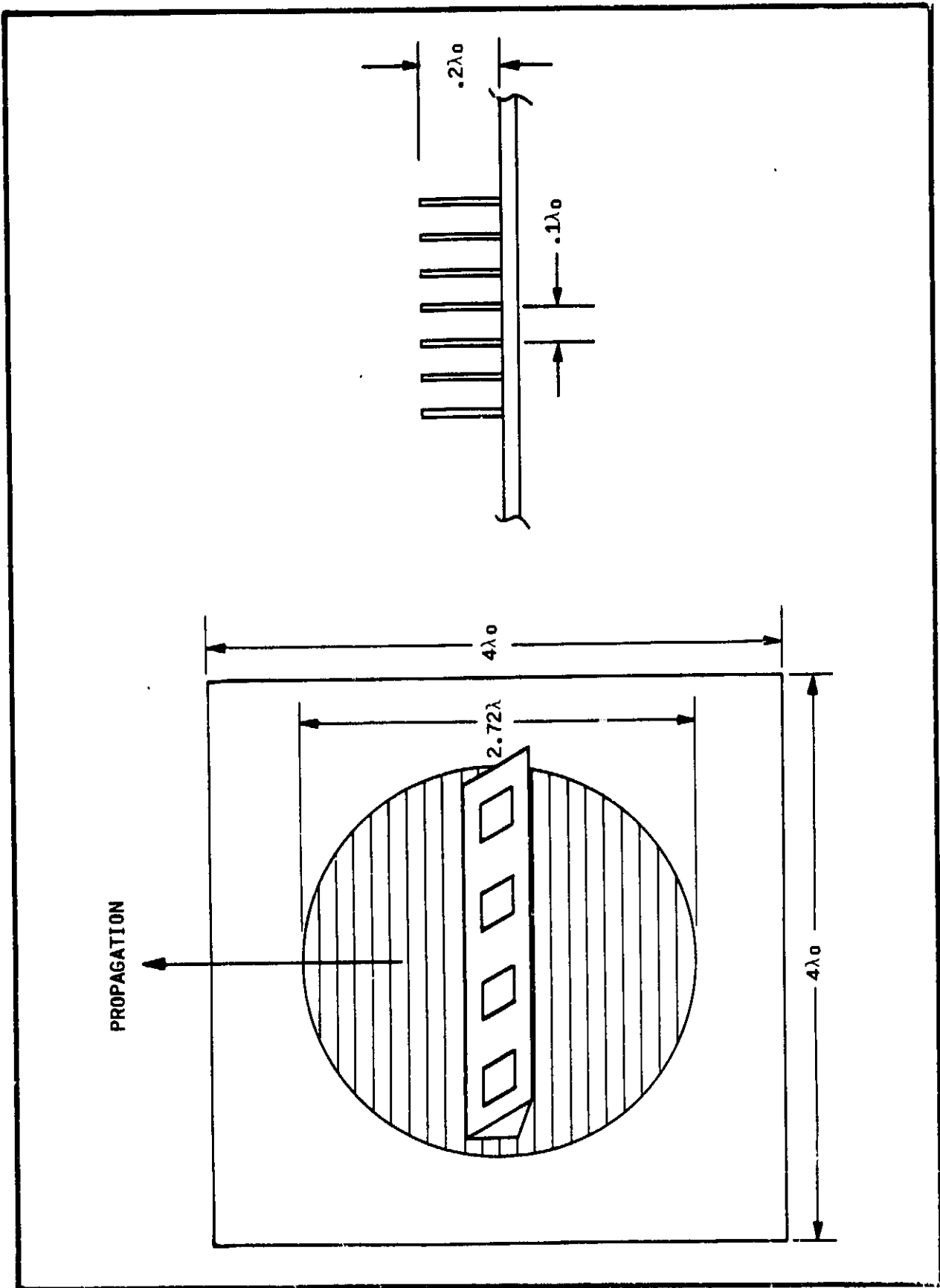
- This rate decreased rapidly with increasing patch height  $H'$  from corrugated surface.
- Best results were obtained with an edge of the patch conductor at the  $h'=0$  reference plane.
- The rolloff rate decreases with increasing fin spacing.
- The rolloffs between  $\theta=80^\circ$  to horizon (relative to the patch over a flat ground plane) are:

<u><math>D(\lambda)</math></u>	<u>Rolloff Improvement (dB)</u>
.15	no improvement
.20	4.5
.25	8.0

### UHF Corrugation Studies

Full-scale UHF tests used the same scaled dimensions as the C-band experiments. The primary difference, as seen in Figure 2-13 is the circular corrugation surface (formerly square in the C-band tests). In addition, the  $1 \times 4$  array extends to either edge of the corrugation region (formerly a single patch at the center). As a result, the  $1 \times 4$  array doesn't "see" the same effective corrugation area as the C-band patch and consequently doesn't exhibit as dramatic horizon-rolloff characteristics. In fact, best-case data indicates only a 1.5 dB improvement (6.5 dB from  $70^\circ$  to horizon).

A practical analysis of the UHF model shows that rolloff was limited because of reduced corrugation area, especially for the outer patches. Furthermore, the UHF corrugation model would have to rotate with the array to maintain the orthogonal relationship between propagation direction and corrugation alignment--not a desirable systems configuration. Unfortunately, fixed position concentric corrugations are no longer normal at the periphery to the direction of propagation and significant changes in phase velocity occur. Thus, it appears that the surface corrugation is not a viable method to increase horizon



UHF Corrugation Model with Finite Ground Plane  
Figure 2-13



rolloff for the LMV antenna (rolloff improvements are minimal and corrugation implementation increases the effective height).

### 2.1.1.3. Multiple Satellite Isolation

The most accurate method of determining the relative isolation between satellites is to compare the amplitude of the radiation pattern at the main beam when pointed at the desired satellite with the amplitude at the location of the undesired satellite (the main beam is still pointed at the desired satellite). All calculations/measurements were performed in this manner. However, in order to visualize the mechanism by which the isolation is achieved, two-dimensional contour plots were drawn so that overlays with desired/undesired satellite locations could be superimposed. These plots help to determine whether the undesired satellites lie in the sidelobe region, the main beam, or both.

In order to investigate adjacent satellite isolation, clear mylar overlays were developed and placed over computer-generated and range-measured radiation distribution plots (RDP's). In total four plots were analyzed: ideal and actual 1 x 4 array without a taper; ideal and actual 1 x 4 array with a taper. This information may be seen in Figures 2-14 to 2-17. The measured data are for antennas with a tilt angle of 35 degrees over a finite ground plane.

The contour plots show the magnitude of the radiation pattern as a function of theta and phi. Theta values are measured from antenna broadside. Therefore, if the antenna broadside corresponds to zenith, theta equal to 60 degrees is equivalent to a 30 degree elevation angle from horizon. The horizontal axis is the phi-axis (azimuth) and the vertical axis is the theta-axis (elevation). Broadside is the bottom of the vertical axis at the center of the phi-axis. By plotting the points from the bottom center of the graph to the top center, an elevation cut can be made in the main beam.

The multiple satellite isolation data for the 80° and 113° and the 105° and 135° W longitude satellites can be seen in Tables 2-5 and 2-6. For both tables, a close correspondence between predicted and measured values is observed.



ORIGINAL PAGE IS  
OF POOR QUALITY

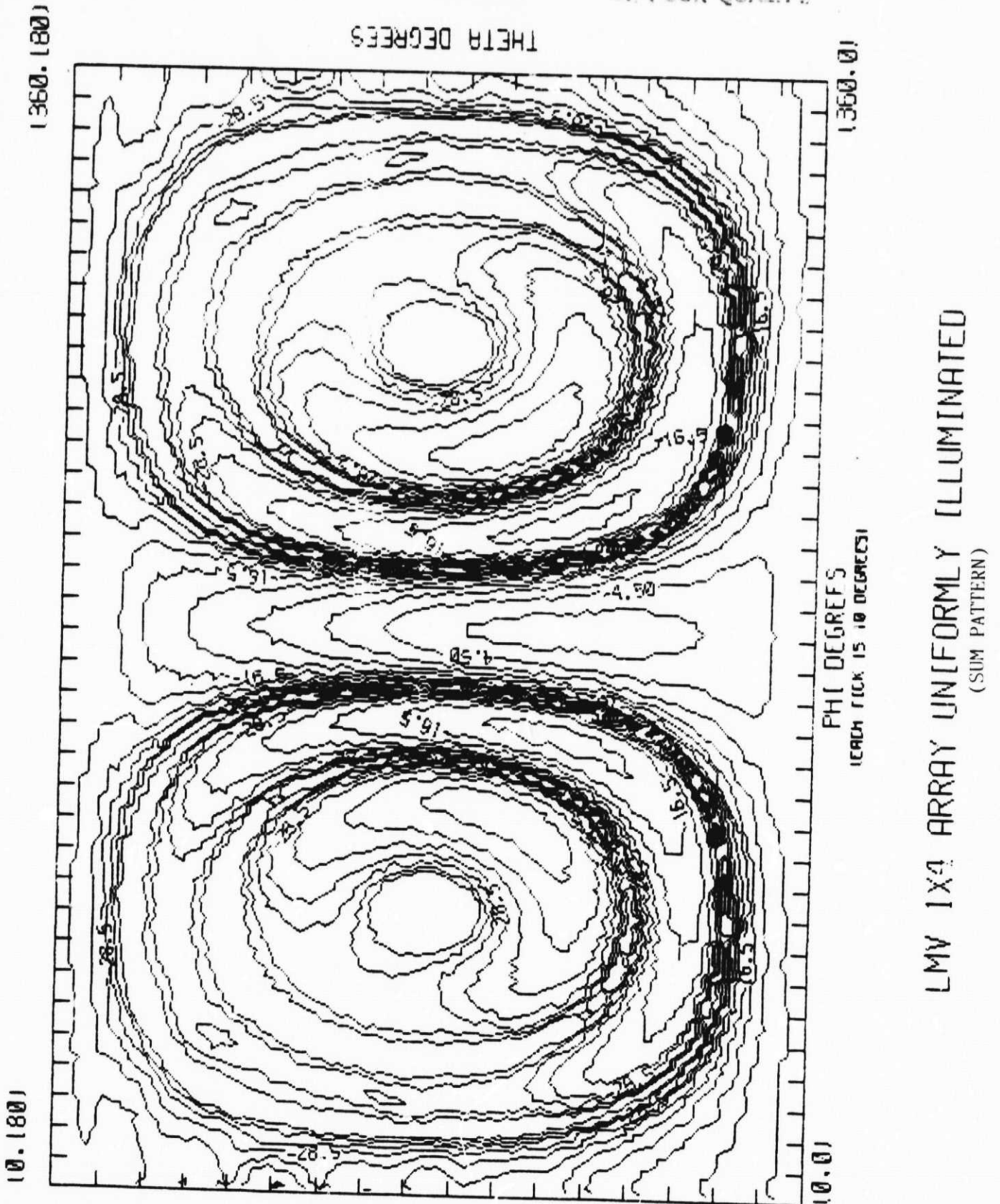


Figure 2-14. Calculated Pattern of the Uniformly Fed Tilted 1 x 4 Array



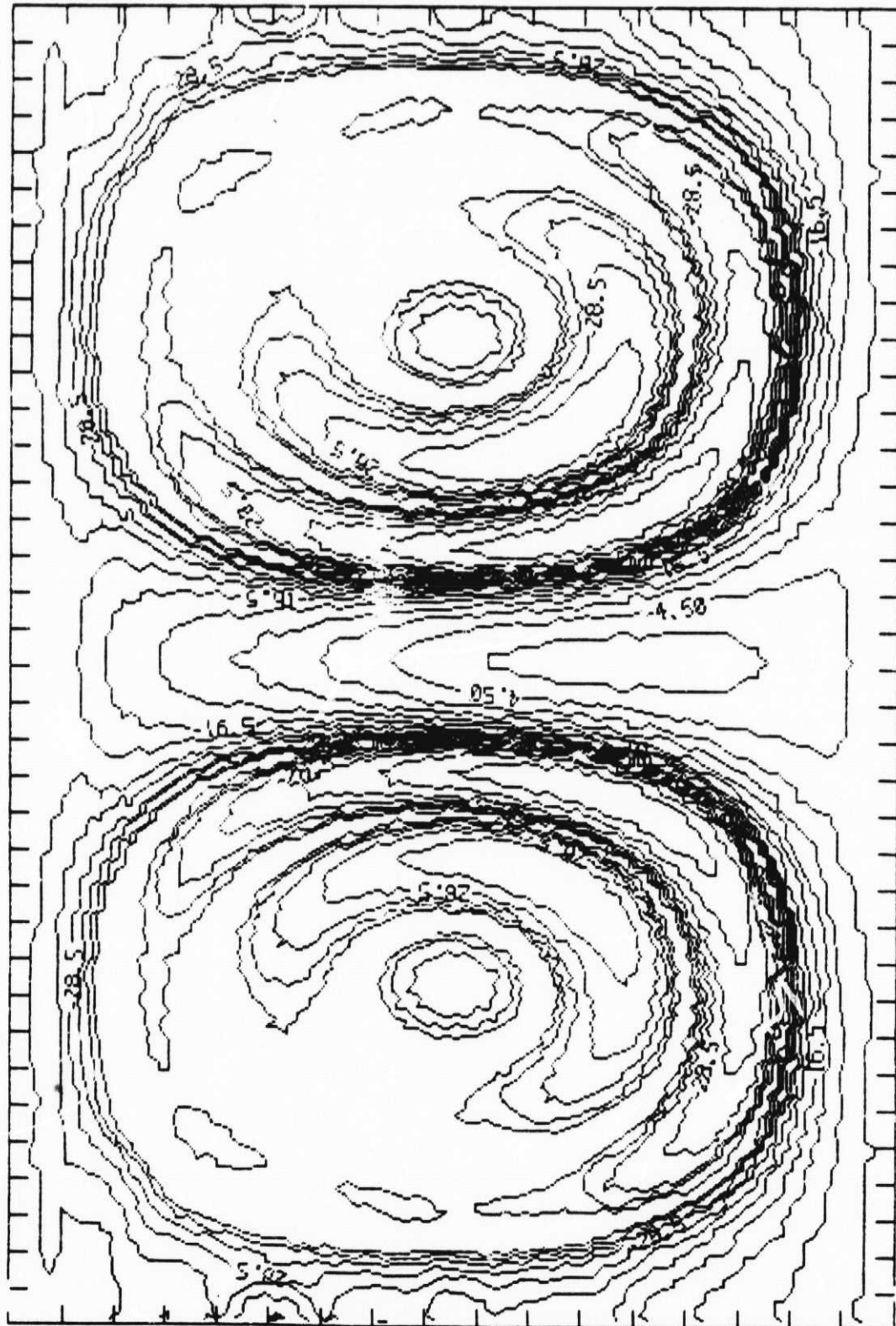


1360.180)

THETA DEGREES

1360.0)

10.180)



PHI DEGREES  
(EACH TICK IS 10 DEGREES)

10.0)

LMV 1X4 ARRAY WITH A .707 TAPER ON THE OUTER ELEMENTS  
(SUM PATTERN)

Figure 2-16. Calculated Pattern of the Tapered Tilted 1 x 4 Array



ORIGINAL PAGE IS  
OF POOR QUALITY

THETA DEGREES  
NUMBER OF SCANS

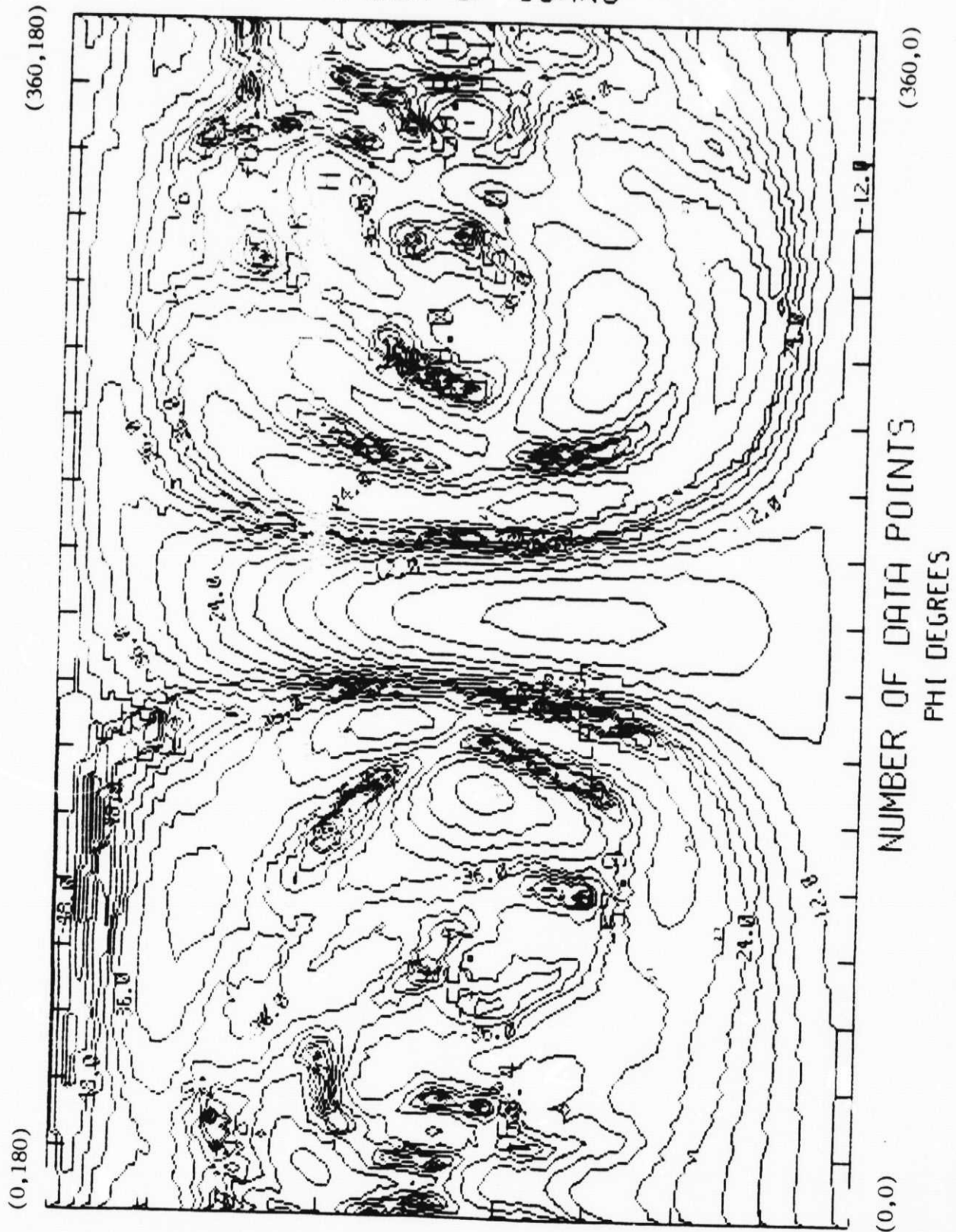


Figure 2-17. Measured Pattern of the Tapered Tilted 1 x 4 Array



Table 2-5

CALCULATED/MEASURED PATTERN ISOLA. N (dB DOWN FROM MAIN LOBE)  
TWO SATELLITE SYSTEM LOCATED AT 80° AND 113° W LONGITUDE  
MEASURED VALUES IN PARENTHESES ( )

	WA	CA	TEX	FL	ME
1 x 4 Tilted Array with No Taper					
pointed at 113° W	16(14)	19(15)	16(13)	16(18)	13(14)
pointed at 80° W	12(11)	15(16)	16(18)	18(17)	14(12)
1 x 4 Tilted Array with Taper					
pointed at 113° W	21(24)	24(26)	22(24)	25(21)	19(23)
pointed at 80° W	19(24)	21(22)	21(24)	22(24)	19(21)

Table 2-6

CALCULATED/MEASURED PATTERN ISOLATION (dB DOWN FROM MAIN LOBE)  
TWO SATELLITE SYSTEM LOCATED AT 105° AND 135° W LONGITUDE  
MEASURED VALUES IN PARENTHESES ( )

	WA	CA	TEX	FL	ME
1 x 4 Tilted Array with No Taper					
pointed at 135° W	15(14)	15(14)	22(14)	18(8)	12(16)
pointed at 105° W	25(20)	16(15)	15(18)	16(16)	16(16)
1 x 4 Tilted Array with Taper					
pointed at 135° W	19(23)	20(21)	25(19)	13(13)	21(24)
pointed at 105° W	20(22)	20(23)	22(22)	26(26)	23(27)



For comparison purposes, with the computed sum patterns of Figures 2-14 and 2-16, we show in Figures 2-18 and 2-19 their respective difference patterns.

### 2.1.2 Conformal Fixed-beam Array

The proposed design of the mechanically steered conformal array is stripline fed crossed slots with integral polarization hybrids and power divider. The crossed slots have good low angle elevation radiation characteristics; the stripline design allows the polarization hybrids and power divider to be fabricated within the element layer. Figure 2-20 shows the detailed antenna configuration. Performance summary is shown in Table 1-1.

The major disadvantage of the mechanically steered conformal array is the gain degradation at low scan angles (as is the case for the electrically steered conformal array). In addition, if a single design is used for the CONUS coverage, the mechanically steered version requires the beam to be shaped for the desired elevation coverage region. Therefore, it has less gain than the electronically steered array. For preselected elevation coverage regions, the mechanically steered version would have higher gain than the phased array. It would then be a worthwhile consideration, especially for southern or mid CONUS regions where very high gains could be achieved in a low profile package at lower cost than the phased array.

The mechanically steered conformal array investigation has centered primarily around the type of steering mechanism which we have already discussed and with reducing the conformal antenna height. Basically, by placing the motor along with the rotary joint at the center of the antenna, the antenna may be lowered by as much as an inch. However, there will be some pretrusion from the center region where the motor and rotary joint are located (see Figure 2-3). This allows an overall lower height of 3.5 inches, possibly lower depending on the final detail design of the antenna.

Approximate cost of this antenna in 100, 10,000 and 100,000 units is summarized in Table S-1. Major cost drivers and cost breakdown are discussed in Section 4.



ORIGINAL PARTS  
OF POOR QUALITY

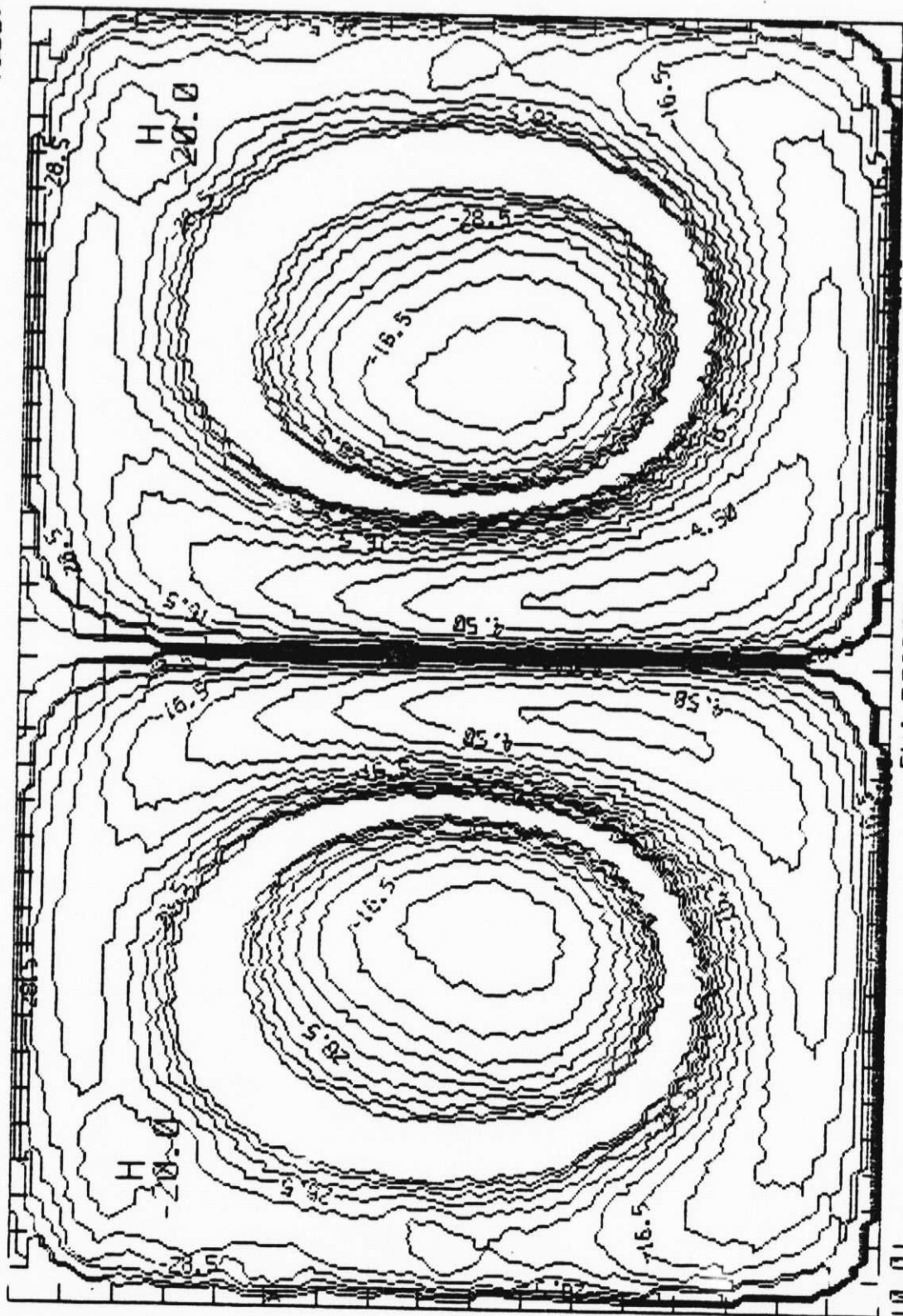
THETA DEGREES

(180, 1360)

(0, 1360)

(180, 10)

(0, 10)



PHI DEGREES

(EACH TICK IS 10 DEGREES)

LMV MONOPULSE WITH UNIFORM ILLUMINATION

(DIFFERENCE PATTERN)

Figure 2-18. Calculated Difference Patterns of the Uniformly Fed Tilted 1 x 4 Array



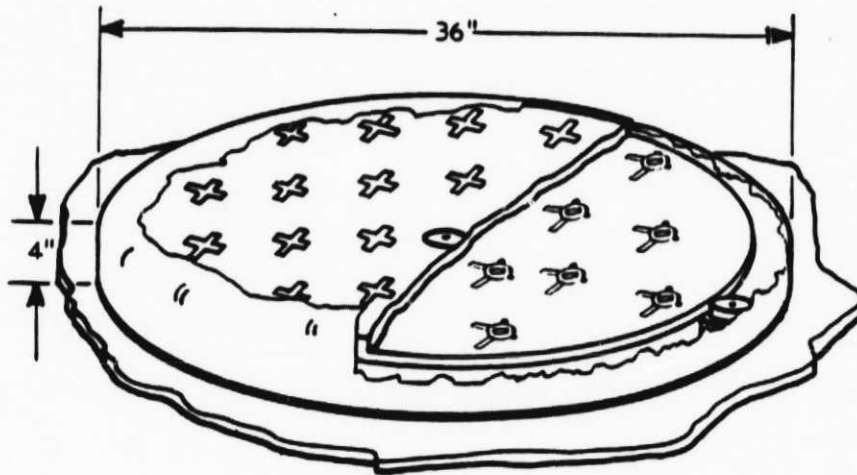


Figure 2-20. Mechanically Steered Fixed-Beam Conformal Array



## 2.2 Electronically Steered Conformal Array

The electronically steered phased array may be configured as follows: 19 stripline-fed crossed slots with integral polarization hybrids. Phase shifters are located beneath the stripline element layer on a microstrip board which contains the RF feed network and DC control circuitry for the phase shifters. The stripline-fed crossed slots were chosen based on their superior low angle radiation characteristics which minimize gain reduction at low elevation angles. The 19 element triangular lattice was chosen to minimize the number of elements within the given aperture and at the same time avoid formation of grating lobes (which could reduce the array gain). A performance summary is shown in Table 1-1.

The low profile conformal physical characteristics of the electronically steered phased array is the most important and obvious advantage (see Figure 2-21). However, many factors contribute to the poor operation of this antenna at low elevation scan angles. The gain of the array is degraded by such characteristics as scan loss which varies as the  $\cos \theta$ , where  $\theta$  is measured from zenith, increased polarization loss due to poor axial ratio, and pattern gain losses due to the inability to actively scan to low elevation angles. The other obvious disadvantage of the conformal phased array is the high cost per dB of gain when compared to the other concepts.

In applications where the conformal property of the electronically steered phased array is a major concern, it offers a solution with a premium price. However, even at the higher cost, performance at low elevation angles will suffer when compared to non-conformal solutions (which also have a lower cost).

In summary, the conformal electronically steered array is a very low profile antenna with 2 inches in thickness, possibly lower. It can be scanned rapidly for acquisition and tracking and finally, it does not have the wear and tear problems associated with the mechanically steered antennas.

A summary of the cost estimates is shown in Table S-1. Major cost drivers and cost breakdown are addressed in Section 4.

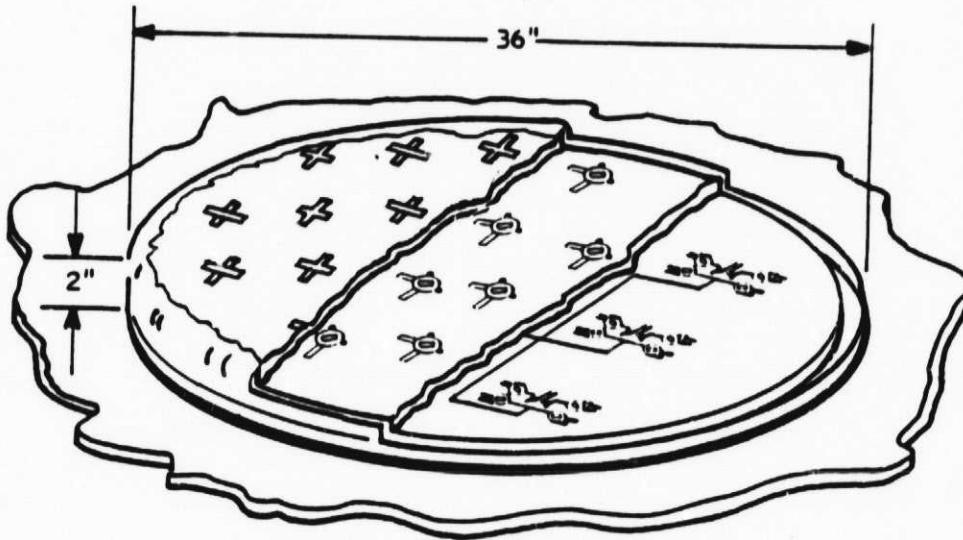


Figure 2-21. Electronically Steered Conformal Phased Array



## SECTION 3.0

### VEHICLE ANTENNA POINTING SYSTEMS

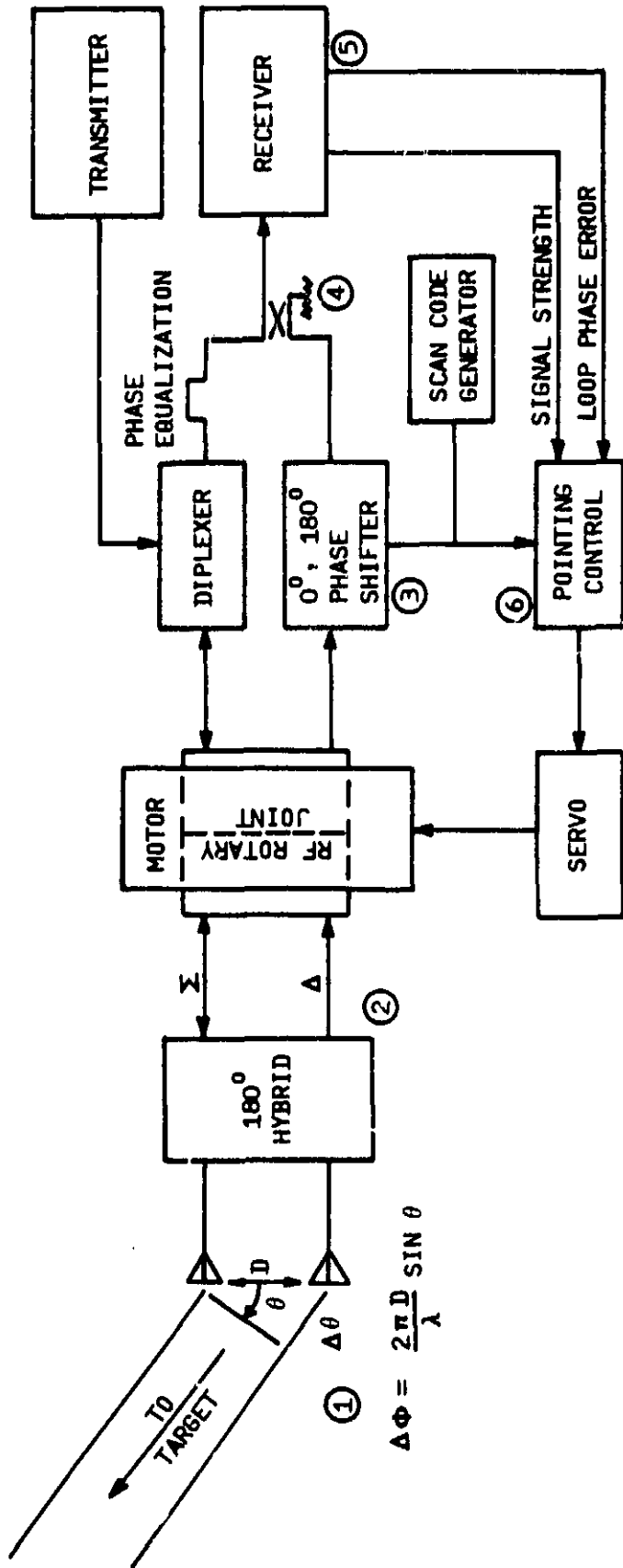
Four types of antenna pointing systems are investigated, three of which are "closed-loop" systems and the fourth is an "open-loop" system. The three closed-loop systems are classified according to their method of tracking. The first two use variations of monopulse tracking and the third uses sequential lobe tracking. The monopulse tracking systems can only be used by the mechanically steered systems while the sequentially lobe method is intended primarily for the electrically steered antenna. The reason for this distinction is because it is difficult for the electrically steered antenna to generate the sum and difference signals needed for monopulse tracking, however, by its very nature it is ideally suited to sequential lobe tracking. The open-loop system that was investigated uses a magnetometer (compass) to determine pointing errors.

#### 3.1 MONOPULSE TRACKING SYSTEMS - PHASE DETECTION

##### 3.1.1 System Concept Description

One of the best methods of tracking a target, in this case the MSAT-X satellite, is to use a monopulse tracking system. The simplest and least expensive method of implementing this technique is to use what is commonly referred to as a single channel monopulse tracking system. The advantage of this system is that it needs very little additional hardware to achieve excellent pointing. Simply stated, this system senses pointing errors and modulates this information onto the signal input into the receiver. It then uses the existing capabilities of the receiver to detect and demodulate this information. Special steps must be taken, however, to make this system work in an environment where the signal is fading rapidly.

One method of solving the fading problem is to use a monopulse tracking system which detects the phase offset inherent in an array antenna when it receives a signal at an off-boresight angle. Figure 3-1 is a block diagram of a mobile



- ① PHASE DELAY DIRECTLY RELATED TO OFF-BORESIGHT ANGLE (  $\theta$  ) AND IS UNAFFECTED BY FADING
- ②  $\Sigma$  AND  $\Delta$  SIGNALS GENERATED BY HYBRID COUPLER
- ③ PHASE OF  $\Delta$  SHIFTED  $0^\circ$  AND  $180^\circ$
- ④  $\Delta$  SIGNAL PHASE MODULATES (PM)  $\Sigma$  SIGNAL. AMOUNT OF PM IS DIRECTLY RELATED TO  $\theta$
- ⑤ PHASELOCK LOOP IN RECEIVER DETECTS PHASE MODULATION
- ⑥ POINTING SYSTEM DEMODULATES PM AND DETERMINES POINTING ERROR.

A/N 5090

Figure 3-1 Single-Channel Monopulse Tracking - Phase Detection



terminal which does this in a simple, yet effective manner. The pointing system can be divided into two major subassemblies; the direction sensing system and the steering mechanism. The operation of these systems and their interfaces with each other and with the transceiver are described in detail in the following.

### 3.1.1.1 Direction Sensing System

This system is configured like a conventional single channel monopulse tracking system. It uses two identical antennas which are pointed in the same direction (note, each antenna may consist of an array of radiating elements). The signals received by these two antennas will be equal in amplitude and both will experience the same variations due to shading and pointing errors. However, since the two antennas are physically separated, the phase of the signals at the two antennas will be off-set by an amount which is directly related to the off-boresight angle. The relationship between the phase off-set and the off-boresight angle can be expressed as:

$$\Delta\phi = \frac{2\pi D}{\lambda} \sin \theta$$

where,

- D is the separation between antennas
- $\lambda$  is the wavelength of the received signal
- $\theta$  is the off-boresight angle.

It is this phase difference which is eventually detected and used to generate antenna pointing information.

The received signals are routed from the two antennas to the A and B input ports of a hybrid coupler where sum ( $\Sigma$ ) and difference ( $\Delta$ ) signals are generated. The  $\Sigma$  and  $\Delta$  output signals are routed across the antenna-vehicle interface by means of a dual channel RF rotary joint. Transferring both the  $\Sigma$  and  $\Delta$  signals across the rotary joint is necessary because this system must also be used to transmit the return-link signal. The return-link signal is routed



from the transmitter through the diplexer to the  $\Sigma$  port of the hybrid. The hybrid acts like a power divider equally splitting the input signal between the A and B output ports and thereby providing equal power to all of the radiating elements of the antenna. In this way, the direction sensing system is transparent to the return-link signal.

After crossing the rotary joint, the  $\Delta$  signal is input to a phase shifter which shifts its phase either  $0^\circ$  or  $180^\circ$  depending upon the state of the control signal from the scan code generator. The rate at which the phase of  $\Delta$  is shifted determines how accurately the antenna can be pointed during perturbations. A rate of 10 Hz is used in order to comply with the maximum allowed rate for modulating the received signal. This factor limits pointing errors to about  $5^\circ$  during  $90^\circ$  turns taken at a  $45^\circ/\text{second}$  rate. A portion of the  $\Delta$  signal is then added to the  $\Sigma$  signal by means of a directional coupler and the resultant signal is input to the receiver. If the coupling factor ( $k$ ) is equal to unity, then it can be shown (see Appendix A) that resultant signal can be expressed mathematically as:

$$R_0 = \sqrt{2} A \cos (\omega t)$$

when the phase of  $\Delta$  is 0 degrees, and as:

$$R_{180} = \sqrt{2} A \cos (\omega t + \Delta\phi)$$

when the phase of  $\Delta$  is shifted 180 degrees.

where,

A is the amplitude of the received signal.

$\omega$  is the frequency of the received signal.

$\Delta\phi$  is the difference in phase of the received signal at the two antennas.

The important thing to notice is that by shifting the phase of  $\Delta$  between 0 and 180 degrees, the signal input to the receiver (R) is phase modulated by an amount ( $\Delta\phi$ ) which is directly related to the off-boresight angle ( $\theta$ ). This



can be seen graphically in Figure 3-2. Figure 3-2 is a phaser diagram showing the addition of the  $\Sigma$  and  $\Delta$  signal and the resultant phase modulation of the signal input to the receiver. Notice that as the antenna is steered toward the target, the amount of phase modulation gets smaller and that the amount of phase modulation at a given off-boresight angle can be adjusted, choosing the appropriate coupling factor ( $k$ ). Most important, however, is the fact that the phase modulation is unaffected by signal fading. The next step is to detect this phase modulation and then provide it to the steering mechanism in some useful form.

A block diagram of the receiver used in the mobile terminal is shown in Figure 3-3. This receiver uses a phaselock loop (PLL) in the narrowband pilot channel in order to achieve the desired SNR. The analysis in Appendix A shows that this same PLL can be used to detect the phase modulation induced by the direction sensing system.

A simplified block diagram of a typical PLL is shown in Figure 3-4. It consists of three basic components; a phase detector, a low-pass filter, and a voltage controlled oscillator (VCO). The phase detector compares the phase of the input signal against the phase of the VCO. The output of the phase detector is a measure of the phase difference between the two inputs. This difference voltage is then filtered and applied to the VCO. This control voltage, commonly referred to as the loop-phase-error, changes the frequency of the VCO in a direction which reduces the phase difference. The loop-phase-error is given by:

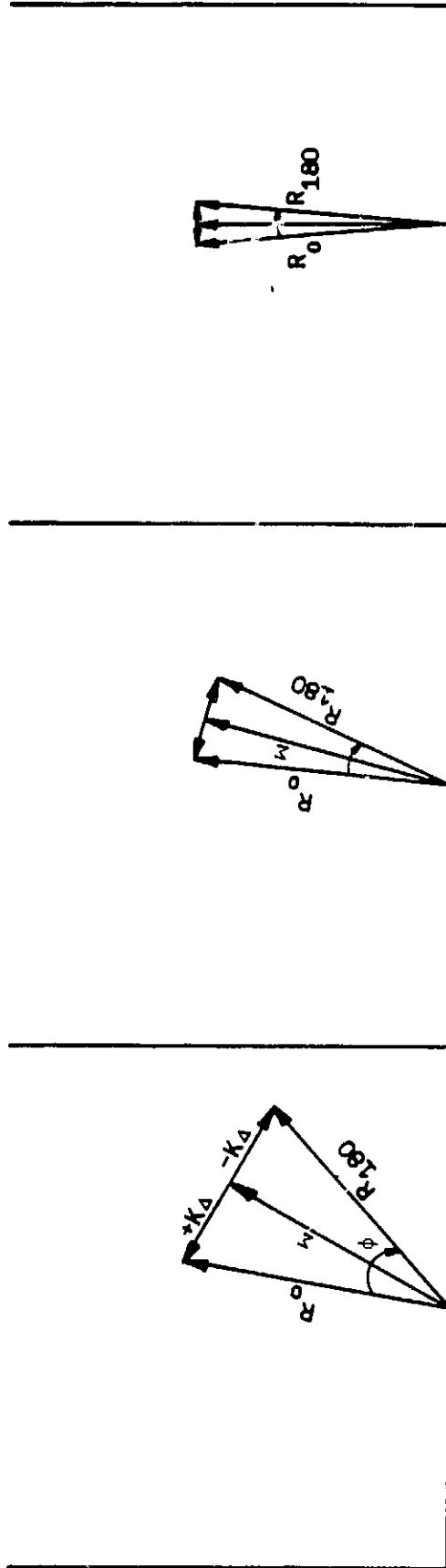
$$V_d = K_d \sin (\phi_i - \phi_v)$$

where,

$K_d$  = phase detector gain constant (volts/radian)

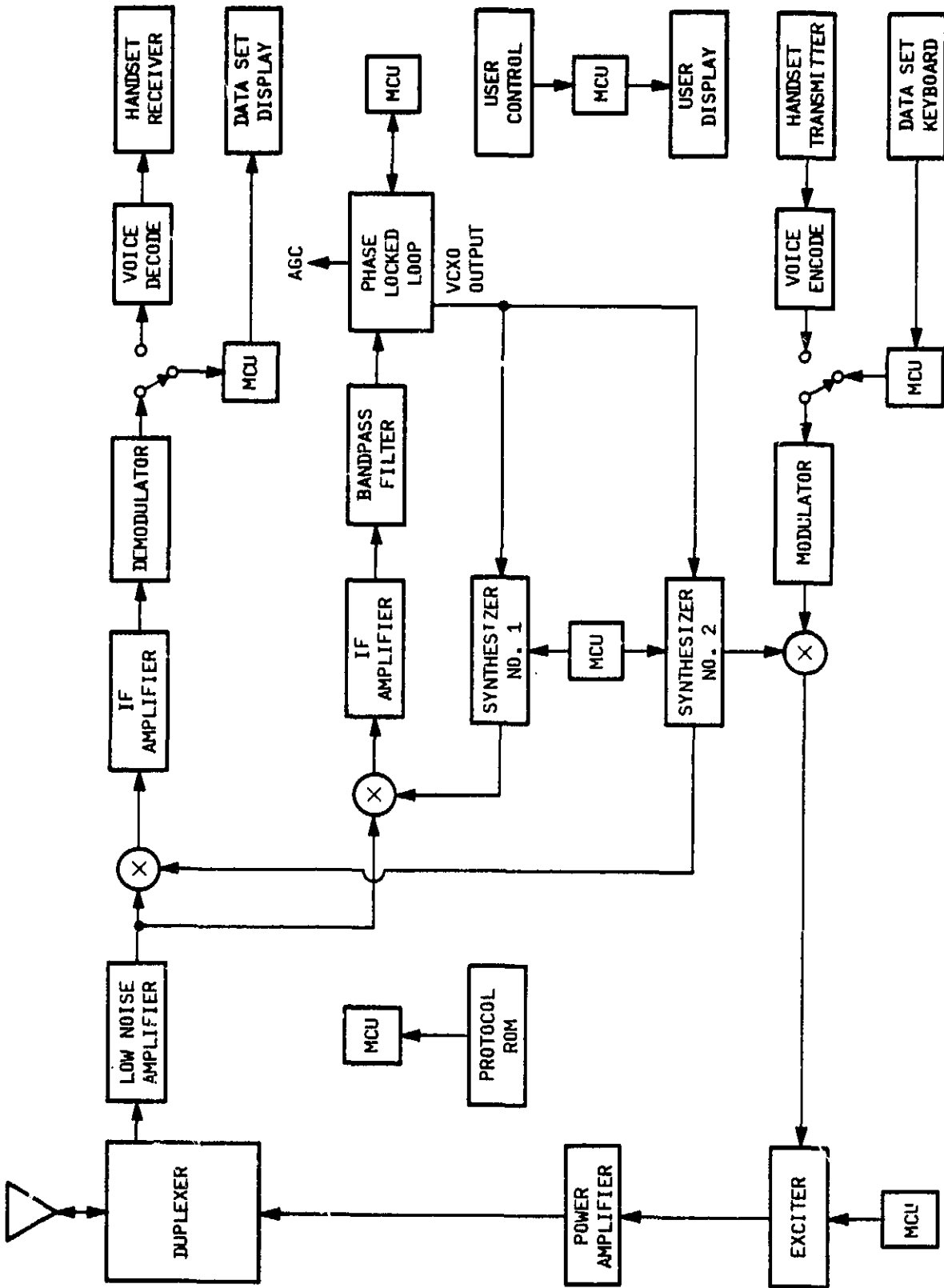
$\phi_i$  = phase of input signal

$\phi_v$  = phase of VCO signal



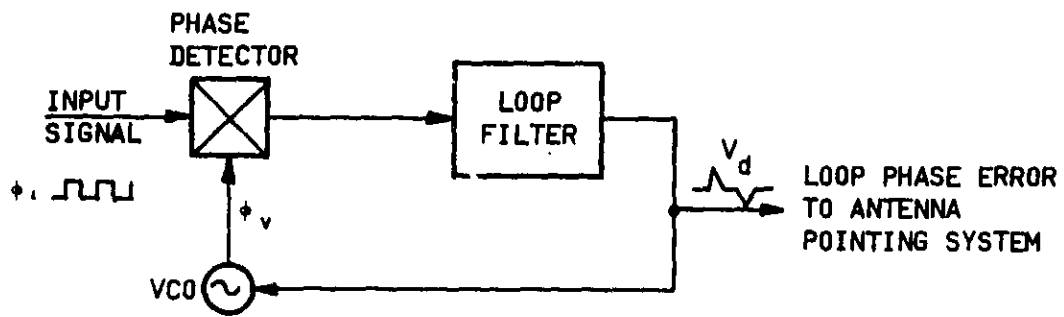
A/N 5090

Figure 3-2 Phasor Diagram Showing Phase Modulation ( $\phi$ ) Caused by Shifting Phase of  $\Delta$  Signal  $0^\circ$  and  $180^\circ$



A/N 5090

Figure 3-3 Mobile Terminal Block Diagram



A/N 5090

Figure 3-4 Basic Phaselock Loop can Detect Pointing Errors

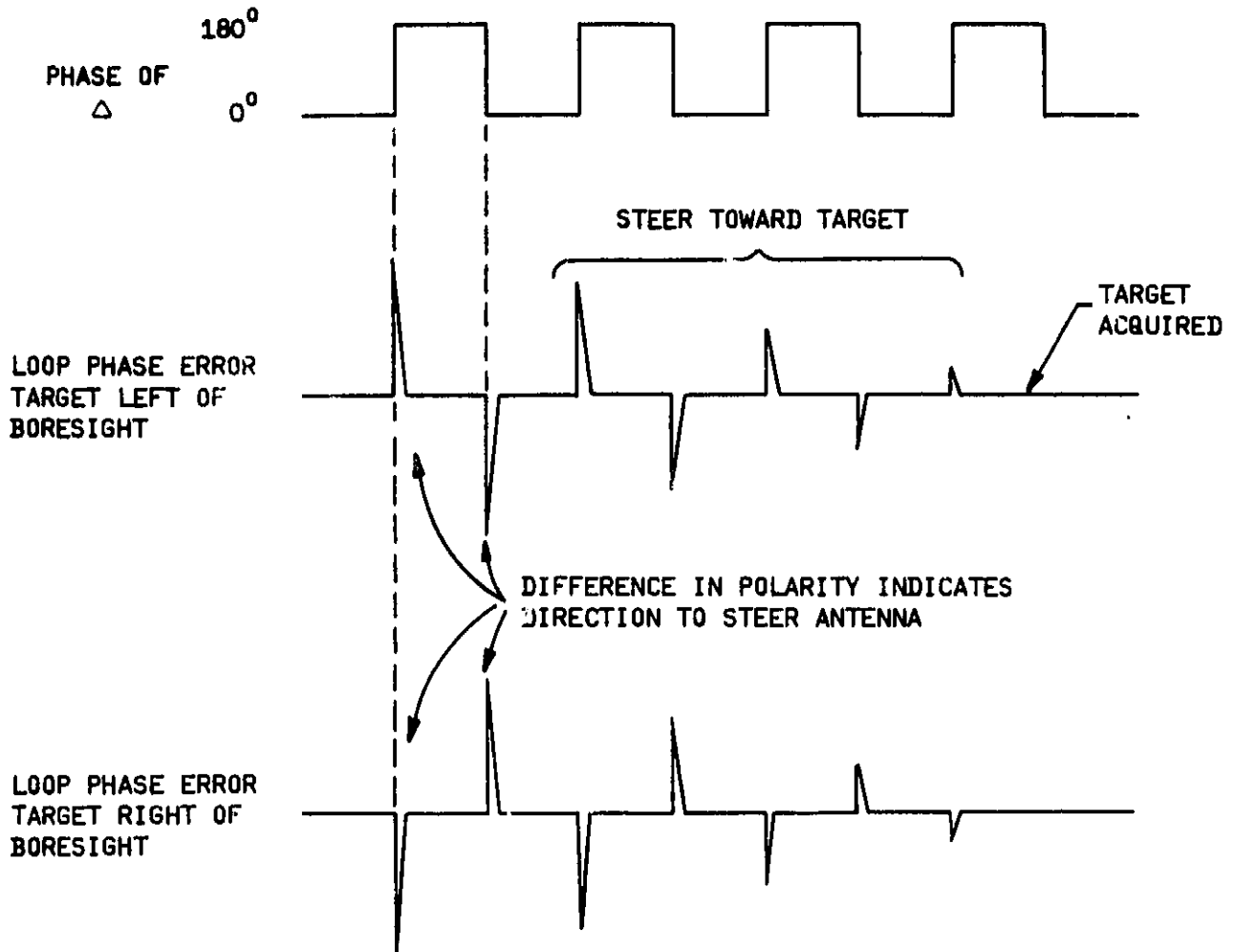


Ideally, when the loop is locked, the loop-phase-error is zero ( $\phi_i = \phi_v$ ). This assumes the rest frequency of the VCO is equal to the frequency of the input signal. In practice this may not be true and the loop-phase-error will have a constant offset, or static phase error; however, this offset will not affect the operation of the pointing system.

A step change in the phase of the input signal will cause a sudden change in the loop-phase-error. The magnitude of the change in the loop phase error is directly related to the magnitude of the phase shift of the input signal. The PLL will eventually track out this phase shift and the loop phase error will return to zero; however, this transient will provide the steering mechanism with the information it needs to determine the antenna pointing error. The final step then is to decode this information and generate the appropriate antenna steering signals. The example shown in Figure 3-5 shows how this is done.

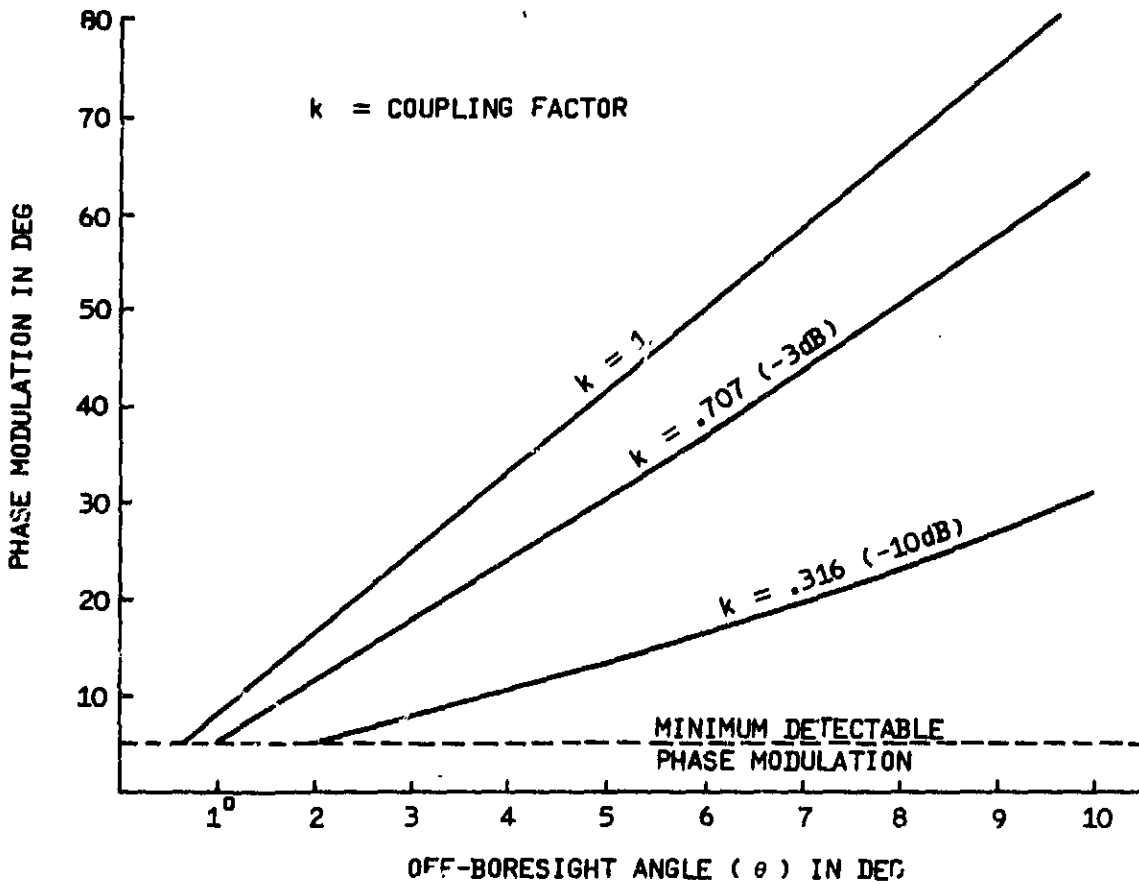
If shifting the phase of the  $\Delta$  signal between 0 and 180 degrees causes a transient in the loop-phase-error, the steering mechanism knows the target is off-boresight. It determines which direction to steer the antenna by detecting the difference in amplitude of the loop-phase-error in synchronism with the phase shift of the  $\Delta$  signal. If the target is to the right of boresight, then the loop-phase-error will experience a positive transient when the phase of  $\Delta$  is shifted from 0 to 180 degrees followed by a negative transient when the phase of  $\Delta$  is shifted from 180 to 0 degrees. If the target is to the left of boresight, then the polarity of the transients will be reversed relative to the phase shift of  $\Delta$ . As the antenna steers toward the target, the amplitude of the transients will get smaller giving the steering mechanism an indication of how close it is to the target.

Phaselock loops are very good devices for measuring phase errors. The typical PLL used in receivers is capable of detecting phase errors of only a few degrees. Figure 3-6 shows the phase shift that will be induced in the input signal as a function of the off-boresight angle  $\theta$  for various coupling factors ( $k$ ). This graph shows that, with  $k=1$ , an off-boresight angle as small as 0.5 degrees will cause an easily detected phase shift of approximately 4 degrees.



A/N 5090

Figure 3-5 Pointing Error Determined by Synchronously Demodulating Transients in Loop Phase Error and Phase Shifts of  $\Delta$  Signal



A/N 5090

Figure 3-6 Phase Modulation of  $R = \Sigma + k\Delta$  as a Function of Off Boresight Angle and Coupling Factor ( $k$ )



Therefore, it is reasonable to expect that, under ideal conditions, the pointing knowledge using this technique will be less than 0.5 degree.

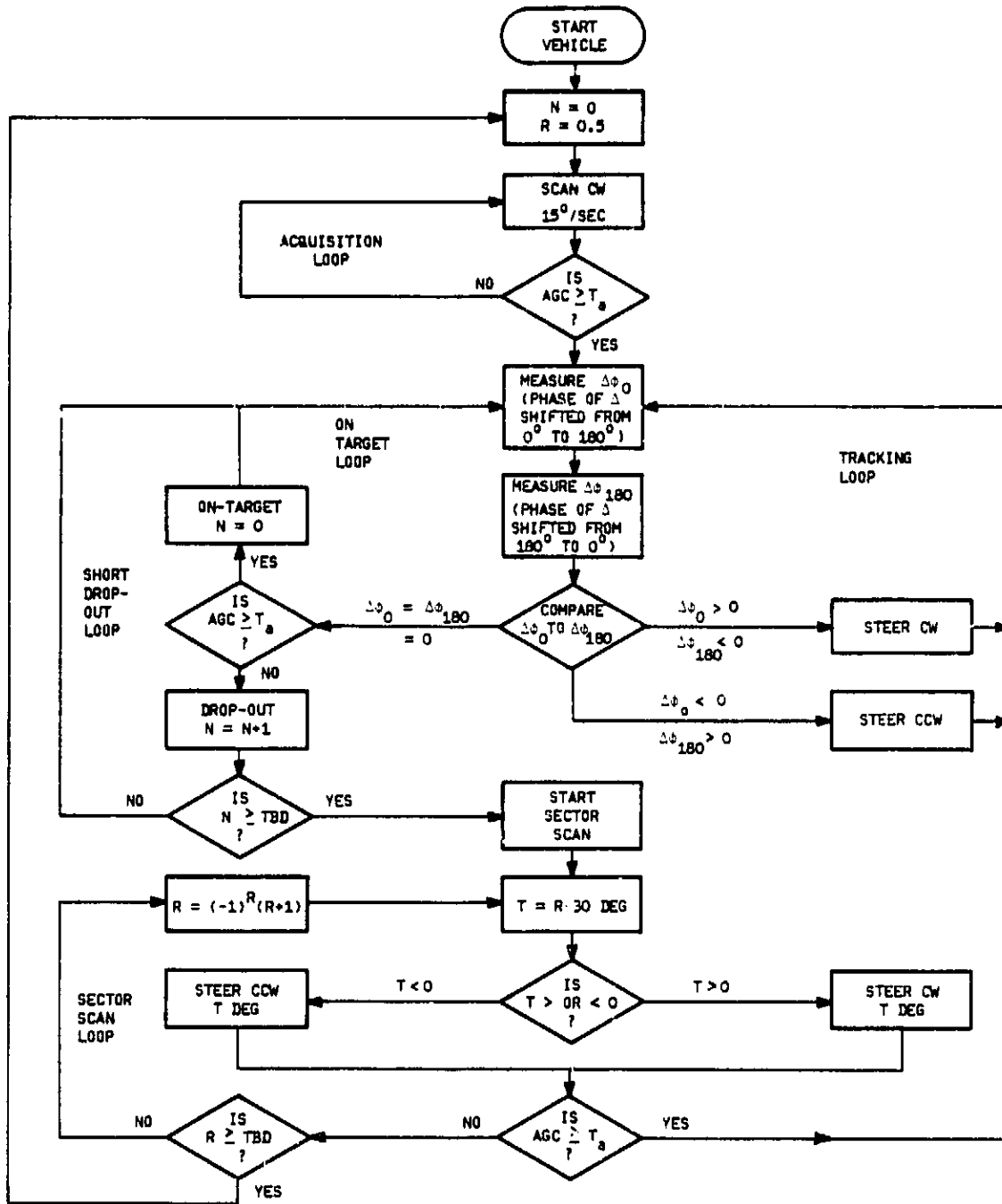
Appendix B presents an analysis of pointing knowledge as a function of loop signal-to-noise ratio (SNR). This analysis confirms that, under strong signal conditions (loop SNR = 30 dB), pointing knowledge will be on the order of 0.5 degrees. Pointing knowledge decreases with decreasing SNR. However, this analysis shows that it should be possible to maintain a pointing knowledge of less than 3° even under weak signal conditions (loop SNR = 10 dB).

This tracking system, as with most tracking systems, has a drawback in that it has a relatively narrow range over which it can lock onto and track the target. Since the loop-phase-error is given by a sine function, phase shifts in the input signal ( $\Delta\phi$ ) greater than 180° (off-boresight angles greater than 20°) will cause the sign of the transients to be reversed, and using the demodulation scheme described above, the steering mechanism would steer the antenna in the wrong direction. Therefore, a separate acquisition system is needed which gets the target within the "lock-on" range of the monopulse tracking system. The following section describes how this is done.

#### 3.1.1.2 Pointing Algorithms

Figure 3-7 is a flow diagram showing the sequence of events the pointing system follows as it acquires and tracks the target. This figure emphasizes the fact that, due to the improvements in the steering mechanism, the pointing system doesn't have to do anything quickly. Pointing errors increase slowly giving the pointing system ample time to react even under conditions where the vehicle is turning and the signal has been lost due to fading.

To begin with, it is assumed that not only must the vehicle itself be able to initiate a contact at any time, but also that it must be possible for someone else to contact the vehicle at any time. This makes it necessary for the pointing system to acquire the target as soon as the vehicle is started. This means the MSAT-X satellite must continuously transmit the pilot tone so that automatic acquisition can take place.



A/N 5090

Figure 3-7 Monopulse Tracking System Operations Flow Diagram



Once the vehicle is started, the pointing system starts to scan the antenna in a clockwise direction at 15 degrees/second. Since the monopulse system can't be used effectively for the initial acquisition of the target, the pointing system monitors the received signal strength (AGC) output of the receiver to determine when the antenna is pointed in the general direction of the target. When the AGC exceeds a predetermined acquisition threshold ( $T_a$ ), the pointing system switches from the acquisition to the track mode of operation.

The acquisition threshold is set equal to the signal level expected when the line of sight to the target is approximately 15 degrees off boresight (approximately -5 dB point on the antenna pattern). There are several reasons for setting the acquisition threshold at this point. First of all, it assures the pointing system won't lock onto weak interfering signals and second, it gets the target within the "lock-on" range of the monopulse tracking system.

One of the major features of the pointing system is that it is capable of acquiring the target even in an environment where the signal is fading badly. The scan rate is set at 15 degrees/seconds so that the antenna is scanned a full 360 degrees within the required acquisition time of 30 seconds. At this rate, the target will be within the "lock-on" range for approximately 2 seconds. The pointing system will acquire the target, regardless of how bad the fading is as long as the received signal exceeds the acquisition threshold at some time during the 2 second window.

After the pointing system has acquired the target, the monopulse tracking system takes over. The steering mechanism determines the antenna pointing error by demodulating the transients in the loop-phase-error and steers the antenna in the appropriate direction. Here again the pointing system provides exceptional performance during fading since it is capable of tracking the target, regardless of how bad the fading is, as long as the narrow band pilot channel remains locked to the received signal. Once the antenna is on-target, there won't be any transients in the loop-phase-error, so the pointing system verifies it is on-target by verifying the AGC exceeds the acquisition threshold at some time during the tracking sequence ( $\approx 100$  msec). As long as the loop-phase-error is zero and the AGC periodically exceeds the acquisition



threshold, then the pointing system knows it has the main beam of the antenna locked on the target.

If the AGC does not exceed the acquisition threshold at some time during the cycle, the pointing system knows the signal has faded (>5 dB down for 100 msec) and it starts the reacquisition sequence. In the first phase of the reacquisition sequence the pointing system doesn't do anything different except to count how long it has been since the signal was lost. The reason for this is as follows:

- If the AGC is below the acquisition threshold but the pilot channel in the receiver is still locked then, if the vehicle makes a turn, the tracking system will still detect transients in the loop phase error and will react accordingly. Therefore, no action is needed.
- If the pilot channel in the receiver has dropped lock (signal drop-out), then, because of the improvements in the steering mechanism, the target will stay within the lock-on range even if the vehicle makes turns up to 75 degrees. Therefore, no immediate action is needed.

This means the pointing system can stay in this "do nothing" mode for several seconds and still have a high probability of being in the right position to reacquire the target the moment the signal returns. This feature will enable rapid reacquisition of the signal as the vehicle drives through tunnels, or under bridges, etc.

The longer the drop-out lasts, the greater the likelihood the vehicle has made a large turn and the antenna is no longer pointed in the right direction. Therefore, after about 4 seconds (320 ft. of travel at 55 mph), the pointing system assumes it has lost the target and it enters the second phase of the reacquisition sequence. Once again the improvements in the steering mechanism help speed up reacquisition, this time because the pointing system can assume the target is nearby, allowing it to enter a sector scan mode. In this mode, the pointing system scans the antenna back and forth in an ever increasing arc



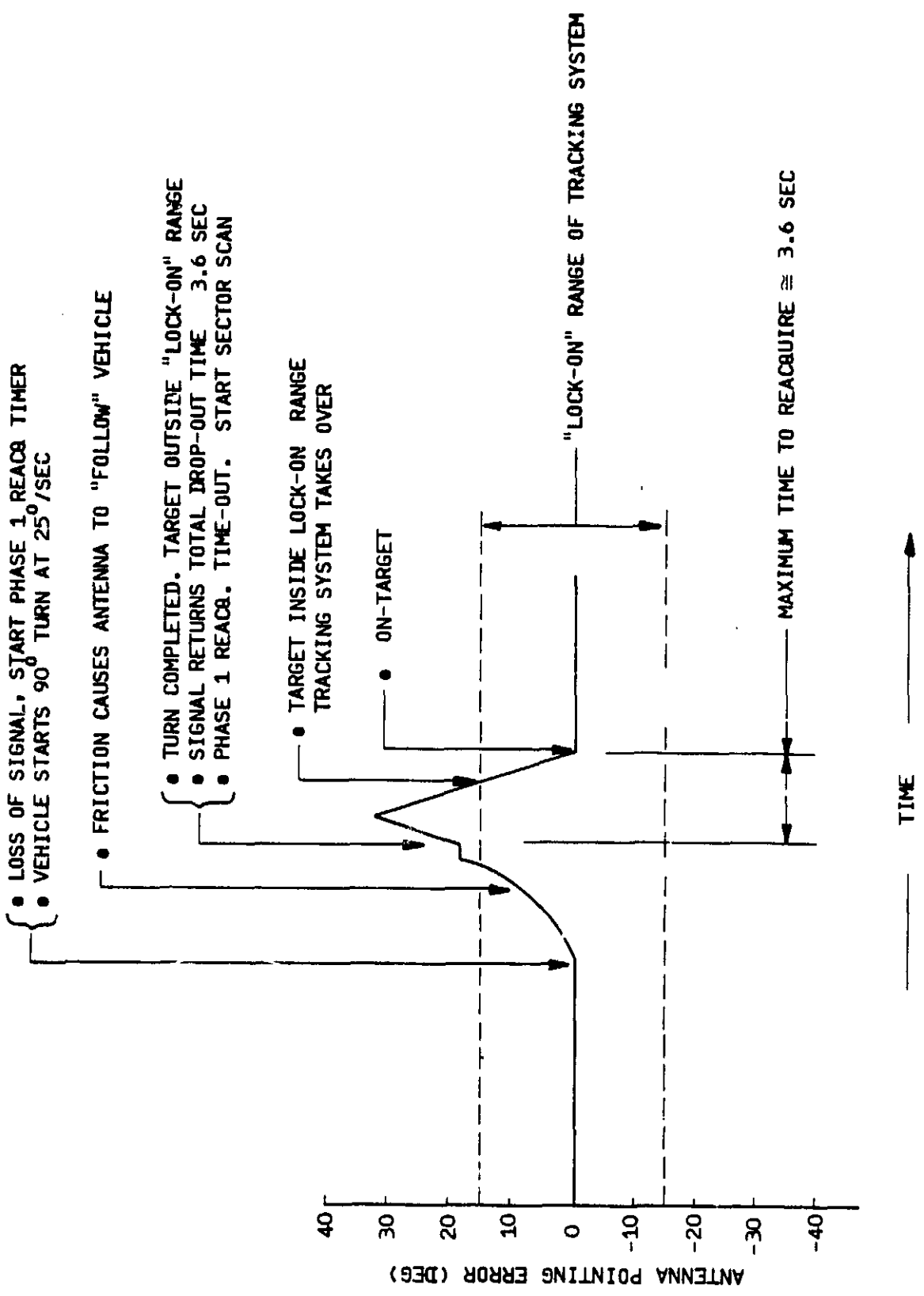
while monitoring the AGC. The length of the arc is increased by the size of the lock-on range of the tracking system (about 30 degrees) on each cycle. This makes it possible to reacquire the target in the shortest possible time. If the target hasn't been reacquired after approximately 9 seconds (total area of 105 degrees has been searched), the pointing system gives up and goes back to the initial acquisition sequence.

Figure 3-8 illustrates the obvious advantages of this system. This figure shows the antenna pointing error as a function of time for a reasonable worst-case design condition. In the example, it is assumed the signal is lost just as the vehicle starts a 90° turn at 25°/second and doesn't return until the turn has been completed (signal is lost for approximately 4 seconds). Our analysis shows that under these conditions the antenna will be off-pointed by less than 20° and it will reacquire in less than 4 seconds. A system not using our "pivot-point" approach would, under these same conditions, be off-pointed by 90° and it could take up to 30 seconds to reacquire.

### 3.1.1.3 Interfaces

Transceiver Interfaces. The interfaces to the receiver are simple and straightforward. The receiver must provide two signals to the steering mechanism. The AGC which is used during the initial acquisition phase and the loop-phase-error which is used during the tracking phase. Both of these signals are typically provided at an external connector to facilitate test and check-out of the receiver; therefore, no additional circuitry should be required. The characteristics of these signals can be the customary 0 to 5 volt analogs. The AGC monitor should be able to detect differences in received signal strength of 1 dB or less, and the phaselock loop monitor must be able to detect phase errors of 4 degrees or less (for 0.5 degree pointing accuracy). Neither of these requirements is considered unreasonable.

The major interface problem that must be carefully considered is whether phase modulating the received signal will affect the performance of the data channel. This is particularly true if the data channel also uses phase modulation. When the antenna is on target, the phase modulation will be small (less



A/N 5090

Figure 3-8 Worst Case Reacquisition Sequence - Mechanical Steered Antenna



than  $8^\circ$ ), however, due to the 10 Hz limit on the allowed modulation by the pointing system, pointing errors during  $45^\circ/\text{second}$  turns will be approximately  $5^\circ$  and the phase modulation caused by the pointing system will be  $25^\circ$ - $45^\circ$  depending upon the coupling factor (k) used. The PLL will quickly track out these phase shifts, however, the length of the transient must be short compared to a bit period. This factor may affect the design of the PLL.

Vehicle Interfaces. The vehicle must provide power to the pointing system.

User Interfaces. This system does not require any user interfaces, however, options such as an "on-target" indicator and "reset button" may be desirable.

### 3.1.2 PERFORMANCE

#### 3.1.2.1 Pointing System Performance

This pointing system satisfies all requirements. The performance of this system in comparison to other pointing systems considered is summarized in section 3.5.

#### 3.1.2.2 Performance Variations

Multiple Satellites. This system will perform very well in a multiple satellite system because it can point the antenna very accurately. This means the gain in the direction in the desired satellite is maximized while the gain in the direction on the adjacent satellites is minimized. However, since the antenna pointing error is detected using information derived from the pilot channel, there is the danger the pointing system will lock onto the wrong satellite if all satellites use the same frequency for the pilot tone. In a two satellite system, the use of cross-polarization does not eliminate this problem. In the three satellite system, two satellites use the same polarization. The simplest way to solve this problem is if these two satellites must use a different frequency for the pilot tone; otherwise the pointing system must go through a complicated procedure of finding both satellites and then determine which is the desired one.



Shadowing. This pointing system is nearly immune to the effects of shadowing. The operation description given in section 3.1.1.4 shows that the pointing system will acquire the target during the first scan of the antenna as long as the antenna can "see" the target (i.e., no shadowing) once during the two seconds "lock-on" window of the monopulse tracking system. Once the monopulse tracking system is locked onto the target, it can maintain antenna pointing regardless of how bad the fading is as long as the pilot channel in the receiver stays locked. Finally, it allows a rapid reacquisition after the signal is lost for prolonged periods (i.e., shadowing caused by buildings, tunnels, etc.) because the steering mechanism acts like a pivot point and keeps the antenna pointed close to the proper direction even if the vehicle is maneuvering.

Different Antennas. This pointing system is compatible with either of the two mechanically steered antenna concepts. It cannot easily be used with the electronically steered antenna because this antenna requires a complex and costly feed network in order to be able to develop the  $\Sigma$  and  $\Delta$  signals needed by the monopulse tracking system.

Half-Duplex Operation. This system will work equally well for the half-duplex mode of operation provided the pilot tone is transmitted on a separate frequency. In the half-duplex mode of operation, the mobile terminal transmits and receives on the same frequency making it necessary to "blank" the communication channel in the receiver during transmissions. If the frequency of the pilot tone isn't the same as that used for communication, the pilot channel doesn't have to be blanked during transmission allowing the pointing system to function normally.

### 3.1.3 RELIABILITY

#### 3.1.3.1 Failure Modes

There are only two elements in the pointing system that can be considered wear-out items. They are the RF rotary joint and the motor. The RF rotary joint has a life expectancy of  $10E6$  revolutions where life is defined as not



being able to meet the specified values of insertion loss and VSWR. Making the conservative assumption that the vehicle makes one turn per minute for eight hours per day results in a system operating life of 57 years. Using the same assumptions the motor (including bearings) has an operating life much greater than this.

#### 3.1.4 HERITAGE

The concepts used in this pointing system are all well known. The single channel monopulse tracking system has seen wide application and complete systems offering two axis pointing are commercially available. The system proposed for MSAT-X is a straightforward application of this technique but using a detection scheme better suited to a rapidly fading signal. The concept of a "pivot-point" steering mechanism has been used extensively by BASD, and others, in spacecraft to point science instruments and communication antennas. In short, there aren't any new technology developments required to meet MSAT-X requirements.

#### 3.1.5 COST

The cost of the direction sensing system is minimal. The 180 degree hybrid is a very simple device often used by BASD in our antennas and can be fabricated as part of the antenna feed network. The cost of this item will be negligible.

The 0-180 degree phase shifter used to modulate the  $\Delta$  signal is also a very simple device. Its main component is two pin diodes used to switch the input signal through the 0 or 180 degree phase shift paths. The cost of this item should only be a few dollars. To reduce packaging costs, the phase shifter and diplexer and pointing control system could be fabricated as a single unit. A cost estimate of the complete antenna system is given in Section 4.0.



## 3.2 MONOPULSE TRACKING - AMPLITUDE DETECTION

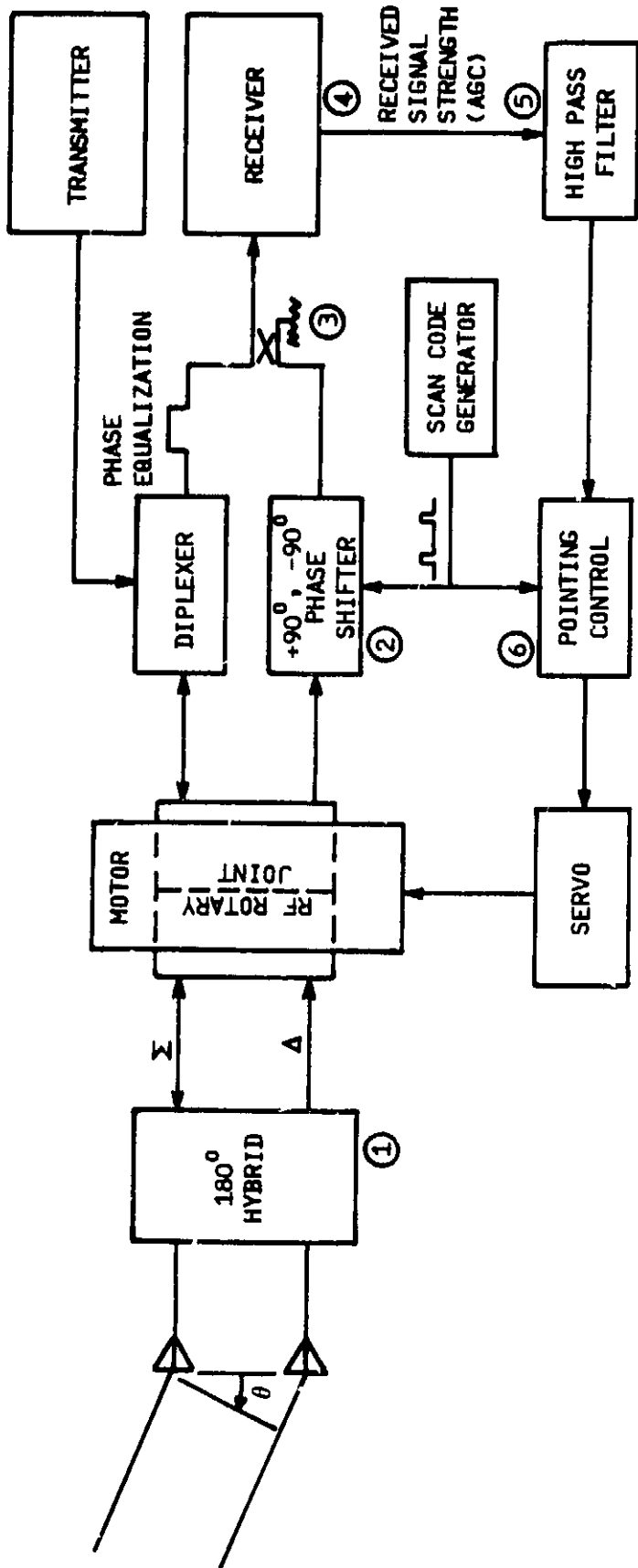
### 3.2.1 System Concept Description

By making some very minor modifications, the monopulse tracking system described in the previous section can be changed such that pointing errors cause amplitude rather than phase modulation of the signal input to the receiver. Here again, special steps must be taken to make this system work in an environment where the amplitude of the received signal is varying rapidly due to shading. With this system, the solution to the fading problem is to sample the pointing information at a rate which is fast compared to the rate at which fading occurs. In this way, amplitude variation caused by shading is small during the sample period, and has a negligible effect on the pointing error information. Figure 3-9 shows a block diagram of a monopulse tracking system which uses amplitude detection. The differences between this system and the system using phase detection are described in the following.

#### 3.2.1.1 Direction Sensing System

As can be seen from Figure 3-9, the amplitude detection system is very similar to the phase detection system. The first major difference between the two tracking techniques is that with the amplitude detection system, the phase of the  $\Delta$  signal is shifted plus and minus 90 degrees (rather than 0 and 180 degrees) before it is added to the  $\Sigma$  signal (in the directional coupler). The net result, as shown in Figure 3-10, is that the  $\Sigma$  signal is amplitude (rather than phase) modulated by the  $\Delta$  signal. By referring back to Figure 3-2, it can be seen how we got from phase to amplitude modulation by simply changing the phase shift of the  $\Delta$  signal. As with the phase detection system, the amount of modulation is directly related to the off-boresight angle, and it can be varied to meet system requirements by adjusting the coupling factor (K).

The resultant signal is then input to the receiver where the AGC is used to detect the amplitude modulation. At this point the AGC will reflect the fact that the signal input to the receiver is amplitude modulated by both pointing



- ①  $\Sigma$  AND  $\Delta$  SIGNALS GENERATED BY HYBRID COUPLER
- ② PHASE OF  $\Delta$  SHIFTED  $-90^\circ$  AND  $+90^\circ$ . RATE IS FAST COMPARED TO RATE OF FADING.
- ③ SIGNAL AMPLITUDE MODULATES  $\Sigma$  SIGNAL. AMOUNT OF AMPLITUDE MODULATION (AM) DIRECTLY RELATED TO OFF-BORESIGHT ANGLE ( $\theta$ ).
- ④ AGC IN RECEIVER DETECTS AM
- ⑤ AM CAUSED BY FADING IS REMOVED BY FILTER
- ⑥ POINTING SYSTEM DEMODULATES AM AND DETERMINES POINTING ERROR.

A/N 5090

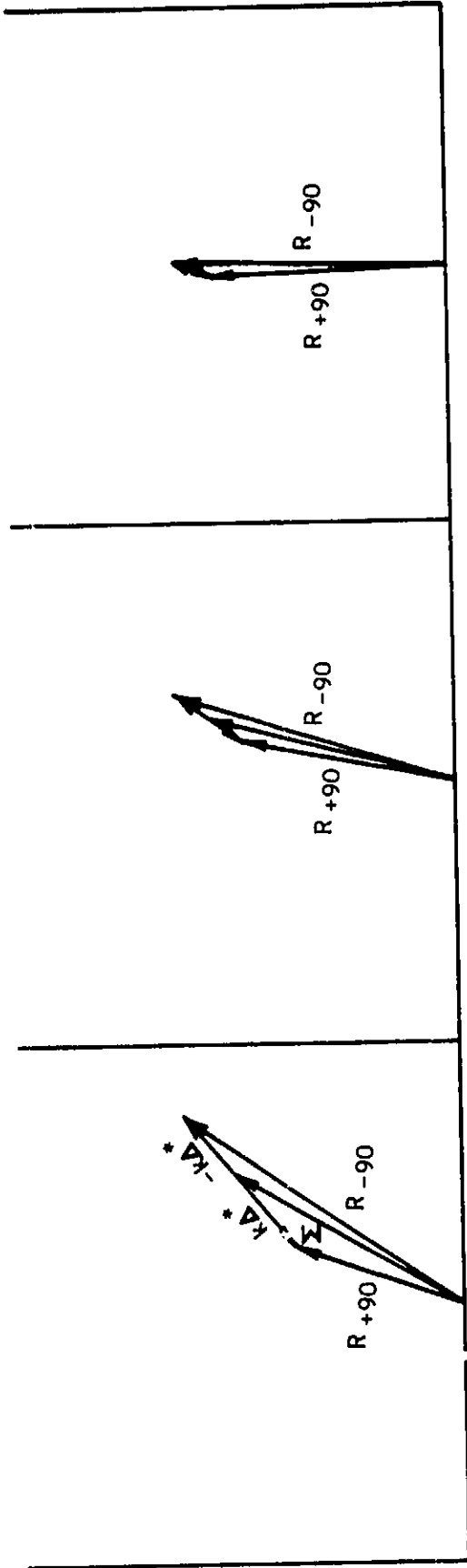
Figure 3-9 Single-Channel Monopulse Tracking - Amplitude Detection



error information and fading. The AGC signal is then input to a high pass filter which is a part of the pointing control system. Since the pointing error information is modulated onto the received signal at a rate which is fast compared to the rate at which fading occurs, the high pass filter can be designed such that it removes the modulation caused by fading thereby providing the pointing control electronics with a "clean" signal containing only the pointing error information. Finally, the pointing error is determined by synchronously demodulating the filtered AGC with the scan code signal used to shift the phase of the  $\Delta$  signal.

JPL has conducted tests, using balloons, which were designed to simulate the effects of shading on MSAT-X transmissions. From these tests, it is known that the maximum rate at which fading is expected to occur is roughly 200 Hz. In order to make it easy to distinguish between pointing errors and fading (i.e., keep filtering easy), it is desirable to make the pointing error sample rate roughly ten times faster than the rate of fading, or approximately 2 kHz. If this sample rate is used continuously, however, we violate the requirement that the pointing system not modulate the received signal at frequencies greater than 10 Hz. Figure 3-11 shows how we can get around this limitation. By keeping the phase shift of the  $\Delta$  signal fixed at one value for a relatively long period of time (approximately 95.5 msec.) and then rapidly shifting the phase of  $\Delta$  to the second value and back (approximately 0.5 msec), we are able to satisfy both requirements. The phase of the  $\Delta$  signal is shifted from  $-90^\circ$  to  $+90^\circ$  and back to  $-90^\circ$  at a 2 kHz rate which causes a transient in the filtered AGC (assuming the target is off-boresight) and the transients will occur at a 10 Hz rate. The pointing system determines which direction to steer the antenna by noting the sign of the transient. A positive transient means the target is to the right of boresight and a negative transient means the target is to the left of boresight. As the antenna is steered toward the target, the amplitude of the transients gets smaller.

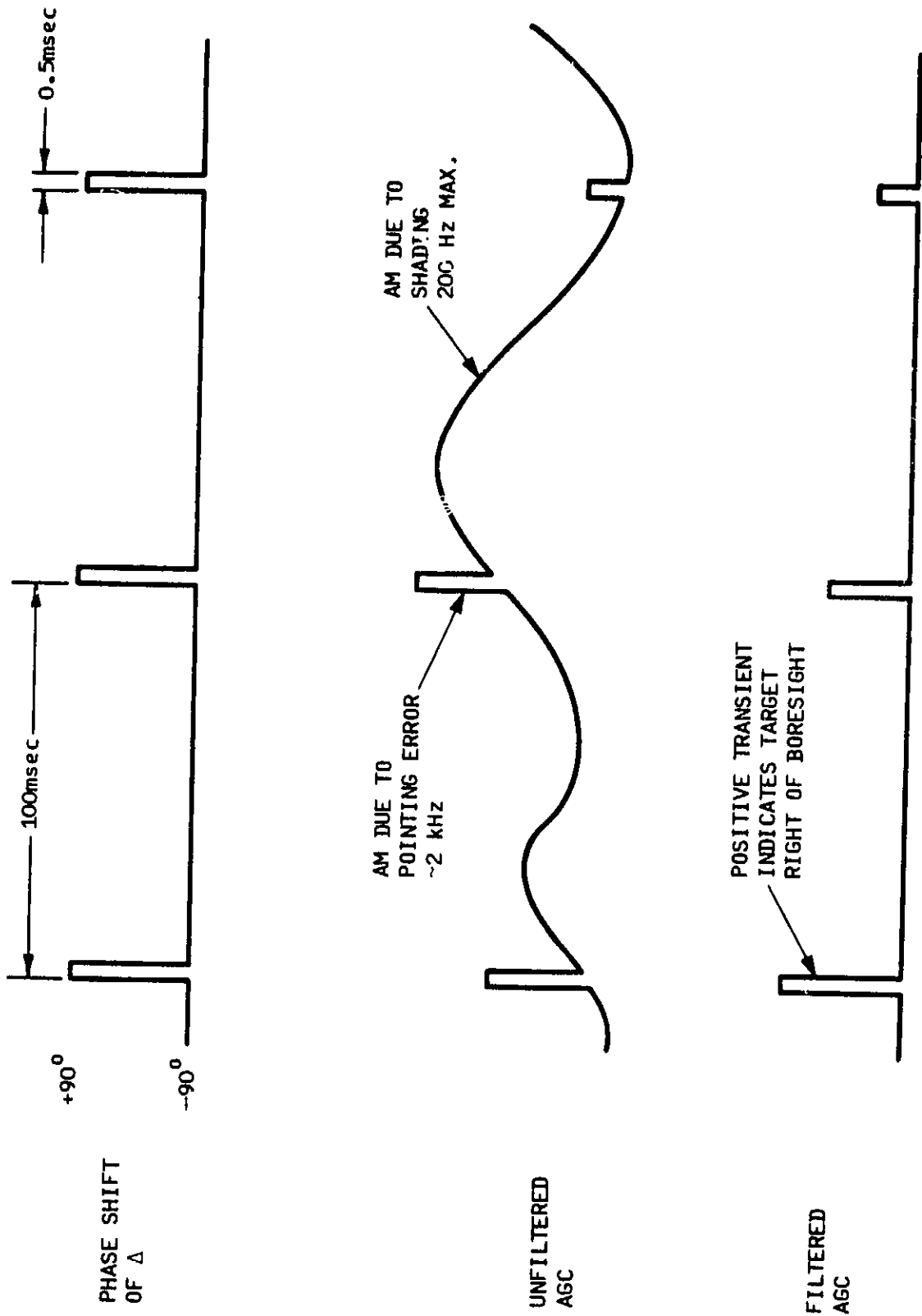
The final requirement that must be satisfied is that the pointing system not introduce signal variations of greater than 3 dB. Since the tracking error can only be updated at a maximum rate of 10 Hz, the antenna pointing error will be approximately 5 degrees during a 45 degree/second turn. By referring



\*SHOWN WITH SOME PHASE SHIFT FOR CLARITY

A/N 5090

Figure 3-10 Phasor Diagram Showing Amplitude Modulation Caused by Shifting Phase of  $\Delta$  Signal  $\pm 90^\circ$



A/N 5090

Figure 3-11 Pointing Error Determined by Synchronously Demodulating Transients in AGC and Phase Shifts of  $\Delta$  Signal



to Figure 3-12, it can be seen that in order to keep signal variation less than 3 dB when the pointing error is 5 degrees, the coupling factor ( $k$ ) of the directional coupler must be between -3 and -10 dB. This factor then determines the steady-state (i.e., not turning) pointing error. The AGC system in typical receivers is capable of detecting signal variation of 1 dB or less. Assuming the receiver in the mobile terminal has this capability results in a steady-state pointing error of between 1 to 2 degrees.

There are two drawbacks of this system. First, since this system uses amplitude modulation, the effective signal range over which the system can track a target is roughly 3 dB less than the system using phase detection (i.e., during turns the amplitude modulation caused by pointing errors will cause the receiver to lose lock sooner). Second, since the sample period for measuring tracking errors is short means the signal-to-noise ratio needed for acceptable performance will most likely need to be greater. A detailed analysis would have to be performed to be able to determine the exact signal-to-noise ratio requirements.

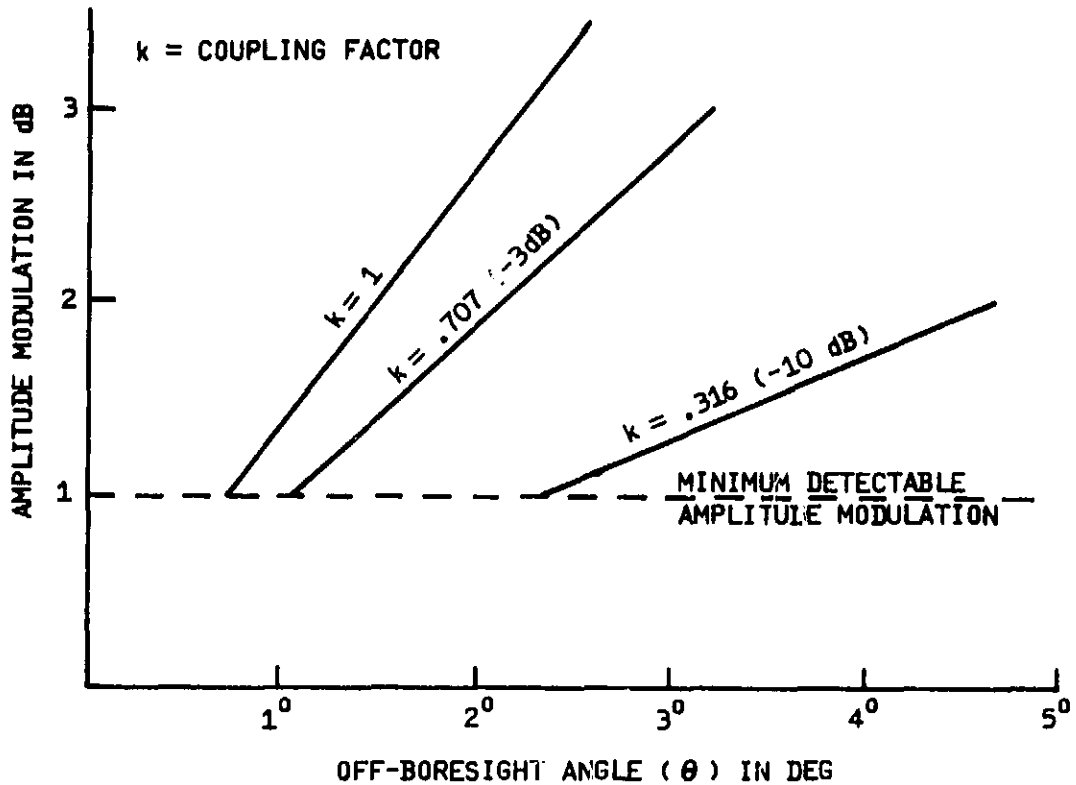
#### 3.2.1.2 Pointing Algorithms

The pointing algorithms for this system are basically the same as that used for the phase detection system. The only difference is that the pointing control system will monitor the AGC rather than the loop-phase-error to determine pointing errors. Please refer to paragraph 3.1.1.2 for a detailed description of the pointing algorithms.

#### 3.2.2 PERFORMANCE

##### 3.2.2.1 Pointing System Performance

The monopulse tracking system using amplitude detection is capable of satisfying all requirements. The performance of this system, in comparison to the other systems considered in this report, is summarized in paragraph 3.5.



A/N 5090

Figure 3-12 Amplitude Modulation of the Received Signal as a Function of Off-Boresight Angle and Coupling Factor (k)



### 3.2.2.2 Performance Variations

Multiple Satellites. This system suffers from the same limitation as the phase detection system in that in the multiple satellite system it is highly desirable to have all satellites use different frequencies for the pilot tone.

Shadowing. This pointing system will perform well in a shadowing environment; however, it probably will be more susceptible than the system using phase detection. Its ability to reacquire after a drop-out will be as good as the phase detection system because it uses the same pivot-point steering mechanism.

Different Antennas. This pointing system, like the phase detection system, is compatible with either of the two mechanically steered antenna concepts. It cannot be used with the electronically steered antenna because this antenna requires a complex and costly feed network in order to be able to develop the sum and difference signals.

Half-Duplex Operation. This pointing system will work well in the half-duplex mode of operation provided: 1) the pilot tone is transmitted on a separate frequency that doesn't have to be blanked during transmission by the mobile terminal, and 2) the AGC signal is derived from the pilot channel.

### 3.2.3 RELIABILITY

The failure modes for this system are the same as for the phase detection system. Please refer to paragraph 3.1.3.

### 3.2.4 HERITAGE

The heritage of this system is the same as the heritage of the phase detection system. Please refer to paragraph 3.1.4.



### 3.2.5 COSTS

The cost of this system is the same as the cost for the phase detection system. A cost breakdown of the complete pointing system is given in Section 4.0.

## 3.3 SEQUENTIAL LOBE TRACKING

### 3.3.1 System Concept Description

The sequential lobe tracking technique is simply the one dimensional version of the conical scan tracking technique used by many radar systems. With this system, pointing errors are determined by steering the peak of the antenna beam to the right and left of boresight. If the target is off-boresight, the antenna gain in the direction of the target will be greater for one beam position than it will be for the other. This causes the received signal to be amplitude modulated by an amount which is directly related to the pointing error. The pointing system determines the pointing error by demodulating the resultant amplitude modulation. Once again, special steps must be taken to make this system work in an environment where the amplitude of the received signal is varying rapidly due to shading. Once again, the solution to the problem is to modulate the pointing error information onto the received signal at a rate which is fast compared to the rate at which fading is expected to occur. In this way, the amplitude variations caused by fading during a sample period are small and have a negligible effect of the pointing error information.

The chief disadvantage of this technique is that it is unsuitable for mechanically steered antenna systems simply because the mechanical systems are incapable of steering the antenna at a rate which is fast compared to fading. However, the electronically steered antenna is, by its very nature, ideally suited to this tracking technique. It would be possible to electronically "dither" the beam of a mechanically steered antenna to produce the required effect. But this adds a great deal of complexity to these antennas and the performance is not as good as with monopulse tracking. For this reason, the



sequential lobe tracking system is considered in conjunction with the electronically steered antenna only.

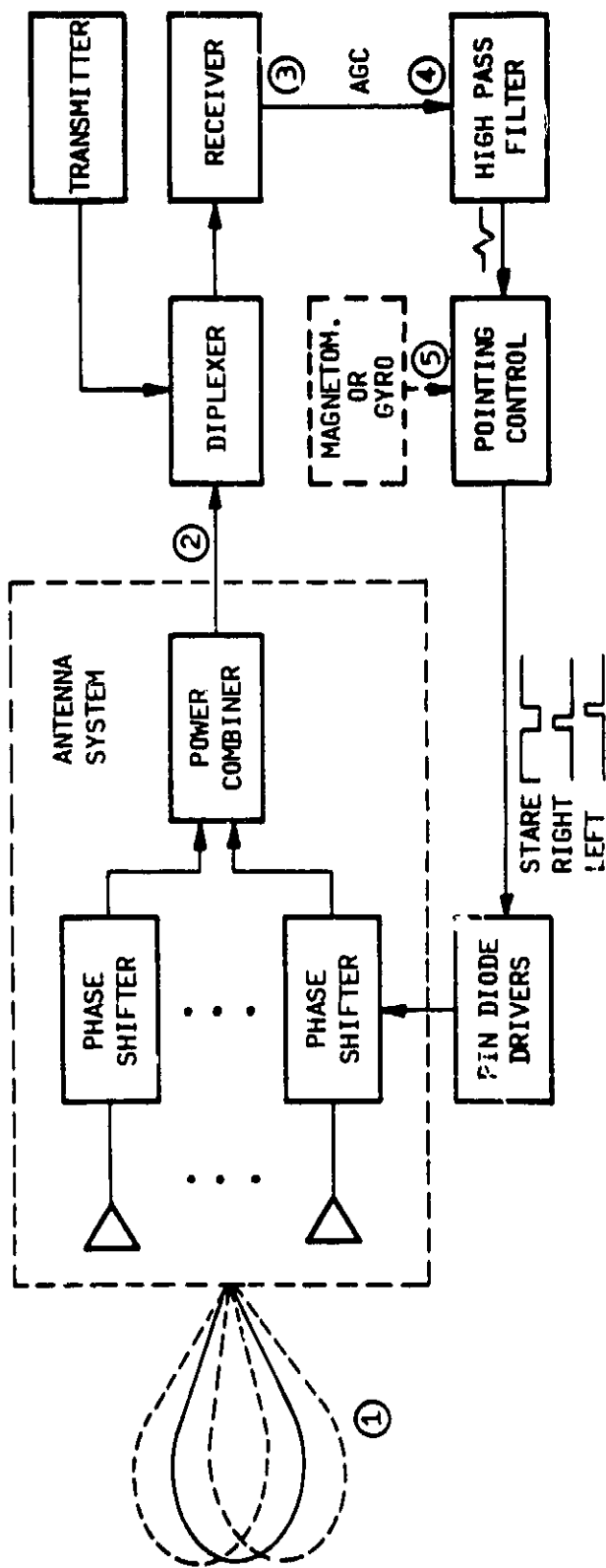
Since this system uses amplitude modulation like the monopulse system using amplitude detection, much of the analysis for this system is the same as that in paragraph 3.2. It is repeated here, however, for completeness.

### 3.3.1.1 Direction Sensing System

Figure 3-13 shows a block diagram of an electronically steered antenna system which uses sequential lobe tracking. The pointing system operates in "stare-scan" mode. The pointing system points the antenna in what it thinks is the right direction for a relatively long period and then quickly steers the antenna beam right then left at a rate fast compared to fading. The net result is to amplitude modulate the received signal with the pointing error information and the amount of modulation is directly related to off-boresight angle.

The resultant signal is input to the receiver where the AGC circuitry is used to detect the amplitude modulation. At this point, the AGC reflects the fact that the signal input to the receiver is amplitude modulated by both pointing error information and fading. The AGC signal output from the receiver is routed to the pointing control system where it is high-pass filtered. Since the pointing error information is modulated onto the received signal at a rate which is fast compared to fading, the high-pass filter can be designed such that it removes the modulation caused by fading, thereby providing the pointing control electronics with a "clean" signal containing only pointing error information. Finally, the pointing error information is determined by synchronously demodulating the filtered AGC signal with the scan code signal used to steer the antenna beam.

Once again, we use the balloon test data provided by JPL to define system parameters. From the JPL balloon tests, it is known that fading will occur at a maximum rate of approximately 200 Hz (assuming the vehicle is traveling at 55 mph). In order to make it easy to distinguish between pointing error information and fading (keep filtering easy), it is desirable to make the pointing



- ① • USES STARE/SCAN TRACKING METHOD
  - STARE - POINT BEAM AT TARGET FOR >90% OF THE TIME
  - SCAN - SCAN BEAM RIGHT AND LEFT ( $\pm 10^\circ$ ) AT FAST RATE ~10% OF THE TIME
- ② • SCANNING CAUSES AMPLITUDE MODULATION (AM) OF RECEIVED SIGNAL. AMOUNT OF AM IS DIRECTLY RELATED TO OFF-BORESIGHT ANGLE
- ③ • AGC IN RECEIVER DETECTS AM
- ④ • AM CAUSED BY FADING IS REMOVED BY FILTER
- ⑤ • POINTING SYSTEM DEMODULATES AM AND DETERMINES POINTING ERROR

A/N 5090

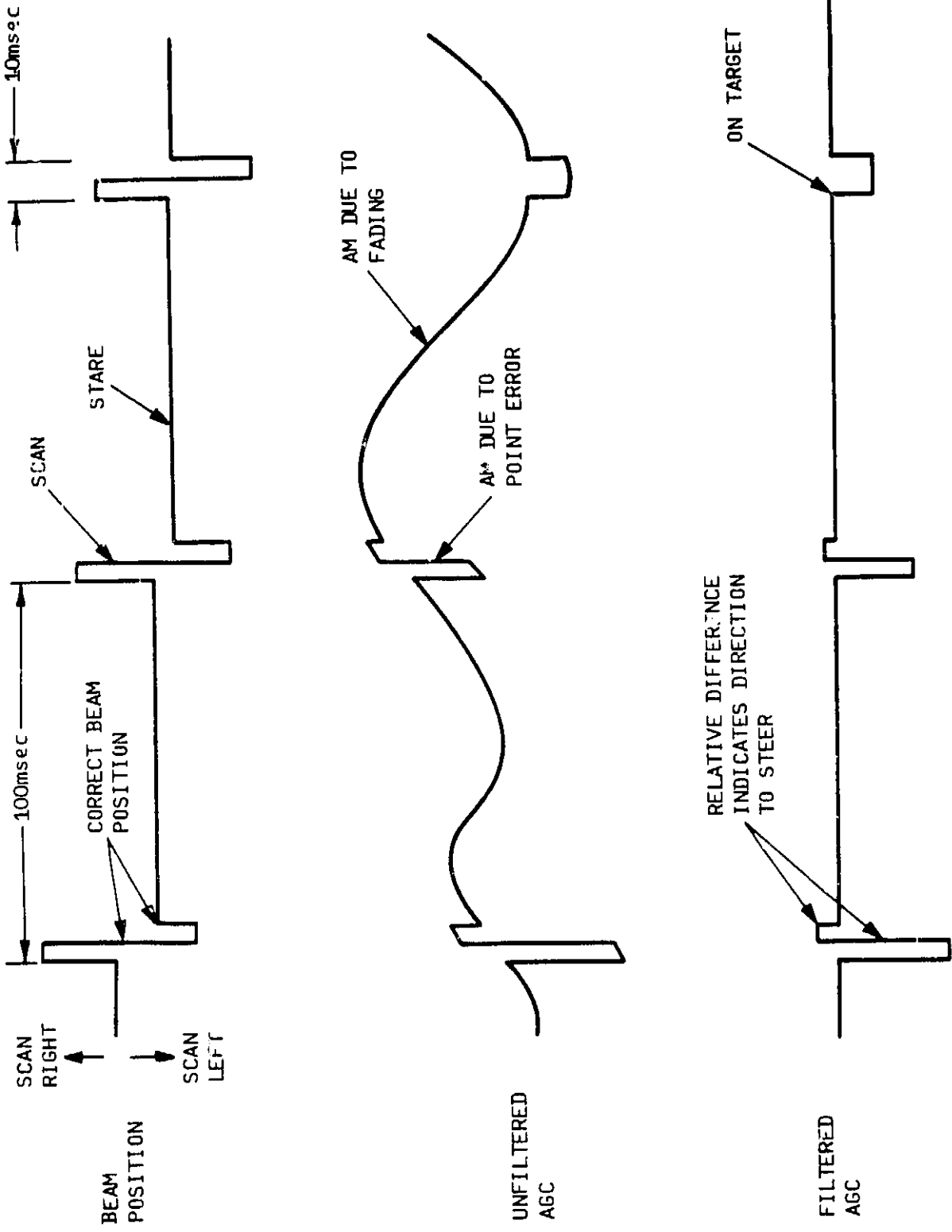
Figure 3-13 Sequential Lobing Tracking System



error sample rate roughly ten times faster than the fading rate, or, approximately 2 kHz. If this sample rate is used continuously, however, we violate the requirement that the pointing system not modulate the received signal at frequencies greater than 10 Hz. Figure 3-14 shows how we get around this problem. By keeping the antenna pointed in one direction for a relatively long period ("stare" mode - approximately 90 milliseconds) and then rapidly steering the beam to the right and left ("scan" mode - approximately 10 milliseconds), we are able to satisfy both requirements. The beam is scanned at a 2 kHz rate and causes a transient in the AGC (assuming the target is off-boresight) and the transients occur at a 10 Hz rate. The pointing system determines which direction to steer the beam by noting the relative difference in amplitude in the AGC for the two beam positions.

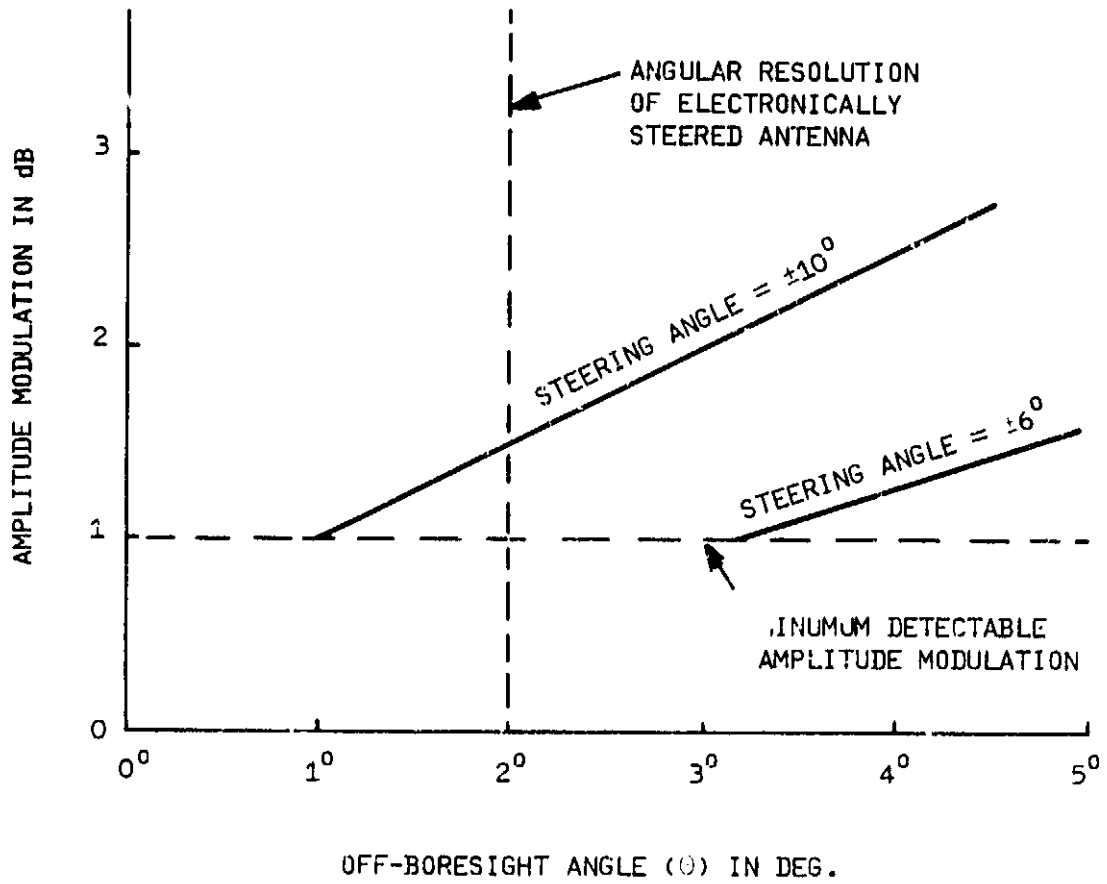
The final requirement that must be satisfied is that the pointing system not introduce signal variation of greater than 3 dB. Figure 3-15 is a graph which shows the amount of amplitude modulation of the received signal for various steering angles. Since the tracking error can only be updated at a maximum rate of 10 Hz, the antenna pointing error will be approximately 5 degrees during a 45 degree/second turn. By referring to Figure 3-15, it can be seen that in order to keep the signal variation less than 3 dB when the pointing error is 5 degrees, the antenna must be steered approximately 10 degrees. This factor then determines the steady-state (i.e., not turning) pointing error. The AGC in a typical receiver is capable of detecting signal variations of approximately 1 dB. Assuming the receiver in the mobile terminal has this capability results in a steady-state pointing error of less than 2 degrees. This matches nicely with the 2 degree beam position increments of the electronically steered antenna.

There are several disadvantages to this approach. The principle one is that during the period when the beam is being scanned, it may not be possible to meet the isolation specification. Figure 3-16 shows a plot of the antenna radiation pattern with the location of the two and three satellite systems superimposed when viewed from a location in Texas. As can be seen, steering the beam  $\pm 10$  degrees can cause wide variations in the gain in the direction of adjacent satellites. It is very difficult to predict exactly what the effect



A/N 5090

Figure 3-14 Pointing Error Determined by Synchronously Demodulating Transients in AGC and Beam Position



A/N 5090

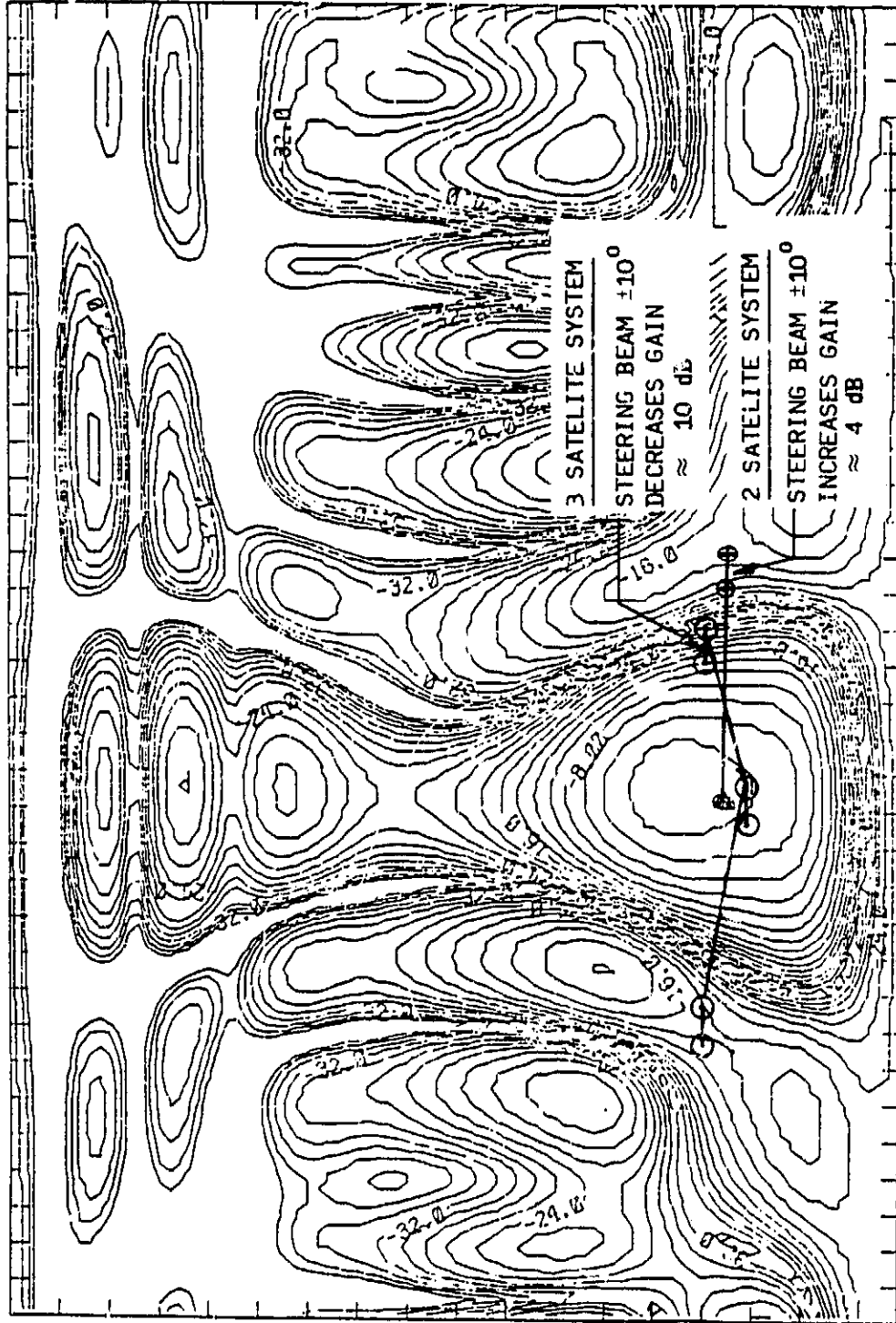
Figure 3-15 Amplitude Modulation can be Adjusted by Adjusting Steering Angle



(0.180)

TEXAS

(360.180)



(360.0)

PHI DEGREES  
(EACH TICK IS 10 DEGREES)

(0.0)

PHASED ARRAY WITHOUT TAPER (TEXAS)

A/N 5090

Figure 3-16 Effects of Steering Beam  $\pm 10^\circ$



on isolation will be since it is necessary to also account for changes in polarization losses as well as different locations within CONUS; however, it is reasonable to expect the isolation to decrease by a maximum of 3 to 5 dB. The potential for interference with adjacent satellites can be lessened by making the length of the scan cycle as short as possible and by making the steering angle as small as possible. Unfortunately, reducing the scan cycle increases the signal-to-noise ratio needed for acceptable performance and reducing the steering angle reduces the pointing accuracy. A detailed trade-off study must be performed in order to define the optimum value for these parameters.

A second problem with this system is that the electronically steered antenna does not have the open-loop inertia feature of the mechanically steered antennas. This means that if the signal is lost during a turn, the beam could be off-pointed by a large amount. This problem is mitigated by the fact that the electronically steered antenna can be steered at very high rates, allowing it to reacquire the target in about the same amount of time as the mechanically steered antenna.

### 3.3.1.2 Pointing Algorithms

Figure 3-17 is a flow diagram showing the sequence of events the pointing system follows as it acquires and tracks the target. It is assumed that both the vehicle and base station must be able to make contact at any time. This makes it necessary for the the MSAT-X satellite to continually transmit the pilot tone. Once the vehicle is started, the pointing system scans the beam in a clockwise direction at 180 degrees/second while it monitors the AGC. Since the electronically steered antenna has two elevation beam positions, it must first scan a full 360 degrees at one elevation and then make another 360 degree scan at the second elevation. The pointing system "remembers" the location where the maximum AGC reading was observed. If the AGC at this location exceeds a predefined "acquisition" threshold (maximum expected signal level minus 5 dB fade), the pointing system switches the beam to that location. If the AGC at this location does not exceed the acquisition threshold the pointing system repeats the acquisition sequence. In a non-fading environment, the entire acquisition sequence is expected to take less than 4 seconds.

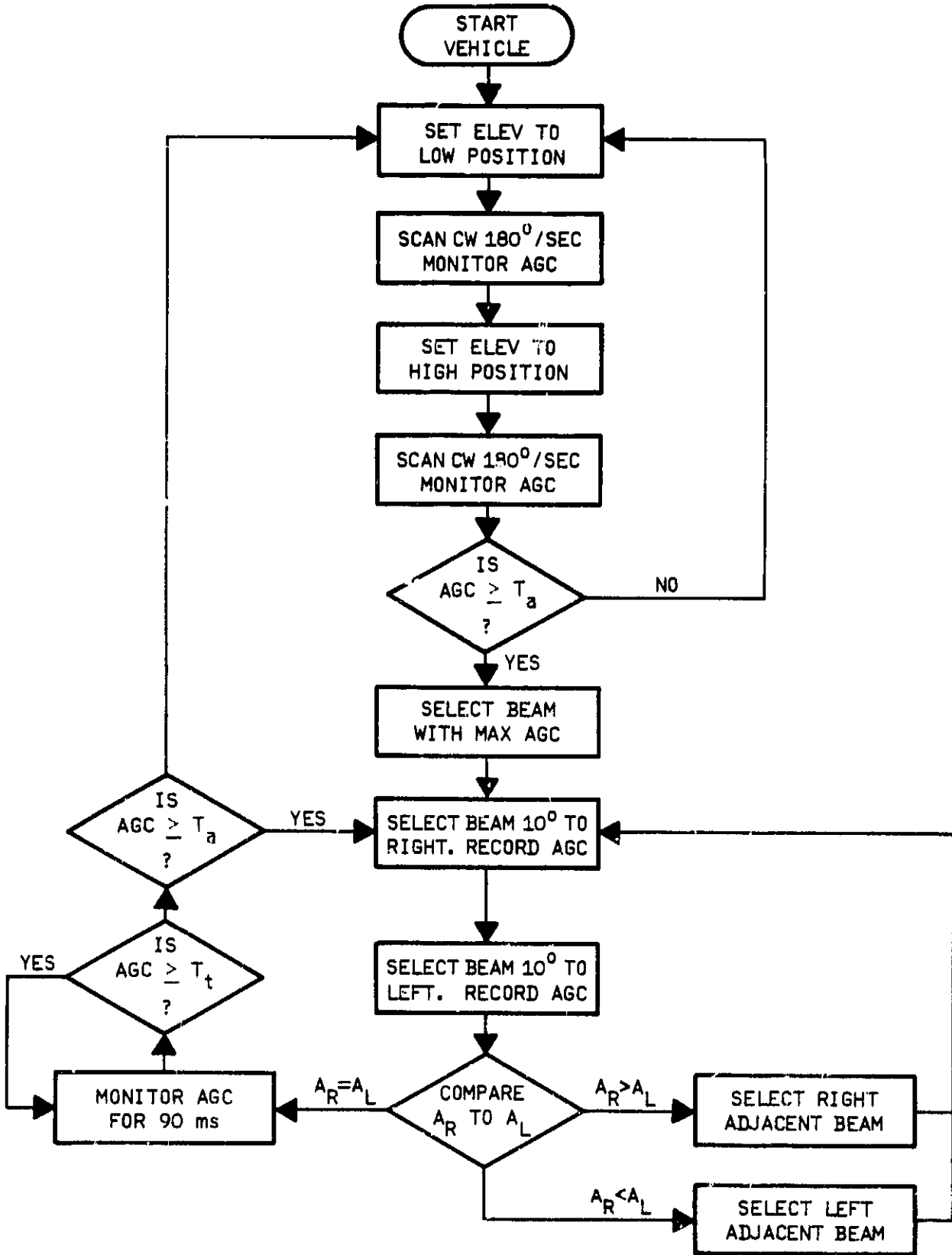


Figure 3 17 Sequential Lode Tracking System Operations Flow Diagram

A/N 5090



Once the target is acquired, the pointing system enters the scan mode. The pointing system determines the antenna pointing error by noting the relative difference in AGC as the beam is steered to the right and left 10 degrees. It then makes the appropriate corrections.

Once the antenna is locked on target, the operation of the system is designed to minimize the time the antenna spends in the scan mode in order to minimize the potential for interference with adjacent satellites. The pointing system monitors the AGC for approximately 90 milliseconds. If the AGC exceeds a pre-defined "tracking" threshold (signal level expected when the target is within 2 degrees of boresight) at some time during this period, the pointing system assumes it is on target (no corrections needed) and proceeds to monitor the AGC for another 90 milliseconds. If the AGC does not exceed the tracking threshold, the pointing system verifies that it is within the "lock-on" ( $\pm 10^\circ$ ) range by checking to see if the acquisition threshold has been exceeded within the last 90 milliseconds. If it has, the pointing system assumes the vehicle has turned and it enters the scan mode. If the signal hasn't exceeded the acquisition threshold the pointing system assumes it has lost the target and it reenters the acquisition sequence. This feature allows the pointing system to track targets during fades of up to 5 dB which last for up to 90 milliseconds.

### 3.3.1.3 Interfaces

Transceiver Interfaces. The interfaces for this pointing system are simple and straightforward. The receiver must provide an AGC signal which is accurate to within 1 dB. The interface characteristics of this signal can be the customary 0 to 5 volt analog.

Vehicle Interfaces. The vehicle must provide power to the pointing system.

User Interfaces. This system does not require any user interfaces; however, options such as an "on-target" indicator and "reset button" may be desirable.



### 3.3.2 PERFORMANCE

#### 3.3.2.1 Pointing System Performance

This pointing system satisfies all requirements. The performance of this pointing system in comparison to the other pointing system considered in this report is summarized in Section 3.5.

#### 3.3.2.2 Performance Variations

Multiple Satellites. This system will work well in a multiple satellite system; however, there is a greater potential for interference with adjacent satellites. The potential for locking onto the wrong satellite is also greater and therefore it is even more desirable for all satellites in the multiple satellite system to use unique frequencies for the pilot tones.

Shadowing. Under normal conditions, the electronically steered antenna works as well as the mechanically steered antennas; however, in a severe fading environment the electronically steered antenna may not perform as well. With the electronically steered antenna system, fades which are more than 5 dB and last longer than approximately 90 milliseconds cause the pointing system to reenter the acquisition sequence whereas the mechanically steered antenna systems can tolerate a total loss of signal for up to 4 seconds. Although the electronically steered antenna does not perform as well in this environment, it can still fully satisfy requirements and its ability to scan the beam at high rates allows it to rapidly reacquire the target.

Different Antennas. As was explained earlier, the sequential lobe tracking system is best suited to the electronically steered antenna system. It can be used with mechanically steered antennas but the ability to electronically "dither" must be added which increases cost and the performance of this system is not as good as the monopulse systems.

Half-Duplex Operation. This pointing system, like the other active pointing systems, will work well in the half-duplex mode provided, 1) the pilot tone is



transmitted on a separate frequency that doesn't have to be blanked during transmission by the mobile terminal, and 2) the AGC is derived from the pilot channel.

### 3.3.3 RELIABILITY

This pointing system has an advantage over the mechanically steered systems in that it does not have any wear-out items but it suffers from the fact that it is more complex. The life expectancy of the system is expected to be equal to or better than the mechanically steered systems.

### 3.3.4 HERITAGE

The concepts used in this pointing system are well known and have seen wide application in radar systems. Only simple straightforward adjustments have been made to make this system better suited to environments where the signal is fading rapidly.

### 3.3.5 COSTS

The cost of the direction sensing system is minimal since all it requires is the electronics needed to demodulate the AGC signal output from the receiver. The cost of the electronics is expected to be about \$150 per unit in large quantities. A cost breakdown of the complete pointing system is given in Section 4.0.

## 3.4 MAGNETOMETER POINTING SYSTEM

### 3.4.1 System Concept Description

The open-loop pointing system considered for this report uses a magnetometer (compass) to determine the location of magnetic north and, from that information, derive the location of the MSAT-X satellite. Magnetometers have seen wide application in satellite attitude control systems, as direction finding systems in aircraft, and to correct drift in gyroscopes.



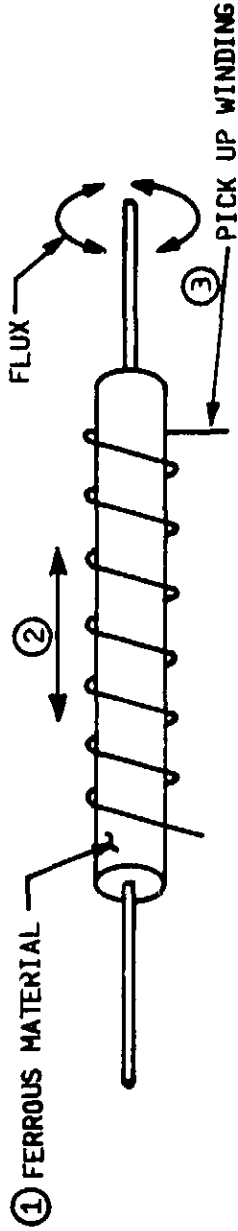
#### 3.4.1.1 Direction Sensing System

The heart of the magnetometer is the fluxgate. It is the transducer that converts a magnetic field into an electrical voltage. Its main component is a piece of easily saturable ferrous material wrapped about a cylinder. An alternating current is passed along the axis of the cylinder creating a magnetic field normal to the axis of the cylinder that periodically saturates the material first clockwise and then counterclockwise (see Figure 3-18).

A pick-up winding is wrapped around the cylinder. While the ferrous material is between saturation extremes, it maintains a certain average permeability. While in saturation, this permeability ( $\mu = dB/dH$ ) becomes one (an increase in driving field  $H$  produces the same increase in flux  $B$ ). If there is no component of magnetic field along the axis of the cylinder, the flux change seen by the pick-up winding is zero since the excitation flux is normal to the axis of the winding. If, on the other hand, a field component is present along the cylindrical axis, then each time the ferrous material goes from one saturation extreme to the other it produces a pulse output on the signal pick-up winding that is proportional to the external magnetic field and the average permeability of the material.

A block diagram of a typical magnetometer electronics is shown in Figure 3-19. Basically, the purpose of this electronics is to generate the AC signal that is passed along the axis of the fluxgate and to convert the AC signal output on the pickup winding into a DC signal whose amplitude is directly related to the amplitude of the external magnetic field.

Two fluxgates oriented at 90 degrees to each other are needed in order to be able to generate a north pointing vector; however, one set of electronics which is switched between the two fluxgates would be adequate. The pointing control system would read the outputs of the two fluxgates, determine the magnetic north vector, calculate the off-set to the MSAT-X satellite and finally steer the antenna to the appropriate direction. Magnetometers can be designed to provide very good accuracy (less than 2 degrees) but for this application,



• **MAGNETOMETER: A TRANSDUCER THAT CONVERTS MAGNETIC FIELDS INTO ELECTRIC VOLTAGE**

• **THEORY OF OPERATION**

- ① **MAIN COMPONENT IS EASILY SATURABLE FERROUS MATERIAL WRAPPED AROUND CYLINDER (FLUX GATE)**
- ② **AC CURRENT IS PASSED ALONG AXIS OF CYLINDER CREATING MAGNETIC FIELD NORMAL TO AXIS OF CYLINDER WHICH SATURATES FERROUS MATERIAL CLOCKWISE THEN COUNTER-CLOCKWISE.**
- ③ **IF EXTERNAL MAGNETIC FIELD ALONG CYLINDER AXIS IS PRESENT, THEN PULSE IS OUTPUT ON PICK-UP WINDING EACH TIME FERROUS MATERIAL GOES FROM ONE SATURATION EXTREM TO THE OTHER.**

**TWO FLUX GATES ARE NEEDED TO DEFINE NORTH VECTOR**

**A/N 5090**

**MAGNETOMETER (COMPASS) POINTING SYSTEM**



Figure 3-18 Magnetometer Fluxgate

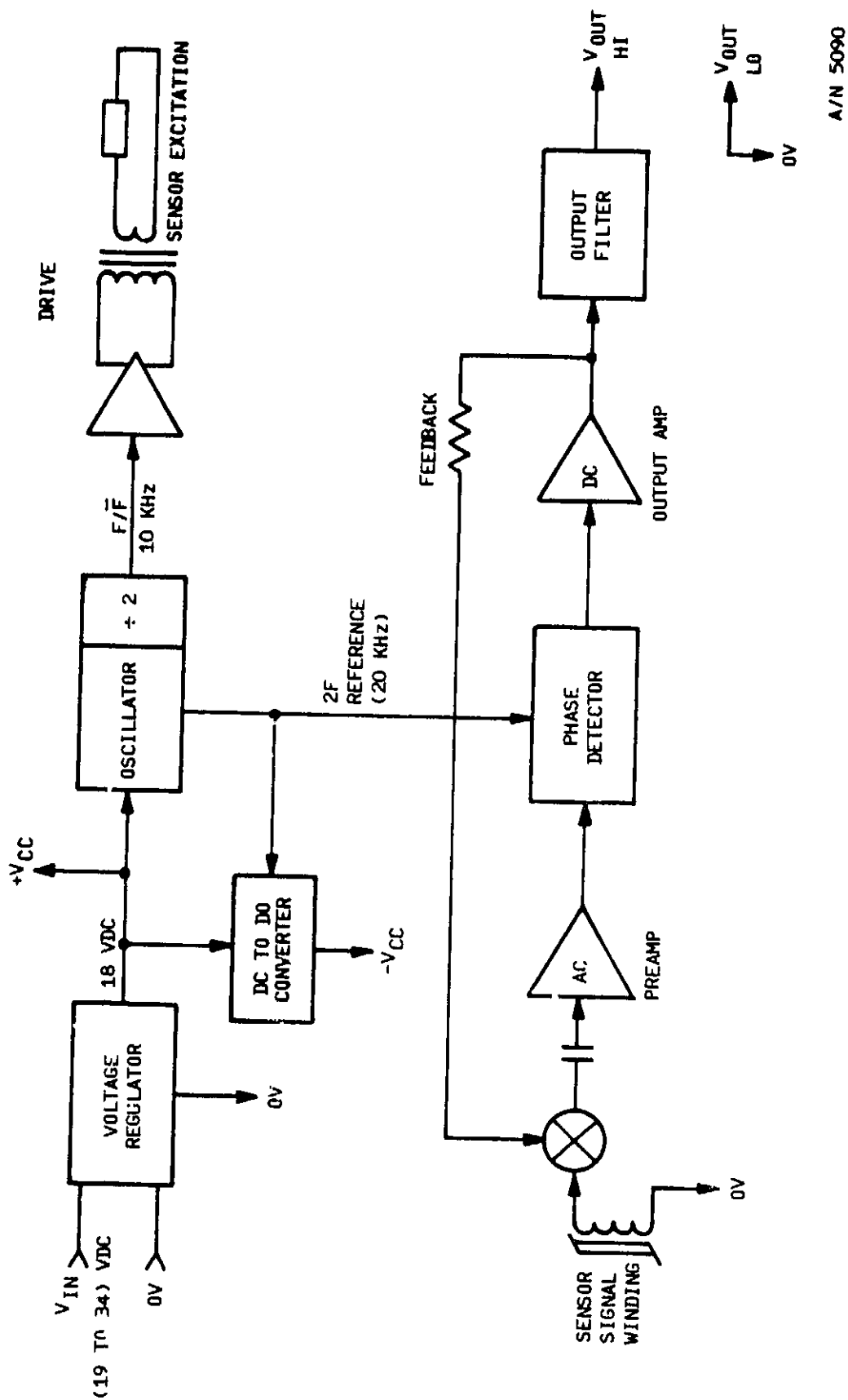


Figure 3-19 Magnetometer Block Diagram



a 2 to 3 degree accuracy is probably adequate when the other sources of error are taken into account.

There are a number of disadvantages to using a magnetometer pointing system. The principle one is that the angle between north and the direction to the satellite varies across the continental United States. For example, if the MSAT-A satellite is located at 105 degrees west longitude, a user in New York must steer his antenna approximately 200 degrees clockwise from north while a user in California must steer his antenna 160 degrees clockwise from north. Then on top of this is the fact that across CONUS magnetic north differs from true north by as much as 22 degrees. To complicate the picture even more is the fact that the local magnetic field can be perturbed by large iron ore deposits and other large metal objects such as bridges and other vehicles.

A user interface is the most practical way to overcome these obstacles. A meter which displays the received signal strength and a knob which controls the antenna azimuth angle would be provided. After the user starts his vehicle, he adjusts the position of the antenna while monitoring the AGC meter until the maximum signal strength is achieved. He then pushes a button which "loads" the antenna location relative to the magnetometer reading into the pointing control system. The pointing system then maintains that orientation from that point on. Once the pointing system has been initialized, a user traveling cross country would only need to update his system every few hours. A user traveling locally would probably never need to update his system.

There are several features which may be desirable upgrades to the basic system. First, to simplify acquiring the target, it may be desirable to provide an audible tone which varies in frequency depending on received signal strength. This would allow the user to tune his terminal while driving in much the same way he would tune his radio. Also to help speed up acquisition, the pointing system should "remember" the antenna/magnetometer orientation even after the vehicle is turned off. Finally, to help maintain tracking, a warning light triggered by the loss of signal may be desirable.



### 3.4.1.2 Pointing Algorithms

Since acquisition of the target is controlled by the user, the pointing algorithm is minimal. The pointing system is only required to maintain a fixed relationship between the antenna orientation and the magnetometer reading.

### 3.4.1.3 Interfaces

Transceiver Interfaces. The transceiver must provide an AGC signal which is accurate to within 1 dB. The interface characteristics of this signal can be the customary 0 to 5 volt analog.

Vehicle Interfaces. The vehicle must provide power to the pointing system and a location for a control and status panel.

User Interfaces. This system requires a fair amount of user interfaces in order to acquire the target. These processes are described in Section 3.4.1.1.

## 3.4.2 PERFORMANCE

### 3.4.2.1 Pointing System Performance

This pointing system is capable of satisfying all requirements; however, it probably will provide the poorest performance. The performance of this system, in comparison to the other pointing system considered in this report, is summarized in Section 3.5.

### 3.4.2.2 Performance Variations

Multiple Satellites. This pointing system will work in a multiple satellite environment; however, its pointing accuracy is not as good as the active systems and it is easily perturbed (i.e., improper tuning, metal objects, etc.). Therefore, the probability of interference with adjacent satellites is greater. In order for the user to be able to easily acquire the proper satellite, it is imperative for all satellites in the multiple satellite system to transmit the pilot tone on unique frequencies in addition to using cross



polarization. This will allow him to manually select the desired satellite by "dialing" the correct frequency.

Shadowing. The chief advantage of any open-loop pointing system is that it is completely impervious to shadowing. It will maintain the proper antenna orientation regardless of how deep the fades are or how long they last.

Different Antennas. This pointing system is compatible with either the electronically or mechanically steered antenna systems.

Half-Duplex Operation. Another major advantage of open-loop pointing systems is that they allow half-duplex operation without putting any restriction on the satellite or transceiver. Unlike the active pointing systems, both the data and pilot channels can be transmitted on the same frequency and both can be blanked during transmission without affecting the ability of the system to point the antenna.

#### 3.4.3 RELIABILITY

The reliability of this pointing system is determined mainly by the type of steering mechanism it is used with. The addition of the magnetometer should not affect the overall reliability of the system.

#### 3.4.4 HERITAGE

Magnetometers have seen wide application as part of spacecraft attitude control systems, direction finding equipment on aircraft, and as a means of correcting gyroscope drift. BASD has had personal experience with magnetometers, having flown them on more than ten spacecraft.

#### 3.4.5 COST

The cost of the direction sensing system, which includes the electronics and fluxgate, is expected to cost about \$150 in large quantities which is comparable to the cost of the monopulse or sequential lobing electronics. A cost breakdown of the complete pointing system is given in Section 4.0.

C-2



### 3.5 PERFORMANCE SUMMARY

The performance of the four types of pointing systems addressed in this report are summarized in Table 3-1. It is difficult to say one system is better than the other since each has some things it does better than the others. However, based on pointing performance and ease of operation, the closed-loop systems are better than the open-loop system. Of the three types of closed-loop systems considered, the monopulse tracking systems are better than the sequential lobe system since it performs better in a fading environment and has fewer problems with adjacent channel interference. Of the two monopulse tracking systems, the one using phase detection has a slight advantage over the one using amplitude detection since it performs better in a fading environments.



Table 3-1  
POINTING SYSTEM PERFORMANCE COMPARISON

Parameter	Single-channel Monopulse <sup>1</sup>		Sequential <sup>2</sup> Lobing	Magnetometer <sup>1</sup>	
	Phase Det.	Amplitude Det.			
<ul style="list-style-type: none"> <li>Acq. Time               <ul style="list-style-type: none"> <li>• Typical</li> <li>• Min.</li> <li>• Max.</li> </ul> </li> <li>Reacq. Time<sup>3</sup> <ul style="list-style-type: none"> <li>• Typical</li> <li>• Min.</li> <li>• Max.</li> </ul> </li> </ul>	2 Sec 2 Sec 24 Sec	2 Sec 2 Sec 24 Sec	4 Sec 4 Sec 4 Sec	10-20 Sec <sup>4</sup> " Sec " Sec	
	<ul style="list-style-type: none"> <li>Tracking               <ul style="list-style-type: none"> <li>• Rate</li> <li>• Accel.</li> <li>• Accuracy</li> </ul> </li> <li>Ops in Fade</li> </ul>	3 Sec 2 Sec 4 Sec	3 Sec 2 Sec 4 Sec	4 Sec 4 Sec 4 Sec	0 Sec 0 Sec 0 Sec
		15°/Sec 15°/Sec 1° Stat; 5° Turn	15°/Sec 15°/Sec 2° Stat; 5° Turn	180°/Sec NA 2° Stat; 6° Turn	0°/Sec NA 3° - 22°
Excellent - operates down to level where RCVR drops lock		Good - amplitude modulation reduces allowed fade by 3 dB	OK unless mag. or gryo	Unaffected	

1. Assumes mechanically steered antenna  
 2. Assumes electronically steered antenna  
 3. Assumes drop-out during 90° turn  
 4. Assumes manual acquisition



Table 3-1  
POINTING SYSTEM PERFORMANCE COMPARISON (CONTINUED)

Parameter	Single-channel Phase Det.	Monopulse <sup>1</sup> Amplitude Det.	Sequential <sup>2</sup> Lobing	Magnetometer <sup>1</sup>
<ul style="list-style-type: none"> <li>• Factors Limiting Performance</li> <li>• Antenna Type</li> <li>• Half Duplex</li> <li>• Multiple Satellite</li> <li>• Interfaces</li> </ul>	<ul style="list-style-type: none"> <li>• Effects on Data</li> <li>• Mech. Steered</li> <li>• Separate Pilot Channel Desirable</li> <li>• Unique Pilot Freq. Desirable</li> <li>• Most Complex AGC &amp; PLL</li> </ul>	<ul style="list-style-type: none"> <li>• Amplitude Mod. Causing Dropout</li> <li>• Mech. Steered</li> <li>• Same</li> <li>• Same</li> <li>• Same</li> <li>• AGC 1 dB Accuracy</li> </ul>	<ul style="list-style-type: none"> <li>• Amplitude Mod. Causing Dropout</li> <li>• Elec. Steered</li> <li>• Same</li> <li>• Same</li> <li>• AGC 1 dB Accuracy</li> </ul>	<ul style="list-style-type: none"> <li>• Geographic Loc. Dependent</li> <li>• All</li> <li>• Excellent</li> <li>• Same</li> <li>• Complex User Interface</li> </ul>



## SECTION 4.0 ANTENNA SYSTEM COST

In evaluating the cost drivers for the production of three types of antennas, the Mechanically Steered 1 x 4 Tilted Microstrip Array Antenna, the Mechanically Steered Conformal Array Antenna and the Electronical Scanned Conformal Phased Array Antenna, the following major cost factors are identified.

- 1) Labor - The largest portion of the cost of producing an antenna is labor costs. Labor costs are dependent on design and quantity produced. Assume the design is as producible as is possible, the production labor is then related to the quantity of units to be produced. If the expected quantity is large enough to justify a large expenditure to automate production and testing, labor cost can be reduced. The amount of reduction that can be achieved can only be estimated by using existing large volume products as a guideline. An automobile radio as an example can be made with a labor cost about equal to the material cost. Material costs are also reduced with large volume usage. To achieve the same level of cost reduction in antennas as achieved with automobile radios requires quantities approaching those of automobile radios. The amount of labor cost reduction depends on the amount of automation justified which is dependent on volume.
- 2) Material - Material costs are dependent on quality of the components and on the quantity used. The reduction in material cost per unit is not near as dependent on volume as is the labor reduction with large volumes.
- 3) Design - The design has an obvious impact on production costs. Again the anticipated volume sets the amount that is justified in design and redesign to achieve lowest production cost. The electronically steered antenna has the potential for greatest cost reduction with increased design effort.



It is a vicious circle. The greater the volume produced the lower the unit cost. The lower the unit cost the greater possibility for marketing a large volume of units.

It is a question, unanswered at this time, what number of units justify the expenditures required to drive cost to a minimum. It is felt that 100,000 units does not justify complete automation.

Production of antennas in quantities of 100,000 units may make it possible to reduce unit cost up to one-half the cost of production quantities of 10,000 or less. However, it is still a matter of producing a few units to determine more accurately large volume unit cost. Table 4-1 shows the relative major cost drivers for the three LMV antenna concepts. In Table 4-2 we show our projected unit cost estimates for production of 10,000 and 100,000 units. The accuracies are estimated to be within  $\pm 25\%$ . However, these accuracies are dependent on the initial details of the designs and on the development of a few prototypes. We believe at this phase of the program, it is very difficult to have highly accurate per unit cost figures with even no breadboard model. In Table 4-3, we show some breakdown costs of the three antenna concepts.

The estimates were performed by highly experienced personnel in the production of large volume antennas. The figures were also based on the experiences gained from a few large volume existing programs.



Table 4-1  
ANTENNA MAJOR COST DRIVER

	Major Cost Driver	
	<u>Labor</u>	<u>Parts and Material</u>
1 x 4 Mechanically Steerable Tilted Array	Low-Medium	Medium
Mechanically Steered Conformal Array	Medium	Medium
Electronically Scanned Conformal Array	High	High

Table 4-2  
COST ESTIMATES

	Cost/Unit (Dollars)	
	<u>10,000</u>	<u>100,000</u>
1 x 4 Mechanically Steerable Tilted Array	800	500-600
Mechanically Steered Conformal Array	1300	700-900
Electronically Scanned Conformal Array	2800	1000-2000



Table 4-3  
PER UNIT COST BREAKDOWN IN QUANTITIES OF 10,000 FOR THREE TYPES OF ANTENNAS

Mechanically Steered 1 x 4 Tilted Microstrip Array	Mechanically Steered Fixed-Beam Conformal Array	Electronically Steered Conformal Array
Radome \$ 20	Radome \$ 20	Radome \$ 20
1 x 4 Antenna (Radiating Elements, Hybrids, & Power Divider) 150	Antenna Hybrids & Power Divider 600	Antenna & Hybrids Board 600
Cables, Phase Shift Switch, Diplexer & Coupler 50	Cables, Phase Shift Switch, Diplexer & Coupler 50	Phase Shifters & Power Divider Board 1250
Rotary Joint 50	Rotary Joint 50	Material Board, \$ 750 Etching, Trim- ing, etc.
Motor 75	Motor 75	PIN, Diodes, 350 Caps, Resistors, etc.
Bearing, Tachometer Shaft & Housing 200	Bearing, Tachometer, Shaft & Housing 200	Parts Placements 150 \$1250
Assembly 75	Assembly 100	Miscellaneous (Feed Pins, 250 Conformal Coatings, Frames, Connectors, Cables, Etc.)
Electronics 125	Electronics 125	Assembly 350
Test 50 \$795	Test 75 \$1295	Electronics 150
		Test 200 \$2820



APPENDIX A  
SINGLE CHANNEL MONOPULSE TRACKING SYSTEM  
USING PHASE MODULATION

In a conventional single channel monopulse tracking system, sum ( $\Sigma$ ) and difference ( $\Delta$ ) signals are generated by a  $180^\circ$  hybrid. The phase of the  $\Delta$  signal is then shifted 0 and  $180^\circ$  at some predefined clock rate and then a portion of the  $\Delta$  signal is added to the  $\Sigma$  signal by means of a directional coupler. The net effect is that the  $\Sigma$  signal is amplitude modulated by the  $\Delta$  signal.<sup>1</sup> However, special steps must be taken in order to make this system work in an environment where the received signal is varying rapidly due to shading. One way to solve this problem is to use phase modulation instead of amplitude modulation. Figure A-1 illustrates how this can be done in a simple, yet effective manner.

As in conventional single channel monopulse systems, this system uses two identical antenna systems which "look" in the same directions. The strength of the received signals from the two antennas will vary both as a function of time ( $t$ ) due to shading and as a function of the angle ( $\theta$ ) between the bore-sight of the antennas and the target. Thus, the real part of the electric field of the signal received by the two antennas can be expressed as;

$$E_A = A(\theta, t) \cos(\omega t + \phi_A)$$

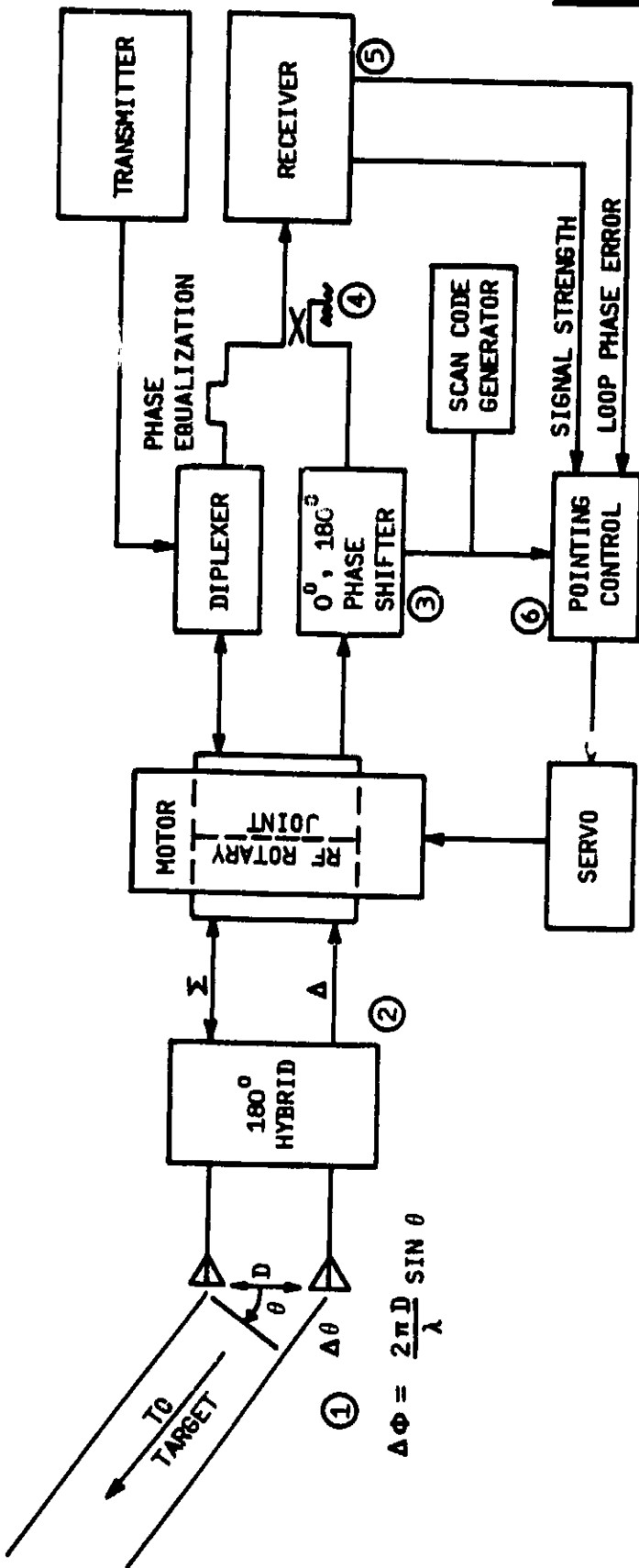
$$E_B = B(\theta, t) \cos(\omega t + \phi_B)$$

where,

$A(\theta, t)$  = the amplitude of the received signal at the A antenna

$B(\theta, t)$  = the amplitude of the received signal at the B antenna

1. Electromagnetic Science Inc., Technical Bulletin No. 022873-1, Single Channel Monopulse Converters.



- ① PHASE DELAY DIRECTLY RELATED TO OFF-BORESIGHT ANGLE (  $\theta$  ) AND IS UNAFFECTED BY FADING
- ②  $\Sigma$  AND  $\Delta$  SIGNALS GENERATED BY HYBRID COUPLER
- ③ PHASE OF  $\Delta$  SHIFTED  $0^\circ$  AND  $180^\circ$
- ④  $\Delta$  SIGNAL PHASE MODULATES (PM)  $\Sigma$  SIGNAL. AMOUNT OF PM IS DIRECTLY RELATED TO  $\theta$
- ⑤ PHASELOCK LOOP IN RECEIVER DETECTS PHASE MODULATION
- ⑥ POINTING SYSTEM DEMODULATES PM AND DETERMINES POINTING ERROR.

A/N 5090

Figure A-1 Single-Channel Monopulse Tracking - Phase Detection



$\omega$  = the angular frequency of the received signal

$\phi_A$  = the phase of the received signal at the A antennas

$\phi_B$  = the phase of the received signal at the B antenna.

Since the two antennas are separated by some distance  $D$ , the phase of signals received by the two antennas will differ by an amount equal to

$$\Delta\phi = \frac{2\pi D}{\lambda} \sin \theta$$

where;

$D$  = distance between antennas

$\lambda$  = wavelength of the received signal

$\theta$  = off-boresight angle.

To simplify the analysis, let us assume the antennas need to be steered clockwise to get "on-target" and that  $\phi_A = 0$ . Under these conditions,  $\phi_B = \Delta\phi$  and since the antennas are identical and look in the same direction,  $A(\theta, t) = B(\theta, t)$ . To make the presentation easier to follow, we will let  $A(\theta, t) = B(\theta, t) = A$  for the remainder of the analysis.

The received signals are routed from the antenna to a  $180^\circ$  Hybrid where  $\Sigma$  and  $\Delta$  signals are generated. The input signal from the A antenna is coupled into both the  $\Sigma$  and  $\Delta$  outputs and both outputs are in-phase with the input signal. Similarly, the input from the B antenna is coupled into the  $\Sigma$  and  $\Delta$  outputs, however, the phase of the signal at the  $\Delta$  output is shifted  $180^\circ$  relative to the input signal while the signal  $\Sigma$  output is in-phase with the input signal. The resultant  $\Sigma$  and  $\Delta$  signals are given by

$$\begin{aligned}\Sigma &= \frac{1}{\sqrt{2}} A \cos(\omega t) + \frac{1}{\sqrt{2}} B \cos(\omega t + \Delta\phi) \\ &= \frac{A}{\sqrt{2}} [\cos(\omega t) + \cos(\omega t + \Delta\phi)]\end{aligned}$$



and

$$\begin{aligned}\Delta &= \frac{1}{\sqrt{2}} A \cos(\omega t) + \frac{1}{\sqrt{2}} B \cos(\omega t + \Delta\phi + 180^\circ) \\ &= \frac{A}{\sqrt{2}} [\cos(\omega t) - \cos(\omega t + \Delta\phi)]\end{aligned}$$

Thus, when two equal amplitude, equal frequency signals are input to a 180° Hybrid, the magnitude of the resultant  $\Sigma$  and  $\Delta$  output signals vary based on the phase of the input signals. For example, when the target is on boresight ( $\theta = 0^\circ$ )  $\Delta\phi = 0$ ,  $\Delta = 0$ , and  $\Sigma = \sqrt{2} A \cos \omega t$  which means when the target is on boresight, the total received signal power of both antennas appears in the  $\Sigma$  output and no power appears in the  $\Delta$  output.

The  $\Delta$  signal is then shifted in phase either 0° or 180° depending upon the state of the "scan code generator". The resultant signals are

$$\Delta_0 = \frac{A}{\sqrt{2}} [\cos(\omega t) - \cos(\omega t + \Delta\phi)]$$

and

$$\begin{aligned}\Delta_{180} &= \frac{A}{\sqrt{2}} [\cos(\omega t + 180^\circ) - \cos(\omega t + \Delta\phi + 180^\circ)] \\ &= -\frac{A}{\sqrt{2}} [\cos(\omega t) - \cos(\omega t + \Delta\phi)]\end{aligned}$$

The rate at which the phase of the  $\Delta$  signal is shifted is determined by the maximum rate at which the antenna must turn. The  $\Sigma$  and  $\Delta$  signals are then added and the resultant signal input to the transceiver. This signal will vary as the phase of the  $\Delta$  signal is shifted and can be expressed as

$$\begin{aligned}R_0 &= \frac{A}{\sqrt{2}} [\cos(\omega t) + \cos(\omega t + \Delta\phi)] + \frac{A}{\sqrt{2}} [\cos(\omega t) - \cos(\omega t + \Delta\phi)] \\ &= \sqrt{2} A \cos(\omega t)\end{aligned}$$



when the phase of  $\Delta$  is zero and as

$$\begin{aligned} R_{180} &= \frac{A}{\sqrt{2}} [\cos (\omega t) + \cos (\omega t + \Delta \phi)] - \frac{A}{\sqrt{2}} [\cos (\omega t) - \cos (\omega t + \Delta \phi)] \\ &= \sqrt{2} A \cos (\omega t + \Delta \phi) \end{aligned}$$

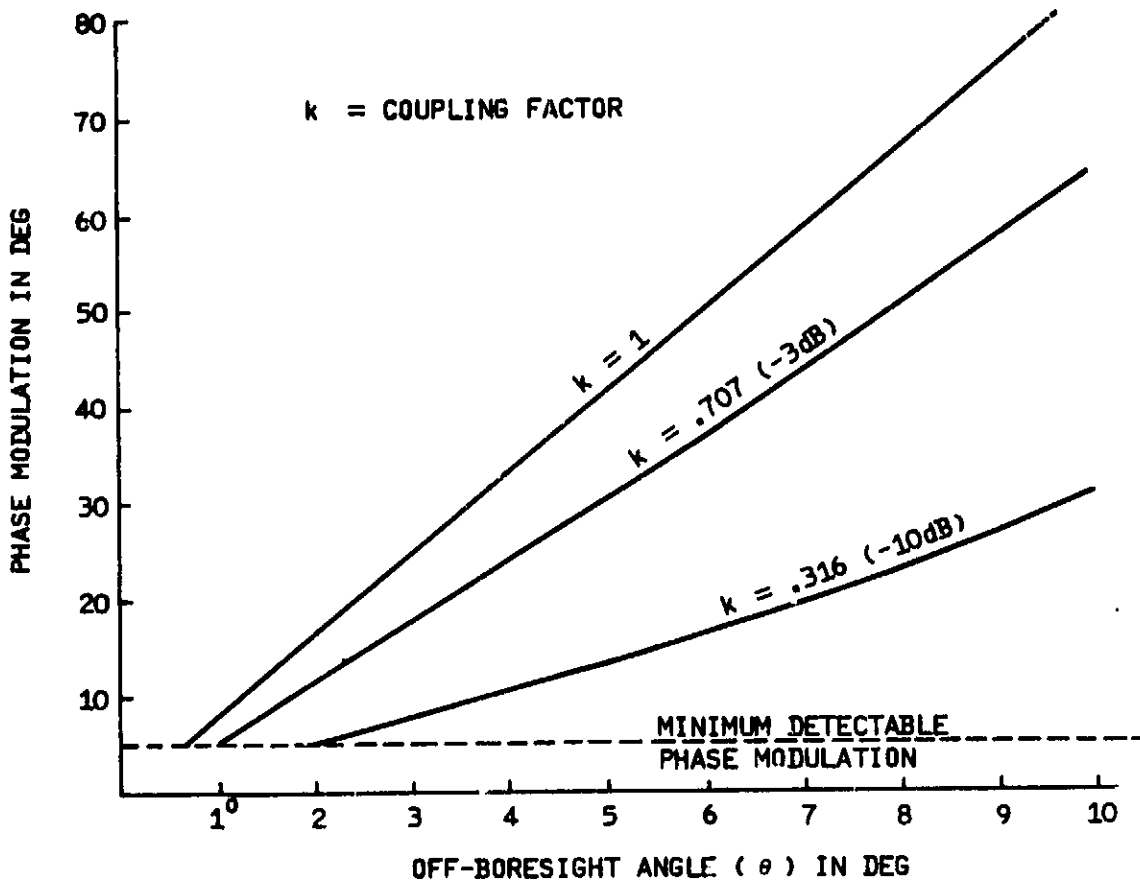
when the phase of  $\Delta$  is  $180^\circ$ .

The important thing to notice is that shifting the phase of the  $\Delta$  signal  $0^\circ$  and  $180^\circ$  causes the resultant signal input to the receiver to be phase modulated by an amount,  $\Delta\phi$ , which is directly related to the off-boresight angle  $\theta$ , and that this phase modulation is independent of the amplitude of the received signal. This means that the phase modulation is constant for a given off-boresight angle even under conditions of severe signal fading. Figure A-2 shows the phase shift of the resultant signal,  $R$ , as a function of the off-boresight angle  $\theta$  for a candidate MSAT-X antenna. The next step is to detect this phase modulation and to supply it to the antenna pointing control system in some useful form.

A receiver which uses a phase-lock-loop (PLL) to track the frequency of the received signal can be used to detect the off-boresight induced phase modulation. A simplified block diagram of a typical PLL is shown in Figure A-3. It contains three basic components, a phase detector, a low-pass filter, and a voltage-controlled oscillator (VCO). The phase detector compares the phase of the input signal against the phase of the VCO. The output of the phase detector is a measure of the phase difference between its two inputs. The difference voltage is then filtered by the loop filter and applied to the VCO. This control voltage, commonly referred to as the loop phase error, changes the frequency of the VCO in a direction that reduces the phase difference between the VCO and the input signal. It can be shown that, after filtering, the output of the phase detector is given by<sup>2</sup>

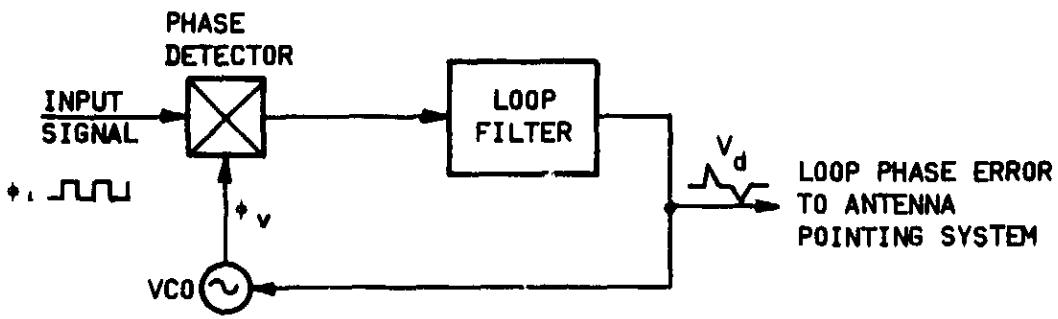
$$v_d = K_d \sin (\phi_i - \phi_o)$$

<sup>2</sup> Phaselock Techniques, Floyd M. Gardner, John Wiley & Sons, Inc., 1966.



A/N 5090

Figure A-2 Phase Modulation of  $R = \Sigma \pm k\Delta$  as a Function of Off Boresight Angle and Coupling Factor ( $k$ )



A/N5090

Figure A-3 Basic Phaselock Loop can Detect Pointing Errors



where

$K_d$  = phase detector gain constant in volts/radian

$\phi_i$  = phase of the input signal

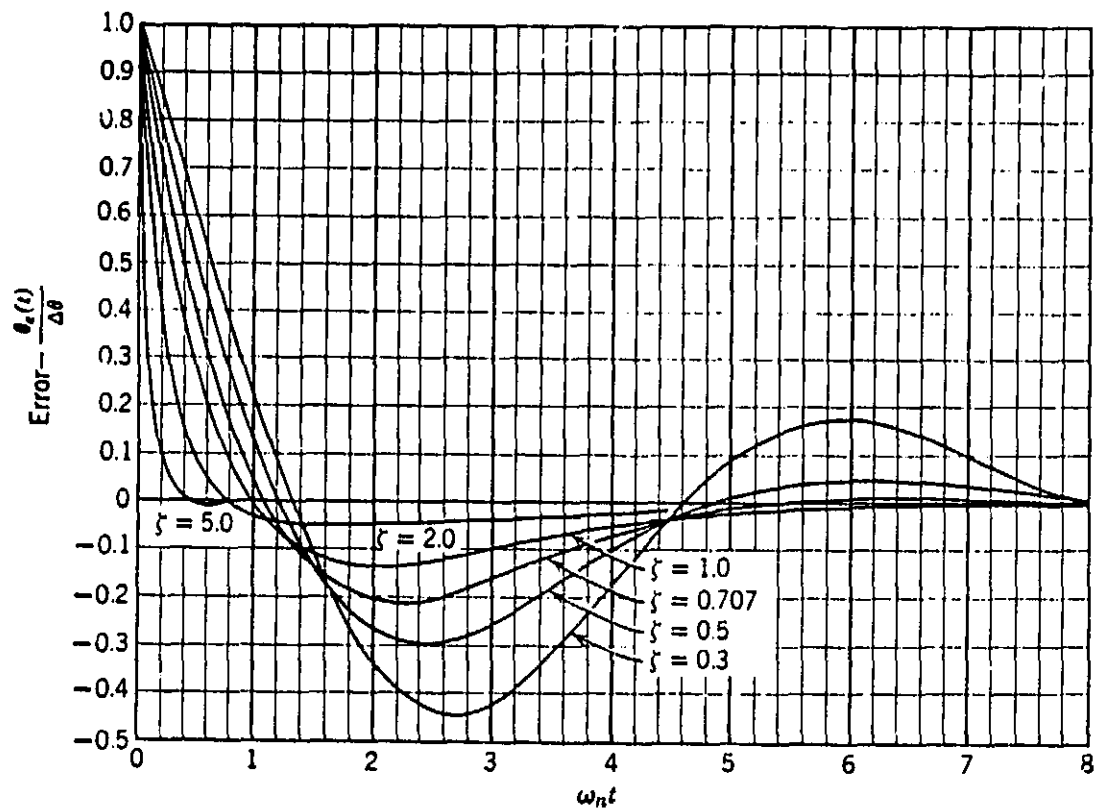
$\phi_v$  = phase of the VCO signal

When the loop is locked, the loop phase error is zero ( $\phi_i = \phi_v$ ). This assumes the loop rest frequency is equal to the frequency of the input signal. In practice this may not be the case, and  $v_d$  will have a constant offset, or static phase error, however, this does not affect the results of this analysis.

A step change in the phase of the input signal of magnitude  $\Delta\phi$  will cause a sudden change in the loop phase error since  $\phi_i$  is no longer equal to  $\phi_v$ . The larger the phase shift is, the larger the change in  $v_d$  will be. The PLL will eventually track out this phase shift and the loop phase error will return to zero. However, the fact that a phase shift in the input signal produces a "transient" in  $v_d$  provides the means to determine antenna pointing error. Figure A-4, which has been extracted from Reference 2, shows examples of the transient in the loop phase error caused by a step phase shift in the input signal for a second order, high gain PLL for various filter damping factors. The final step is to take the information provided by the transient in  $v_d$  and use it to generate antenna steering signals. The following example explains how this is done.

If switching the phase of  $\Delta$  causes a transient in  $v_d$  then the pointing system knows the target is off-boresight. It determines which direction to steer the antenna by comparing the transient induced in  $v_d$  when switching the phase of  $\Delta$  from  $0^\circ$  to  $180^\circ$  with the transient induced when switching the phase from  $180^\circ$  to  $0^\circ$ . If the target is to the right of the boresight, then when the phase of  $\Delta$  is  $0^\circ$ , the phase of the input signal (R) is  $0^\circ$ . When the phase of  $\Delta$  is shifted  $180^\circ$ , the phase of R is shifted  $180^\circ$ . Let us assume the PLL lock up during the  $\Delta\theta$  portion of the cycle. That is, the phase of the signal input to the PLL is  $\phi_{i0}$  and

$$\phi_v = \phi_{i0}$$



$\omega_n$  = LOOP NATURAL FREQUENCY IN RAD/SEC.  
 $\zeta$  = DAMPING FACTOR

FIGURE A-4 PHASE ERROR  $\theta_e(t)$  DUE TO A STEP IN PHASE  $\Delta\theta$



and

$$\begin{aligned} v_d &= K_d (\phi_{i0} - \phi_{v0}) \\ &= 0 \end{aligned}$$

When the phase of the  $\Delta$  signal is shifted  $180^\circ$ , the phase of the signal input to the PLL is shifted  $\Delta\phi$

$$\phi_{i180} = \phi_{i0} + \Delta\phi$$

However, the phase of the VCO signal is still equal to  $\phi_{i0}$  and, as a result,

$$\begin{aligned} v_d &= K_d (\phi_{180} - \phi_{v0}) \\ &= K_d (\phi_{i0} + \Delta\phi - \phi_{i0}) \\ &= K_d \Delta\phi \end{aligned}$$

A POSITIVE TRANSIENT

The PLL eventually tracks out this phase shift, such that

$$\phi_v = \phi_{180} = \phi_{i0} + \Delta\phi$$

and  $v_d = 0$ .

When the phase of the  $\Delta$  signal is shifted back to  $0^\circ$ , the phase of the input signal is  $\phi_{i0}$  and

$$\begin{aligned} v_d &= K_d (\phi_i - \phi_v) \\ &= K_d (\phi_i - (\phi_i + \Delta\phi)) \\ &= K_d (-\Delta\phi) \end{aligned}$$

A NEGATIVE TRANSIENT

If the target is to the left of boresight, then phase shift of R will be reversed relative to the phase shift of the  $\Delta$  signal. That is, when the phase of  $\Delta$  is zero, the phase of R is shifted  $180^\circ$  and when the phase of  $\Delta$  is shifted  $180^\circ$ , the phase of R is  $0^\circ$ . This means the sign (+ or -) of the transient induced in  $v_d$  will be reversed relative to the phase of  $\Delta$ .



To summarize, if  $v_d$  experiences a positive transient when the phase of the  $\Delta$  signal is shifted  $180^\circ$  followed by negative transient when the phase of the  $\Delta$  signal is  $0^\circ$ , then the target is to the right of boresight and the antenna must be steered clockwise. If the reverse is true, the target is to the left of the boresight and the antenna must be steered counter-clockwise.

Figure A-5 is a timing diagram showing the relationship between the phase shift of  $\Delta$  and the transient in  $v_d$ . Notice that, as the tracking system acquires the target, the amplitude of the  $v_d$  transients get smaller which means the pointing system will know when it is getting close to the target.

Phase-lock-loops are extremely good at measuring phase. Typical second order, high-gain, PLL are capable of measuring phase errors of only a few degrees. Figure A-2 shows that an off-boresight angle of  $0.5^\circ$  cause a phase shift of nearly  $4^\circ$ . Therefore, it is reasonable to expect the pointing knowledge using this approach will be less than  $0.5^\circ$ .

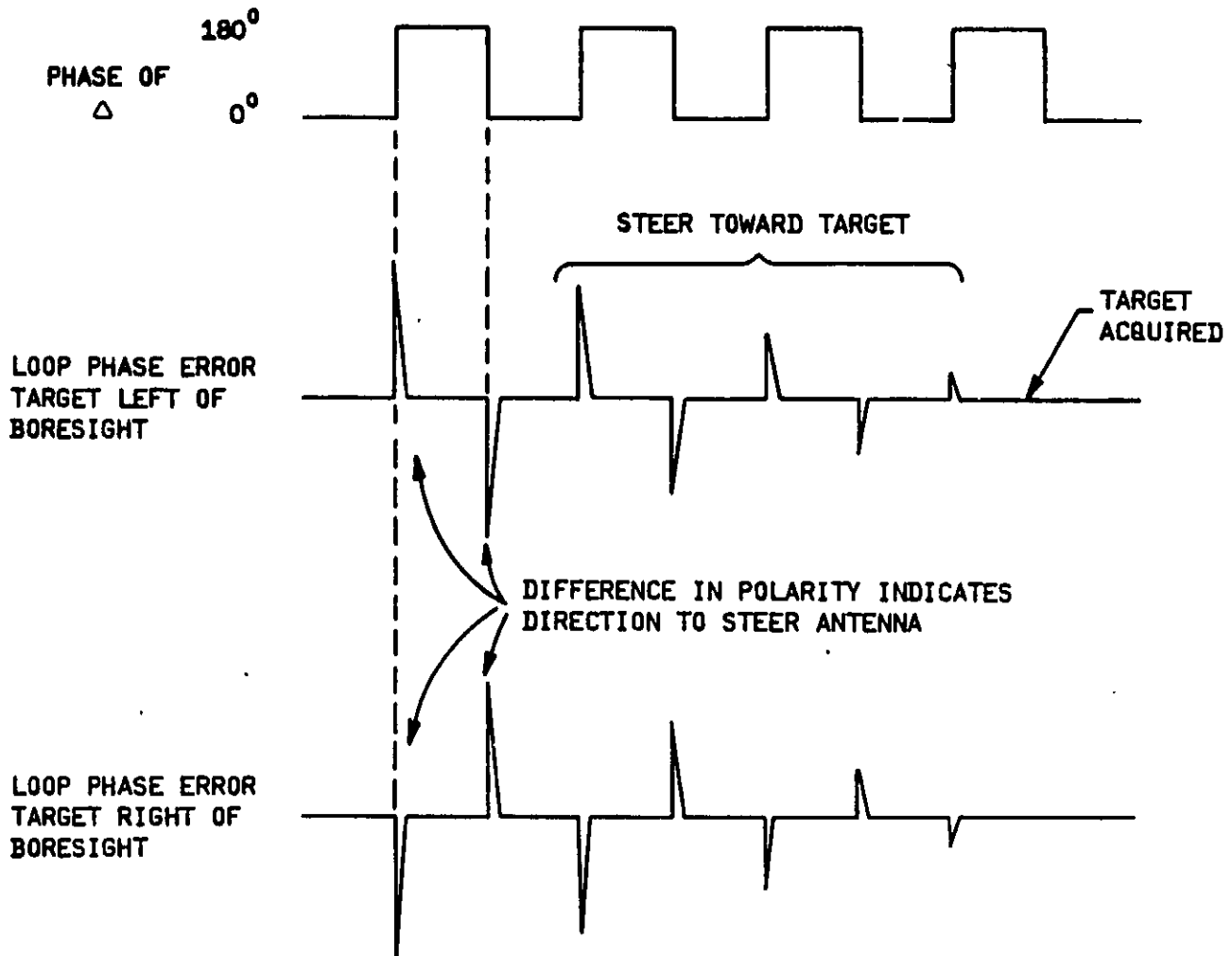


Figure A-5 Pointing Error Determined by Synchronously Demodulating Transients in Loop Phase Error and Phase Shifts of  $\Delta$  Signal



APPENDIX B  
POINTING ACCURACY OF A MONOPULSE TRACKING SYSTEM  
USING PHASE DETECTION

A monopulse tracking system uses two antennas which are pointed in the same direction. Since these two antennas are physically separated, when a signal is received at an off-boresight angle, the phase of the signal seen by one antenna will be delayed relative to the phase of the signal seen by the other antenna by an amount which is directly related to the off-boresight angle. This relationship between the phase delay and off-boresight angle can be expressed as:

$$\phi = \frac{2\pi D}{\lambda} \sin \theta \quad (1)$$

where

- D = distance between antennas
- $\lambda$  = wavelength of the received signal
- $\theta$  = off-boresight angle

The accuracy of the monopulse tracking system is found by considering the derivative of (1):

$$d\phi = \frac{2\pi D}{\lambda} \cos \theta d\theta \quad (2)$$

Replacing the differentials by increments  $\Delta$ , we can evaluate the effects of system errors:

$$\Delta\phi = \frac{2\pi D}{\lambda} \cos \theta \Delta\theta \quad (3)$$

Solving for the pointing error,  $\Delta\theta$ , we get:

$$\Delta\theta = \frac{\Delta\phi}{k} \quad (4)$$

where,



$\Delta\theta$  = the pointing error  
 $\Delta\phi$  = measured phase error  
 $k = \frac{2\pi D}{\lambda}$

Contributions to the measured phase error,  $\Delta\phi$ , are derived from two basic sources, the ability of the equipment to hold phase match and the effect of signal-to-noise ratio (SNR) in the phase-lock-loop. Since these two sources of error are independent, they can be expressed as:

$$\Delta\phi^2 = \Delta\phi_{SNR}^2 + \Delta\phi_{EQ}^2 \tag{5}$$

where,

$\Delta\phi$  = the resultant measured electrical phase error,  
 $\Delta\phi_{SNR}$  = the electrical phase error component due to SNR  
 $\Delta\phi_{EQ}$  = the error component due to equipment electrical phase mismatch.

Errors due to equipment electrical equipment are caused by the phase mismatch of the radiation patterns of the two antennas, the phase mismatch in the  $\Sigma$  and  $\Delta$  channels, and the mechanical alignment of the antennas. It is expected these sources can easily be held to less than 5 degrees of phase error.

The signal-to-noise ratio of the phase-lock-loop affects the ability of the phase detector to measure the difference in phase of the incoming signal and VCO. It can be expressed as (from reference 1):

$$\Delta\phi_{SNR} = \left[ \frac{1}{SNR} \right]^{1/2} \text{ (rad.)}$$

The resultant pointing error can then be expressed as:

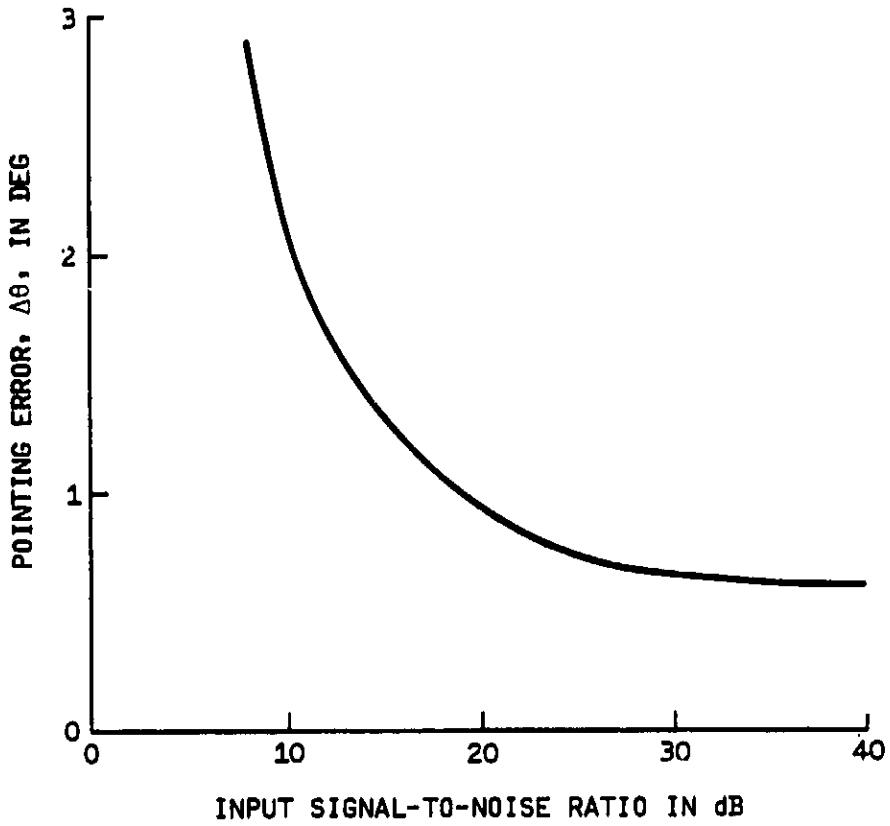
$$\Delta\theta = \frac{1}{k} \left[ \left( \frac{1}{SNR} \right) + \Delta\phi_{EQ}^2 \right]^{1/2}$$



Figure B-1 shows a plot of the expected pointing error as a function of signal-to-noise ratio. It shows the pointing error of less than  $2.5^\circ$  can be maintained even if shading causes the input signal to noise ratio to drop to 10 dB. If the SNR drops much below this level, there is a danger the PLL will drop lock.

#### REFERENCES

1. L.G. Bullock et al., "An Analysis of Wide-Band Microwave Monopulse Direction-Finding Techniques."



A/N 5090

Figure B-1 Pointing Errors As a Function Of Input Signal-To-Noise Ratio